Investigating cross-species immunity and disease modulation in *Babesia* co-infections

2024

Iqra ZAFAR

Doctoral Program of Veterinary Science

Graduate School of Animal and Veterinary Sciences and Agriculture

Obihiro University of Agriculture and Veterinary Medicine

バベシア共感染における種間免疫と疾患調節の研究

令和 6 年
(2024)

帯広畜産大学大学院畜産学研究科
獣医学専攻博士課程

イクラ　ザファー

Table of contents

Abbreviations

ANOVA:	Analysis of variance
ADCI:	Antibody cell-dependent inhibition
BBB:	Blood brain barrier
Bm:	*Babesia microti*
Bm/Br:	*Babesia microti/ Babesia rodhaini*
Bm/PbA:	*Babesia microti/ Plasmodium berghei* ANKA
BSA:	Bovine serum albumin
CDC:	Centers for Disease Control and Prevention
CD:	Cluster of differentiation
CI:	Confidence interval
CM:	Cerebral malaria
DNA:	Deoxyribonucleic acid
DDW:	Deionized distilled water
DW:	Distilled water
dpi:	days post-infection
ECM:	Experimental cerebral malaria
EDTA:	Ethylenediaminetetraacetic acid
ELISA:	Enzyme-linked immunosorbent assay
FACS:	Fluorescence-activated cell sorting
GFP:	Green fluorescent protein
H & E:	Hematoxylin and eosin
IFA:	Immunofluorescence microscopy analysis
IgG:	Immunoglobulin G
IgG1:	Immunoglobulin G1
IgG2a:	Immunoglobulin G2a
IgG2b:	Immunoglobulin G2b
IgG2c:	Immunoglobulin G2c
IgM:	Immunoglobulin M
IFN-γ:	Interferon Gamma
IL-2:	Interleukin 2
IL-6:	Interleukin 6
IL-10:	Interleukin 10
IL-12p70:	Interleukin 12 subunit p70

iRBCs:	Infected red blood cells
MEXT:	Ministry of Education, Culture, Sports, Science and Technology
NBRP:	National BioResource Project
NRCPD:	National research center for protozoan disease
OR:	Odds ratio
PbA:	*Plasmodium berghei* ANKA
PBS:	Phosphate-buffered saline
PBST:	Phosphate-buffered saline with Tween
PCR:	Polymerase chain reaction
pci:	Post-challenge infection
RBC:	Red blood cell
RBCs:	Red blood cells
ROS:	Reactive Oxygen Species
SD:	Standard deviation
RT:	Room temperature
RMCBS:	Rapid murine coma and behavior scale
TNF-α:	Tumor necrosis factor alpha

Unit abbreviations:

°C:	Degree celsius (temperature)
bp:	Base pairs
μM:	Micromolar (concentration)
nm:	Nanometer (length)
h:	Hour (time)
μL:	Microliter (volume)
μm:	Micrometer
mL:	Milliliter
min:	Minute
s:	Second
%:	Percentage

<center>**General introduction**</center>

Babesiosis

Babesiosis, caused by the intraerythrocytic parasite *Babesia*, shares clinical similarities with malaria, affecting both humans and animals. It is increasingly recognized as an emerging zoonotic disease in humans. While having the ability to infect a diverse array of vertebrates, parasites need the presence of both a vertebrate and nonvertebrate host to continue the transmission. So far, all identified babesial parasites have been transmitted by ixodid ticks to their vertebrate hosts. Within the red blood cells of vertebrate hosts, these parasites undergo replication and are referred to as piroplasms, owing to their distinctive pear-shaped appearance when inside the host cells (Homer et al., 2000).
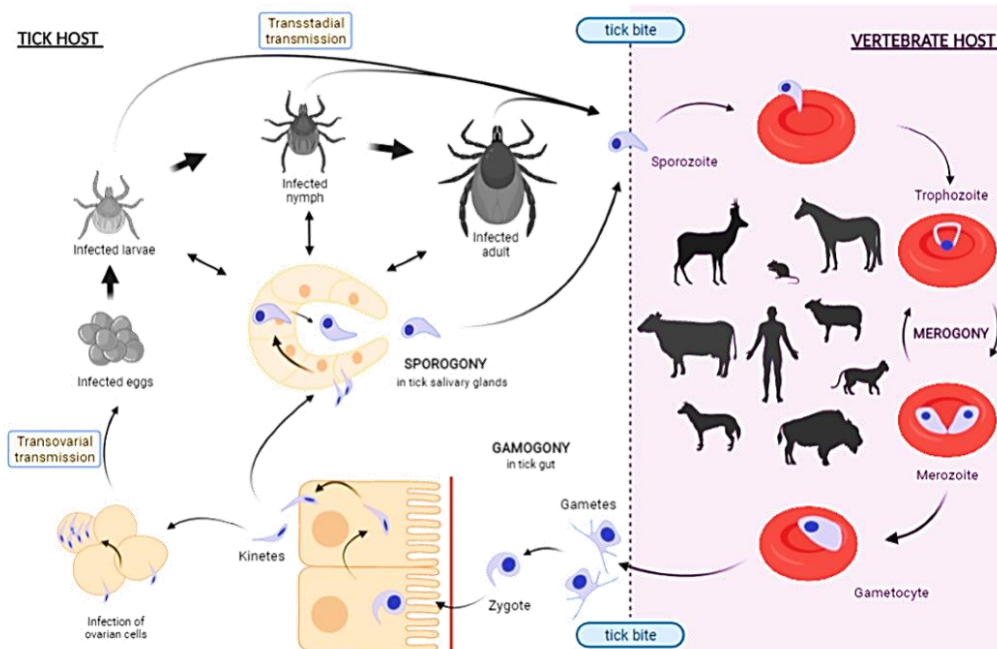

Figure 1. Life cycle of *Babesia* sensu stricto. Adapted from (Bonnet & Nadal, 2021).

Human babesiosis results from infections by various *Babesia* species, each displaying unique geographical distributions dependent on the presence of suitable hosts (Homer et al., 2000), including *Babesia microti*, a pathogen resembling *Babesia crassa*, *Babesia divergens*, *Babesia duncani*, and *Babesia venatorum*, along with other parasites closely genetically related to these pathogens, such as *B. divergens*-like, *B. duncani*-like, and *B. microti*-like. Typically, infections in individuals without underlying health issues are mild to moderate, with severe cases predominantly observed in immunocompromised individuals. *B. microti* is prevalent in the northeastern and upper midwestern regions of the United States, while *B. duncani* is found on the west coast. In Europe, the majority of human cases are attributed to *B. divergens*, whereas

in Asia, they are linked to *B. venatorum*, *B. crassa*-like, and *B. microti* (Krause, 2019). In cattle, *Babesia* spp. exert a substantial worldwide economic, social, and epidemiological impact. Among the most significant species are *B. bovis*, *B. bigemina*, *Babesia major*, and *B. divergens*. *B. bovis* and *B. bigemina* are present in numerous countries across Africa, Asia, Australia, Central and South America, and Southern Europe between 40° N and 32° S. *B. major* is found in Europe, Northwest Africa, and Asia, while *B. divergens* is prevalent in northern Europe (Bock et al., 2004). Ovine babesiosis, caused by *Babesia ovis* and *Babesia motasi*, stands as a critical blood-borne parasitic disease of small ruminants in tropical and non-tropical regions, occurring in South-eastern Europe, North Africa, and Asia (Yeruham et al., 1998). In equids, *Babesia caballi*, is the agent of equine piroplasmosis and is endemic in several countries across Africa, Asia, the Americas, and primarily in the Mediterranean basin for Europe (Nadal et al., 2022). This disease poses a significant animal health concern and results in notable economic losses for the equine industry.

Ultimately, babesiosis is acknowledged as one of the most widely dispersed and swiftly advancing tick-borne illnesses in dogs. *Babesia canis* serves as the leading cause of canine babesiosis in Europe and is intermittently encountered worldwide, with *Babesia gibsoni*, the most commonly found species, and *Babesia vogeli* exhibiting a global distribution. Additionally, *Babesia rossi*, identified as one of the most harmful species, is confined to southern Africa (Petra et al., 2018).

Spleen plays an essential role in protecting against *Babesia* infection (Xue et al., 2021). The spleen consists of B lymphocytes and macrophages and can also produce immunoglobulins and factors that deploy immune functions (Golub et al., 2018). The existing knowledge regarding the host response to babesial infections primarily stems from observations and investigations involving vertebrates other than humans. Across all examined mammalian hosts, the development of immunity to *Babesia* species has been consistently observed, either following infection and subsequent recovery or through prophylactic immunization. Both humoral and cellular components contribute to the establishment of immunity against babesiosis. Multiple factors contribute to the severity of disease, including age, immune status, and concurrent infections with other pathogens (Homer et al., 2000). Some studies indicated that cellular immunity, T cells, and macrophages are critical for the clearance of *B. microti* in mice (Igarashi et al., 1999; Clawson et al., 2002; Li et al., 2012). Still, these studies are uncertain in establishing the crucial function of each of these factors in the resolution of

infection (Skariah et al., 2017). No vaccine has yet proven effective against *Babesia* infection (Man et al., 2017). More importantly, the limited knowledge on the mechanisms of immunity and pathogenesis in babesiosis causes hindrance for the development of effective preventive and therapeutic interventions (Vos & Bock, 2006; Rathinasamy et al., 2019).

Malaria

On the other hand, malaria, a devastating infectious disease caused by unicellular protozoan parasites belonging to the *Plasmodium* genus, continues to pose a global health threat with more than 200 million cases and hundreds of thousands of deaths annually (World Malaria Report, 2022). These parasites infect a wide range of vertebrates, encompassing reptiles, birds, and mammals, not solely humans. Over 200 *Plasmodium* species have been formally identified, each targeting specific hosts. Among the *Plasmodium* species causing malaria in humans worldwide, only five are prevalent; *P. falciparum*, *P. vivax*, *P. malariae*, *P. ovale*, and *P. knowlesi*. The first four are exclusive to humans, while *P. knowlesi* is naturally harbored by macaque monkeys and leads to zoonotic malaria, particularly in South East Asia (Sato, 2021). The transmission of *Plasmodium* species between vertebrate hosts relies on an insect vector, typically mosquitoes belonging to genus *Anopheles* (Sanches-Vaz et al., 2019). These same mosquitoes are also carriers for additional *Plasmodium* species that parasitize other mammals (Perkins, 2014). Malaria caused by *Plasmodium falciparum* malaria has the potential to be life-threatening, and the infection may progress swiftly, leading to cerebral malaria and dysfunction of multiple vital organs, resulting in a mortality rate of 15–20%, even with the use of effective antimalarial drugs and clinical care. In regions with high stable transmission, severe malaria in young children is primarily characterized by anemia. Numerous pathophysiological aspects of severe malaria remain not fully comprehended (Dondorp et al., 2000, Ghazanfari et al., 2018).

There are various approaches to investigate the pathogenesis of cerebral malaria (CM) and they have the potential to complement each other. However, as previously mentioned (Hunt and Grau, 2003), there has traditionally been a lack of integration among research groups employing these diverse approaches. The most well-established methods include clinical studies in malaria-endemic regions (Molyneux et al., 1989), examination of post-mortem material from CM victims (Brown et al., 1999), animal model studies (Grau et al., 1986), and genetic predisposition studies in humans or mice (McGuire et al., 1999, Nagayasu et al., 2002). Given that some malaria cases exhibit severe complications and are at risk of death, another

rational approach is to pinpoint the crucial steps in the pathogenesis of these complications and identify specific treatments to impede them (Mishra & Newton, 2009). Implementing such treatments would be a judicious use of limited health resources in malaria-endemic regions. A comprehensive understanding of its pathogenesis may facilitate the identification of new drug targets in the host that show promise as specific CM treatments.
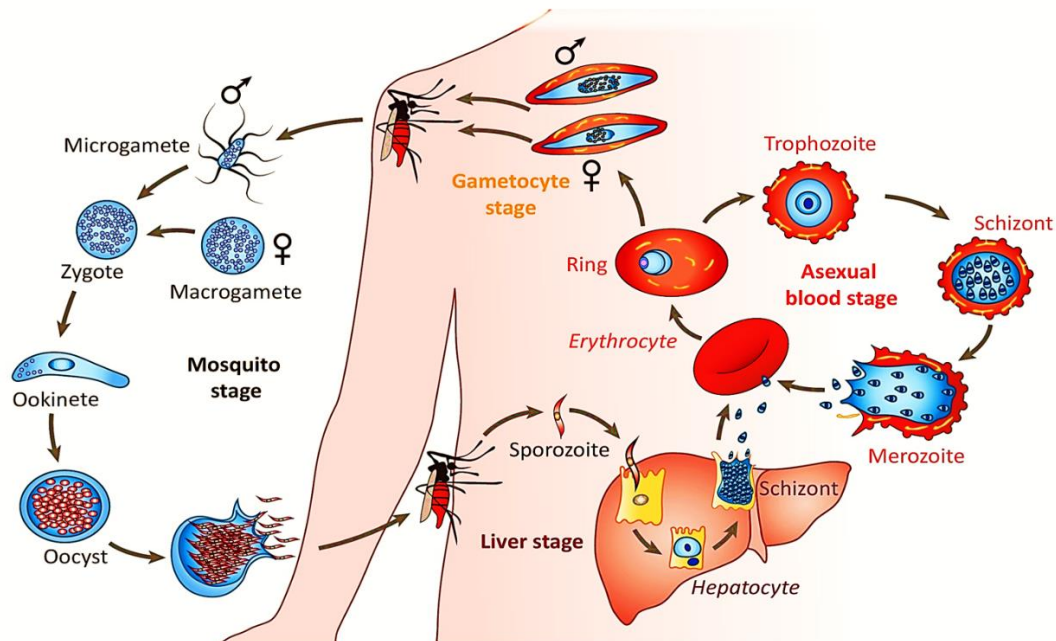

Figure 2. Life cycle of *Plasmodium* Adapted from (Maier et al., 2019).

Despite numerous efforts to combat malaria, there is still no effective remedy for cerebral malaria and a comprehensive understanding of the host-parasite interactions underlying its pathogenesis is urgently needed (Mawson, 2013; Mineo et al., 2013). Hence, the quest for the eradication of malaria requires a deeper comprehension of the disease's pathogenesis (Mawson, 2013; Junaid et al., 2017), which may facilitate the identification of new therapeutic targets in the host that show promise as specific CM treatments. In general, the ANKA strain of *Plasmodium berghei* is characterized by higher virulence and is known to induce experimental cerebral malaria (ECM) in C57BL/6 mice (Dobrescu et al., 2020). Therefore, a model for investigating the intricacies of cerebral malaria, utilizing *P. berghei* ANKA (PbA) infection in C57BL/6 mice, is globally adopted as an alternative to the study of human cerebral malaria (HCM) (Ghazanfari et al., 2018).

Co-infections

Co-infections are a common occurrence worldwide rather than a rare exception. In our daily

lives, we encounter numerous potential pathogens, with many people carrying chronic or latent infections, and hosting various potential pathogens within our resident microbial flora. However, there is still much to learn about which combinations of co-infections have the most significant impact on our health. Co-infections result in various outcomes, including inconsequential, harmful, or potentially beneficial interactions. These interactions can impact the host's immune response (McArdle et al., 2018). A phenomenon known as 'heterologous immunity' or 'cross-protection' occurs when a host develops immunity to one pathogen after exposure to a different, non-identical pathogen (Welsh et al., 2010). Co-infection models have provided valuable insights into cross-protection between *Babesia* and *Plasmodium* species (Cox & Young, 1969; Zivkovic et al., 1984).

The quest for effective preventive and therapeutic interventions for Babesiosis and malaria infections remains a challenge, as no effective vaccine has been developed (Man et al., 2017). This limited understanding of immunity and pathogenesis hinders the development of suitable interventions (Vos & Bock, 2006; Rathinasamy et al., 2019). Furthermore, co-infections, where a host is simultaneously infected with multiple pathogens, have gained increasing recognition for their impact on the course of infections (Cox, 2001; McArdle et al., 2018). While co-infections involving *Babesia* species and *Plasmodium* parasites have been documented in humans, animals, and vectors (Steiner et al., 2008; Mayne, 2014; Young et al., 2019), their prevalence and clinical implications remain relatively unexplored (Moutailler et al., 2016). Co-infection of rodents with both *Babesia* and *Plasmodium* has been documented to trigger cross-protection. In various hosts, including humans, both parasites elicit comparable inflammatory responses and clinical symptoms that exhibit varying degrees of severity (Van Duivenvoorde et al., 2010).

General objectives

Babesiosis and malaria are two vector-borne infectious diseases of significant concern that have attracted the attention of researchers worldwide due to their impact on public health. As mentioned earlier, co-infections of these parasites are found naturally and in laboratory experiments.

The immune dynamics involved in these co-infections, especially during the acute stages, remain poorly understood. In this context, the studies were undertaken to investigate the role of primary *B. microti* infection during the acute phase in influencing susceptibility to *B.*

rodhaini and *P. berghei* ANKA challenge infection, shedding light on various aspects of disease manifestations and immune dynamics. Understanding co-infections and their implications for host immunity is essential for the development of effective interventions against both babesiosis and malaria, including vaccine strategies. The general objectives of these studies were:

1. To decipher the host immune mechanisms associated with the development of protective immunity following a lethal challenge with *B. rodhaini* during acute primary babesiosis in mice.

2. To investigate the outcome of disease in a co-infection disease model of acute stage *Babesia microti* primary infection after *Plasmodium berghei* ANKA challenge infection.

Through these objectives, the study aims to contribute valuable insights into the intricate interplay between the host immune system and parasites, particularly in the context of co-infections, ultimately advancing our understanding of protective immunity and disease manifestation dynamics.

Chapter 1

The Cross-species immunity during acute *Babesia* co-infection in mice

1.1 Introduction

Babesiosis is an emerging tick-borne disease caused by intraerythrocytic parasite *Babesia*, resulting in a malaria-like ailment (Dvoraková & Dvorácková, 2007). *Babesia rodhaini*, a rodent-specific variant of *Babesia* closely related to *B. microti*, which is a primary causative agent of human babesiosis, exhibits the potential to infect human RBCs (Kawabuchi et al., 2005). Even the introduction of a single parasite results in 100% mortality in mice (Clark, 2001). In contrast, *B. microti* (Munich strain) induces a self-limiting disease in mice that ultimately resolves (Igarashi et al., 1999). *B. microti* is responsible for babesiosis in animals and humans globally, attracting increased attention as an emerging zoonosis (Leiby, 2011; Vannier & Krause, 2012). The transmission of *Babesia* extends beyond tick vectors to include blood transfusion or transmission during pregnancy (Young et al., 2019; Xue et al., 2021). According to the Centers for Disease Control and Prevention (CDC), approximately 2,000 cases of babesiosis are reported annually in the United States (Centers for Disease Control and Prevention, 2012). *Babesia* poses a threat to the blood supply and is presently the most prevalent transfusion-transmitted infection in the United States (Lobo et al., 2013). In infants or individuals with compromised immune systems, babesiosis can be life-threatening (Gabrielli et al., 2016). Elderly individuals who have undergone splenectomy face an elevated risk of severe symptoms, including hemolytic anemia, splenomegaly, hepatomegaly, renal failure, and, in extreme cases, death (Bloch et al., 2019; Young et al., 2019).

Thus, as the primary immune organ, the spleen plays a vital role in defending against *Babesia* infection. In *Babesia* infection, despite significant spleen damage, it actively triggers immunomodulatory responses (Xue et al., 2021). Comprising B lymphocytes and macrophages, the spleen is capable of producing immunoglobulins and factors that contribute to immune functions (Golub et al., 2018). Several studies suggest the importance of cellular immunity, particularly T cells and macrophages, in the clearance of *B. microti* in mice (Igarashi et al., 1999; Clawson et al., 2002; Li et al., 2012). However, uncertainties persist regarding the specific roles of these factors in resolving the infection (Skariah et al., 2017).

To date, no vaccine has demonstrated efficacy against *Babesia* infection (Man et al., 2017). Moreover, the limited understanding of the immune mechanisms and pathogenesis in

babesiosis poses a barrier to the development of effective preventive and therapeutic interventions (Vos & Bock, 2006; Rathinasamy et al., 2019).

Co-infections can manifest as inconsequential, deleterious, or even beneficial, involving intricate interactions with the potential to modulate the host response (McArdle et al., 2018). Particularly in underdeveloped countries, the clinical landscape of simultaneous infections encompasses diverse microorganisms that not only influence each other but also impact the host (Lundqvist et al., 2010). Nevertheless, our understanding of the significance of various co-infections to human health remains limited (McArdle et al., 2018). In the context of babesiosis, instances of simultaneous infection with two *Babesia* species have been documented in humans (Mayne, 2014), animals (Young et al., 2019), and tick vectors (Steiner et al., 2008). However, information regarding the prevalence of such co-infections is sparse (Moutailler et al., 2016). Unlike the *Plasmodium* species, the pathogenesis of *Babesia* infection and co-infections remains underexplored, leading to a poor understanding of their substantial impact on human health. Heterologous immunity, demonstrating immunity to babesiosis, has been previously observed. Few studies, utilizing mouse models, have experimentally investigated co-infections with *B. microti* and *B. rodhaini* (Cox & Young, 1969; Zivkovic et al., 1984; Inoue et al., 1994; Li et al., 2012; Wang et al., 2016). Notably, *B. microti* has shown cross-protective immunity against *Babesia rodhaini* (Li et al., 2012). During the chronic stage of the *Babesia* co-infection, a significant decline in antibody levels and blood cytokine levels in mouse sera was observed. Furthermore, macrophages were identified as the primary immune cells responsible for conferring cross-species protection against subsequent lethal challenges (Li et al., 2012). However, whether these immune dynamics persist during acute *Babesia* co-infections remains unknown.

This study emphasizes the significance of exploring simultaneous infections and gaining a deeper understanding of the immune dynamics associated with protective immunity following a lethal challenge with *B. rodhaini* during acute primary babesiosis in mice.

1.2 Materials and methods

Experimental animals

Female wild-type (WT) BALB/c mice, aged 6–8 weeks and weighing 18–22 g, were obtained

from CLEA Japan. The mice were maintained in pathogen-free conditions, as detailed in a previous study (Li et al., 2021). The utilization of female mice was deliberate to eliminate potential interference caused from variations in hormonal profiles that could impact parasitic interactions (Djokic et al., 2019).

Babesia Parasites and experimental infections

Stabilates of *Babesia microti* (Munich strain) and *Babesia rodhaini* (Australia strain) were thawed from the cell bank, and intraperitoneal inoculations were carried out for serial passage and maintenance of the parasites *in vivo* in mice. Initially, two groups (n=6) received intraperitoneal infections with 10^7 *B. microti*-infected red blood cells (RBCs). In this study, infection trials were conducted to assess the impact of an initial *B. microti* infection on a subsequent infection. Three groups were challenge-infected with 10^6 *B. rodhaini*-infected RBCs on day 2 (referred to as bm/br2; n=6), day 4 (referred to as bm/br4; n=6), and day 6 (referred to as bm/br6). Similarly, a separate group (n=6) was intraperitoneally inoculated with *B. rodhaini*-infected RBCs only (referred to as Br), and another group received *B. microti*-infected RBCs only (referred to as Bm). The first trial included the co-infected groups (bm/br2, bm/br4, and bm/br6) and a control group (Br) to determine the time point at which cross-protection occurs. Subsequently, a second trial was conducted, including only groups where cross-protection was observed from the first trial (bm/br4 and bm/br6), control groups for each parasite species (Br and Bm), and one additional group (n=6) of naïve mice to assess immune dynamics during cross-protection (Figure 1.1A).

Assessment of parasitemia and survival rates

Parasitemia, body weight, hematocrit values, and survival rates were systematically monitored every other day. Hematocrit values were assessed using previously described methods (Wang et al., 2016). The percentage of parasitemia was determined through thin blood smears stained with Giemsa, and calculations were based on the examination of 10^3 erythrocytes observed under a 100 × oil immersion Eclipse E200 microscope (Nikon, Tokyo, Japan).

Immunofluorescence microscopy analysis (IFA)

Blood taken from mice was diluted to 1:40 in phosphate-buffered saline (PBS) and subjected to three washes. Blood smears were fixed on glass slides with ethanol/methanol (1:1) for 1 minute at –20°C. Subsequently, the fixed smears were treated with 3% bovine serum albumin (BSA) in PBS for 30 minutes at room temperature (RT). Primary antibodies, mouse anti-*B. microti* P32 (rBmP32), and rabbit anti-*B. rodhaini* P26 (rBrP26) were applied to the fixed smears and incubated at 37°C for 1 hour in a moist chamber. Following three washes with PBS and rinsing with distilled water, secondary antibodies, Alexa Fluor® 594-conjugated goat anti-rabbit IgG or Alexa Fluor® 488-conjugated anti-mouse IgG (Thermo Fisher Scientific, Massachusetts, USA), were applied to the smears. The secondary antibody solution (diluted 1:200 in 3% BSA in PBS) was incubated at 37°C for 30 minutes. The slides were then washed three times and incubated with a Hoechst 33342 solution (Thermo Fisher Scientific) at a concentration of 200 µg/mL, diluted in 3% BSA in PBS containing 50 mg/mL RNase (Qiagen, Hilden, Germany), at 37°C for 10 minutes. After washing with PBS twice, the glass slides were mounted by adding 10 mL of a 50% glycerol–PBS (v/v) solution and covered with a glass coverslip. Microscopic examination and image capture were performed using the All-in-One BZ-9000 microscope (Keyence, Illinois, USA).

Immunophenotyping of splenocytes by fluorescence-activated cell sorting (FACS) analysis

After surgically excising spleen tissues from both naïve and infected mice under sterile conditions, splenocytes were isolated by obtaining single-cell suspensions. Tissues were fragmented into small pieces and passed through a sterile 70 µm cell strainer into 50-mL tubes. The crude splenocyte suspensions were washed twice with cold 1× PBS and centrifuged at 375 × g for 5 minutes at 4°C. The cell pellets were lysed with 1× ACK lysis buffer (Gibco, Massachusetts, USA) for 5 minutes at 25°C. Cold PBS was added to halt the lysis process, and the samples were then centrifuged at 375 × g for 5 minutes at 4°C. The cell pellets were resuspended in 2 mL of cell staining buffer (BioLegend, California, USA) and kept on ice until staining. Viability of cells was assessed after staining with trypan blue (1:5 dilution) using a hemocytometer.

Approximately one million splenocytes were reconstituted in cell staining buffer (CSB) and centrifuged. The cells were resuspended in 70 µL CSB containing CD16/CD32 monoclonal

antibody for Fc blocking (Invitrogen, Massachusetts, USA) at 4°C for 25 minutes. Subsequently, splenocytes were stained in the dark by labeling with respective marker antibodies conjugated with different fluorophores for 30 minutes at 4°C. The antibody panel used in the study is presented in Table 1.1. Following staining, cell samples were fixed with 200 μL of 4% paraformaldehyde (PFA) solution for 15 minutes, washed twice with CSB, and centrifuged at 375 × g for 5 minutes at 4°C. Finally, samples were resuspended in 200 μL CSB. Labeled cells were sorted using a CytoFLEX flow cytometer (Beckman Coulter, California, USA), and the data were analyzed using CytExpert 2.4 software (Beckman Coulter). The gating scheme used is illustrated in Figure 1.2, following the approach of Bayne and Vonderheide (2013).

Spleen histopathological analysis

Spleen samples were initially fixed in 10% neutral buffered formalin. Subsequently, the tissue underwent dehydration through a series of graded alcohols, followed by embedding in paraffin and sectioning at a thickness of 4 μm. Upon deparaffinization of the sections, staining was conducted using hematoxylin & eosin (H & E) for tissue visualization. The slides were then mounted on MGK-S (Matsunami Glass Ind. Ltd., Osaka, Japan) and covered with coverslips. An examination of changes was performed by a histopathologist using a Microphot-FX (Nikon) in a blinded manner. Microphotographs were captured using a Digital Sight DS-5M camera (Nikon) equipped with a microscope.

Quantification of serum cytokines

Mice were exsanguinated to collect serum on days 2, 4, and 6 following the challenge infection with *B. rodhaini*. Commercial enzyme-linked immunosorbent assay (ELISA) kits (Thermo Fisher Scientific) were employed to detect and quantify cytokines, while levels of reactive oxygen species (ROS) were assessed using the OxiSelect™ In Vitro ROS/RNS Assay Kit (Cell Biolabs, Inc., California, USA), in accordance with the manufacturers' protocols. For cytokine detection, serum samples were diluted in PBS to a 1:1,000 ratio. Absorbance values were measured using the MTP-500 microplate reader (Corona Electric Co., Tokyo, Japan), and fluorescence (480 nm excitation/530 nm emission) was recorded with the GloMax®-multi detection system (Promega, Wisconsin, USA). The concentrations of serum IFN-γ, TNF-α, IL-2, IL-6, IL-10, IL-12, and ROS were determined by extrapolating obtained standard curves.

Humoral response determination

Previously established ELISA protocols utilizing GST-fused rBmP32 and rBrP26 antigens were employed to assess the antibody response against each parasite species (Li et al., 2012). Microtiter plates (Nunc, Roskilde, Denmark) were coated with 0.1 µM of rBmP32 or rBrP26 and left to incubate at 4°C overnight. Subsequently, the plates were washed once with 0.05% Tween 20-PBS (PBST) and incubated with 100 µL/well of blocking solution (3% skim milk in PBS) for 1 hour at 37°C. Following a wash, the antigen-coated plates were incubated for 1 hour at 37°C with 50 µL of mouse serum diluted at 1:100 in blocking solution. After six washes with PBST, the plates were incubated for 1 hour at 37°C with HRP-conjugated secondary antibodies (goat anti-mouse immunoglobulins IgG1, Ig2a, IgG2b, IgG2c, IgG2, IgG3, IgM, and IgG) diluted to 1:4,000 in blocking solution. Subsequent to another six washes, 100 µL/well of substrate solution (100 µM citric acid, 200 µM sodium phosphate, 0.3 mg of ABTS [2,2=azinobis (3-ethylbenzthiazolinesulfonic acid)]/mL [Sigma, St. Louis, MO], 0.01% of 30% H_2O_2) was added. After a 1-hour incubation at room temperature (RT), optical density values were measured using the MTP-500 microplate reader (Corona Electric) at a wavelength of 415 nm. Each serum sample was run in duplicates.

Absolute quantification of *B. rodhaini* parasites

For the absolute quantification of *B. rodhaini* parasites, about 100 µL of blood diluted in PBS (1:1) was collected from each mouse (n=4 per group). DNA was extracted using the QIAamp® DNA Blood Mini Kit (Qiagen, Hilden, Germany) following the manufacturer's protocol. A newly designed *B. rodhaini*-specific primer set (F: 5'- CCAGGTCATTGATAACGAAGC-3'; R: 5'-TAACACCACTCATAGCGGCA-3'), amplifying a 113 bp-long β-tubulin gene sequence, was used to quantify B. rodhaini in the DNA samples collected at day 4 post-challenge infection (pci). The reaction involved 5 µL of 2 × PowerUp™ SYBR™ Green Master Mix (Applied Biosystems, Massachusetts, USA), 0.6 µM primers, 1 uL DNA, and distilled water up to a 10 µL volume. The cycling conditions were 50°C for 2 min, 95°C for 2 min, followed by 40 cycles of 95°C for 15 sec and 60°C for 1 min, and a dissociation stage. The reactions were run in the ABI 7900HT Real-time PCR System (Applied Biosystems). Serially diluted plasmids were used to establish standards, from which parasite count was calculated from the mean

quantification cycle values of duplicated samples. Parasite numbers were transformed to log values before performing statistical analysis.

Statistical analyses

Comparison among groups was performed using ordinary one-way analysis of variance (ANOVA) with Tukey's test for multiple comparisons in GraphPad Prism 8 (California, USA), reported as mean $\pm$ standard deviation (SD) of 4-6 mice and are designated as follows: $*p < 0.05$, $**p < 0.01$, and $***p < 0.001$. Survival curves were calculated by Kaplan-Meier non-parametric model.

1.3 Results

Survival of mice with acute *B. microti* infection against *B. rodhaini* lethal challenge

Infection with *B. rodhaini* is associated with high parasitemia and lethality in mice. The combination of different *Babesia* species resulted in different disease outcomes following infection. All mice infected with *B. rodhaini* alone (Br) and those challenged 2 days after *B. microti* primary infection (bm/br2) succumbed at day 8 pci, while complete survival was recorded from bm/br4 and bm/br6 groups (Figure 1.1B). These results demonstrate that cross-species protection against *B. rodhaini* arising from a prior *B. microti* infection can be observed in challenge infected mice as early as day 4 post primary infection.

Parasitemia levels and hematologic indices during acute stage of *Babesia* co-infection

The signs of *B. rodhaini* infection in mice, such as severe intravascular hemolysis associated with significantly increased parasitemia levels (Chiou et al., 2014), were observed in the present study. Parasitemia levels were continually monitored throughout the infection trial by examining Giemsa-stained blood smears for each mouse. At the start of challenge infection (day 0), the *B. microti* parasitemia for bm/br2, bm/br4, and bm/br6 groups were 0.087%, 0.86%, and 1.03%, respectively (Figure 1.3). A consistent escalation in parasite burden was observed in all infected groups during the initial week of *B. rodhaini* infection, reaching its peak before gradually declining. The peak parasitemia levels in Br, bm/br2, and bm/br4 mice were 54.36%, 53.98%, and 47.72%, respectively, recorded at day 6 post-challenge infection (pci). Conversely, the bm/br6 group exhibited a lower peak parasitemia level (37.19%),

observed two days earlier than Br, bm/br2, and bm/br4 groups, but still significantly lower (Figure 1.1C). In the survival groups bm/br4 and bm/br6, the bm/br4 group displayed the lowest average body weight (20.48 ± 1.68 g) at day 8 pci, while the bm/br6 group exhibited an increased average body weight (23.79 ± 1.23 g) (Figure 1.1D). All groups experienced anemia, evident in their below-normal hematocrit values and reduced RBC densities after *B. rodhaini* challenge infection (Figures 1.1E and 1.1F), with the bm/br4 group showing the most severe anemia at day 6 pci. Intriguingly, peak parasitemia at day 6 pci coincided with the recorded lowest hematocrit values in bm/br2, bm/br4, and Br groups, with only the bm/br4 mice surviving two days after (day 8 pci). Normal hematocrit and RBC values were restored and maintained until day 28 pci in survival groups bm/br4 and bm/br6. Our results clearly demonstrated that an increase in parasitemia facilitated RBC lysis, resulting in decreased hematocrit values and ultimately leading to hemolytic anemia, a characteristic feature of babesiosis.

During the peak parasitemia period, parasites exhibited a ring-like morphology within erythrocytes (Figure 1.4A), with multiple parasites observed within a single erythrocyte (Figure 1.4B). Conversely, a significant proportion of intraerythrocytic parasites appeared to be in a degenerated state (Figure 1.4B). Historically termed as "crisis forms," this phenotype becomes pronounced during intraerythrocytic parasitic death (Skariah et al., 2017). At day 4 pci, significantly fewer *B. rodhaini* organisms were detected in co-infected bm/br4 (30.82% parasitemia) and bm/br6 (37.19% parasitemia) groups compared to Br (9.21% parasitemia), indicating that the majority of infected RBCs were parasitized by *B. microti* (Figure 1.4C). Immunofluorescence assay (IFA) micrographs supported these findings, highlighting *B. microti* (stained in green) as the predominant species in co-infected groups (Figure 1.5A). Additionally, it was observed that the majority of the uninfected RBC population consisted of Hoechst-stained reticulocytes (Figure 1.5).

Effects of *B. microti* and *B. rodhaini* infection on splenic immune cell population at the acute phase of co-infection

Spleen, the largest secondary lymphoid organ in the body, plays a crucial role in hematopoietic functions and orchestrates immunological responses against blood-borne pathogens, making it an essential component in coordinating the immune system's actions (Cesta, 2006).

Additionally, the spleen is involved in filtering and clearing parasitized erythrocytes, particularly in cases of babesiosis (White et al., 1998). Ultimately, the host's fate depends on the integrity of the spleen (Roberts et al., 1972). To assess the impact of co-infection on the splenocyte population responsible for immune responses and pathogenesis during the acute phase of infection, FACS analysis was conducted at day 6 post-challenge infection (pci), considering this as the peak parasitemia for both the Br and bm/br4 groups. Examination of splenic immune cells revealed fluctuations in the numbers of B cells, T cells, macrophages, natural killer cells, and dendritic cells (DC) (Table 1.2). Regardless of the infection type and species, *Babesia* infection was significantly associated with a notable reduction in T cells (Figure 1.6A) and B cells (Figure 1.6B), along with a significant increase in NK cells (Figure 1.6C) and DCs (Figure 1.6D). Particularly, macrophages in co-infected spleens exhibited significantly higher populations compared to those with a single infection of *B. rodhaini* and spleens from naïve mice (Figure 1.6E). In summary, there was a decrease in adaptive immune cell populations (T and B cells) and an increase in innate immune cell populations (NK cells, DCs, and macrophages) in the spleens of infected mice (Figure 1.6F).

Downregulation of pro-inflammatory cytokines and upregulation of anti-inflammatory cytokines during acute phase of *Babesia* co-infection

Cytokines play a pivotal role in orchestrating symptoms and pathological manifestations during infections, with IL-10 and IFN-γ being key moderators in this process (Medina et al., 2011). This study aimed to explore the interplay between various cytokines, particularly IL-10 and IFN-γ levels, and to observe the involvement of the pro-inflammatory and regulatory balance during the natural immune response in mice infected with *Babesia*. Serum cytokines (IFN-γ, IL-10, IL-12p70, IL-6, IL-2, TNF-α, and ROS) were assessed in mice acutely infected with *B. microti* and subsequently challenged with *B. rodhaini* to identify changes in the immune response at days 2, 4, and 6 post-challenge infection (pci). By day 6 pci, the IL-10 serum levels in the Br group were comparable to those in the bm/br4 group (Figure 1.7A), while both groups exhibited significantly higher levels of IFN-γ (Figure 1.7B) compared to other groups. Although not significantly different, a relatively higher level of IL-12 p70 was observed in the bm/br6 group at day 6 pci compared to other groups (Figure 1.7C). The highest concentrations of IL-6 (Figure 1.7D), IL-2 (Figure 1.7E), and ROS (Figure 1.7G) were noted in mice with *B. rodhaini*-only infection, and a lack of strong TNF-α levels in the serum was also observed

(Figure 1.7F). Overall, the findings indicated an upregulation of cytokines IL-10, IFN-γ, and IL-6, and a downregulation of IL-12p70, IL-2, and TNF-α during acute stage *Babesia* co-infection in mice.

Immunomodulation of humoral response during acute phase *Babesia* co-infection

Next, we wanted to confirm if the depletion of B and T cells (as confirmed Figure 1.6A and 1.6B) had any effects on the species-specific antibody response; thus, antibodies against *B. rodhaini* (Figure 1.8) and *B. microti* (Figure 1.9) were detected at day 2, 4, and 6 pci. Pronounced IgM- and IgG-specific antibody responses to *B. rodhaini* challenge in mice were most pronounced at day 6 pci (Figure 1.8). IgM reacting to *B. rodhaini* antigen was detected 2 days after infection, indicating primary immune response (Figure 1.8A), suggesting that during the early phase of acute *Babesia* infection, immune responses to parasitized erythrocytes were triggered (Chiou et al., 2014). In addition, substantial levels of IgG, IgG1, IgG3, IgG2a, IgG2b, and IgG2c were detected at day 6 pci (Figure 1.8B-1.8G), confirming the activation of secondary immune response against erythrocytes.

Changes in splenic immune structure during acute stage of *Babesia* co-infection

In HE sections, macrophages were detected as light-stained cells by hematoxylin (blue), and the numbers increased in all groups compared with naïve mouse spleen. Hence, the increase in macrophages in all groups, as revealed in Figure 1.6E, was also confirmed in histopathology, and it was mostly found confined to the marginal zone. However, NK cells cannot be detected in our HE sections. We observed splenic disarray relative to the disorganized germinal center. In infected groups, disruption of the marginal zone starts during the acute phase (Djokic et al., 2018a). Erosion of the marginal zone is more pronounced during *B. rodhaini* only infection (Figure 1.10B), while less obvious during co-infection (Figure 1.10C-1.10D), The most significant abnormality of the marginal zone was in the *B. rodhaini* group, represented by the loss of cellularity of marginal zone (Figure 1.10B). It was characterized by increasing macrophage-like cells and decreased cell density, along with the wider marginal zone as observed in the *B. rodhaini* group than other groups (Figure 1.10A-1.10D).

1.4 Discussion

So far, the immune mechanisms responsible for protection against *Babesia* remain inadequately characterized (Aguilar-Delfin et al., 2003). In the presence of a co-infecting agent, the immune response to one organism can either synergistically or antagonistically induce downstream effects related to the infection process (Homer et al., 2000). Using a murine co-infection model (Li et al., 2012), the immune response during the acute phase of *Babesia* infection was dissected. This study aimed to investigate the influence of *B. microti* acute co-infection on *B. rodhaini* concerning the development of parasitemia, immune response, disease manifestations, hematology, the role of splenic immune effector cells, and cytokine kinetics.

Initially, the goal was to validate the previously established protection observed during *Babesia* co-infection and delve into specific clinical and hematologic characteristics. The results illustrated that primary *B. microti* infection attenuated the parasitemia peak and slightly exacerbated anemia in *B. rodhaini*-challenged mice. In contrast, *B. rodhaini*-infected mice without prior primary infection exhibited a rapid increase in parasitemia and exacerbated anemia (Wang et al., 2016). Thus, current findings affirm that the previously demonstrated cross-protection observed during chronic *B. microti*-*B. rodhaini* co-infection (Li et al., 2012) also occurs and initiates at a specific time point during the acute stage co-infection. Inside the host, *B. microti* infection progresses through three phases: establishment, progression, and resolution (Knapp & Rice, 2015). After the establishment of infection, *Babesia* damages the host's red blood cells (Dvoráková & Dvorácková, 2007). During the progression phase, erythrocyte damage is induced by the parasite's egress (Sevilla et al., 2018), followed by the lysis of the host cell, eventually leading to anemia and reticulocytosis (Homer et al., 2000; Kjemtrup & Conrad, 2000), both observed in the infected mice in this study. The density of erythrocytes decreases as a consequence of the egress (Sevilla et al., 2018). It is hypothesized that the rupture of the plasmatic membrane of erythrocytes is potentially accompanied by the release of hemoglobin during the egress process. This may elucidate the observed hemolysis and hemoglobinuria in babesiosis (Zintl et al., 2003; Gray et al., 2010; Hildebrandt et al., 2013; Narurkar et al., 2017).

Previous investigations into malaria have established that parasites exhibit a tropism for mature erythrocytes. Similarly, *Babesia microti* also demonstrates a distinct tropism for mature erythrocytes (Borggraefe et al., 2006), as evident in the present immunofluorescence assay

(IFA) results where the infection of reticulocytes by *B. microti* and *B. rodhaini* parasites was rarely observed. The reduction in the population of mature erythrocytes during parasite infection leads to a decrease in parasitemia (Okada et al., 2015), potentially contributing to the decline in parasitemia levels immediately after reaching its peak in *Babesia* co-infected mice. This preference for mature erythrocytes may stem from the likelihood that parasite-infected reticulocytes are more susceptible to elimination than those infecting mature erythrocytes (Skariah et al., 2017). Likewise, our results revealed the presence of dead *B. microti* remains (crisis forms) inside erythrocytes (Clark et al., 1975). Crisis forms of parasites are characterized by punctuated and degenerating parasites induced by crisis form factor (CFF) and immune response (Sow et al., 2015). The existence of crisis forms of *Babesia*, coupled with the occurrence of reticulocytosis and a reduced population of mature peripheral erythrocytes, may constitute a potential mechanism for controlling *Babesia* infection.

In this investigation, mice infected with *B. rodhaini* exhibited notably elevated levels of autoreactive IgGs at day 6 post-challenge infection (pci), aligning with the onset of severe hemolytic anemia. During the establishment phase, antibodies are known to contribute to preventing erythrocyte infection either by binding to free sporozoites (Homer et al., 2000; Leitner et al., 2020) or by promoting the phagocytosis of merozoites during the resolution phase, aiding in the clearance of infected RBCs through a mechanism known as antibody cell-dependent inhibition (ADCI) (Marsh and Kinyanjui, 2006). The development of severe anemia, stemming from extravascular hemolysis and increased erythrocyte accumulation in the spleen, might be partially attributed to the presence of anti-erythrocyte autoantibodies. However, the direct impact of these autoantibodies on the pathogenesis of babesiosis remains unclear (Chiou et al., 2014). Additionally, this study's results revealed a decrease in antibody production during the acute co-infection phase, consistent with findings from a previous study (Li et al., 2012). Similarly, the subversion of the adaptive immune response against *B. microti*, observed in various co-infected *Babesia* models (Djokic et al., 2018b, 2019; Efstratiou et al., 2020), may have contributed to the specific immune response documented in this study. In contrast, a study by Yi et al. (2018) reported that despite disorganized splenic architecture during infection, *B. microti*-infected mice were capable of eliciting robust adaptive immune responses. It is hypothesized that cells of the innate immune system regulate the growth rate of the merozoites, thereby influencing the parasitemia rate (Homer et al., 2000). While antibodies play a role in blocking the invasion of merozoites, they do not significantly contribute to the

opsonophagocytosis of *Babesia*- or *Plasmodium*-infected erythrocytes (Djokic et al., 2021).

The spleen serves as the central hub for regulating detrimental immune responses (Bronte and Pittet, 2013). As a crucial organ responsible for clearing infected RBCs, malaria infections can lead to spleen rupture (Lacerda-Queiroz et al., 2017). Previous co-infected models involving *B. microti* and *B. rodhaini* did not provide insights into spleen histopathology and splenocyte composition during the acute stage of *Babesia* co-infection. Therefore, it was imperative to illuminate the status of the spleen under these conditions. In both human and murine malaria, disorganization of splenic architecture and splenomegaly are linked to innate immune activation, monocytic cell extension, and the elimination of infected RBCs (Weiss, 1989; Weiss et al., 1989; Villeval et al., 1990). Alterations in splenic structure, particularly within the germinal centers, can impact the quality of an antibody response during malaria infection, potentially influencing the development of immunity to malaria (Cadman et al., 2008). With *B. microti* initiating early-phase macrophage activation, it effectively curbs parasite replication (Terkawi et al., 2015). Subsequent studies have confirmed that *B. microti* imparts immunity against other *Babesia* species (Li et al., 2012) and *Plasmodium* (Efstratiou et al., 2020), primarily relying on macrophages.

The FACS analysis results corroborate this finding, demonstrating a substantial increase in the macrophage population among splenocytes, an observation supported by the histopathological examination of spleen sections from co-infected mice. Conversely, the decline in B and T cell populations observed in this study aligns with findings from other research (Djokic et al., 2018a; Djokic et al., 2019). These outcomes underscore the pivotal role of innate immunity during the acute phase of *Babesia* co-infection in mouse models. In the acute infection stage, there is robust activation of mononuclear cells, leading to apoptosis of monocytes, dendritic cells, B and T cells, ultimately resulting in thymus apoptosis and a decline in the output of naïve T cells (Rénia and Goh, 2016). Conversely, during reinfection, chronically activated T cells may induce a state of anergy and exhaustion, potentially impacting the T and B cell splenocyte population in co-infected mice in the present study.

Cytokines play a pivotal role in driving symptoms, pathological remodeling, and the outcomes of infections, relying on the reciprocal regulation of pro- and anti-inflammatory cytokines. Prior studies demonstrated reduced cytokine production during the acute stage of *B. microti*

infection in response to lethal *B. rodhaini* challenge (Li et al., 2012). The present findings emphasize the critical timing of *B. rodhaini* challenge during the acute *B. microti* infection stage, influencing the inflammatory cytokine response post-challenge, as evidenced by cytokine levels in the co-infected groups bm/br4 and bm/br6. Elevated cytokine levels may potentially facilitate parasite clearance during peak parasitemia (Bronte & Pittet, 2013; Djokic et al., 2018a). Therefore, the role of cytokines in the pathogenesis of babesiosis is a time-dependent phenomenon (Ahmed, 2002). Cytokines such as IFN-γ (Koch et al., 2005) and IL-10 (Kumar et al., 2019), with the capacity to act as mediators of immunity, exemplify double-edged sword cytokines. Cross-protected mice exhibited lower levels of IFN-γ and IL-10, in contrast to higher levels observed in *B. rodhaini* control mice (Li et al., 2012). During the blood-stage of malaria, IFN-γ plays a pathological role by contributing to anemia through the suppression of erythropoiesis (Okada et al., 2015). Early production of IFN-γ provides protection from experimental cerebral malaria, while the lack of early IFN-γ production leads to fatal infection (Stevenson & Riley, 2004; King & Lamb, 2015).

In both the Br and bm/br4 groups, peak parasitemia and severe anemia occurred at day 6 post-challenge. Concurrently, *B. rodhaini* infection caused extensive spleen damage in mice from both groups, leading to a significant reduction in cell population, especially in the marginal zone. This increase in pathology may result from elevated levels of circulating IFN-γ during infection. Despite comparable levels of IL-10 in the serum of the Br group and bm/br4 group at day 6 post-challenge, *B. rodhaini*-infected mice succumbed to the infection, while the bm/br4 group survived. IL-10 limits the overproduction of IFN-γ and TNF-α during *B. microti* infection (Djokic et al., 2018a). In this study, elevated IL-10 levels at day 6 post-challenge may have contributed to the relatively lower levels of IFN-γ and TNF-α in bm/br4 compared with the Br group, playing a central role in the survival of co-infected mice. Lethality in malaria is attributed to the early overproduction of IL-10 (Li et al., 2012). Regardless of its origin, IL-10 restrains the function of macrophages and dendritic cells, restricting Th1 and Th2 effector responses. Additionally, IL-10 inhibits the production of IL-12 by monocytes, which is essential for inducing a protective immune response against malaria and shifting towards a pro-inflammatory cytokine response (D'Andrea et al., 1992; Crutcher et al., 1995; Xu et al., 2001). However, the impact of IL-10 is contingent on both time and location and is influenced by the specific cell type producing it (Kumar et al., 2019). In the bm/br4 group, the reduced production of IFN-γ at day 6 post-challenge might have slightly diminished parasitemia, thereby averting

lethality. IFN-γ is acknowledged as a crucial cytokine that induces splenic cell death and leads to host lethality following *Plasmodium* infection (Lacerda-Queiroz et al., 2017). Despite both the Br and bm/br4 groups exhibiting proportional levels of IFN-γ, the bm/br4 group experienced less loss of splenic cells, potentially attributed to the cross-protection conferred by *B. microti*. FACS analysis revealed the lowest T cell population in the bm/br6 group (12.82%), explaining the reduced levels of IFN-γ at day 6 post-challenge, given that Th1 cells are major contributors to IFN-γ production.

Earlier studies proposed that macrophages and NK cells play a pivotal role in the response protecting against the pathogenic *Babesia* WA1, likely through early production of IL-12 and IFN-γ, and the induction of macrophage-derived effector molecules like nitric oxide (Aguilar-Delfin et al., 2003). IL-12 is essential in enhancing Th1-associated immunity (Trinchieri, 1993). The early production of IFN-γ by NK cells relies on IL-12 from dendritic cells (DCs). Moreover, the early induction of IFN-γ and IL-12 contributes to survival and protection against babesiosis (Li et al., 2012; Efstratiou et al., 2020). Th1-associated immunity is crucial for controlling the blood-stage replication of *Babesia* and *Plasmodium* parasites (Li et al., 2012; Djokic et al., 2018a). Thus, IL-12 serves as a potent mediator of host-defense mechanisms in various experimental malaria models (Luty et al., 2000; Malaguarnera et al., 2002). The results align with prior findings, wherein IL-12 levels were lowest in control *B. rodhaini* mice and highest in bm/br6 mice, underscoring its role in providing immunity against fatality.

Activation of immune cells relies on intracellular ROS as a messenger in the signaling pathway. Ty et al. (2019) elucidated a mechanism in which oxidative stress triggers macrophage activation, leading to the release of inflammatory cytokines. Conversely, Li et al. (2012) and Johnson et al. (1996) proposed that macrophages can eliminate parasites through the production of reactive oxygen and nitrogen intermediates. The quantity and site of production determine whether these intermediates exert a favorable or detrimental influence on malaria. Reactive oxygen and nitrogen intermediates are implicated in the generation of crisis forms in *Plasmodium* and *Babesia*. A study demonstrated that the inoculation of NO resulted in erythrocyte lysis rather than killing *P. berghei*, suggesting that *Plasmodium* parasites may be shielded from ROS by hemoglobin released during hemolysis, yet the parasite likely possesses intrinsic defense mechanisms against ROS (Sobolewski et al., 2005). Macrophages generate substantial amounts of ROS and RNS, inducing oxidative stress (Percário et al., 2012).

However, there remains uncertainty regarding the role of oxidative stress in malaria, with some authors suggesting protective effects, while others argue for its contribution to the pathophysiology of malaria. Reactive oxygen and nitrogen species (ROS and RNS), along with oxidative stress, are implicated in the systemic complications of malaria. *Plasmodium* parasites, residing in host cells, are susceptible to increased levels of oxidative stress. To defend against this stress, parasites have evolved antioxidant defense mechanisms (Percário et al., 2012). Malaria induces a "cytokine storm" characterized by elevated cytokine levels in the bloodstream (Clark, 2007; Clark et al., 2008). The mechanism by which ROS triggers inflammation during malaria involves xanthine oxide-produced ROS leading to increased IL-1β levels, while the parasite activates caspase-1, thereby activating the NLRP3 inflammasome (Ty et al., 2019). Consequently, a new role for extracellular ROS has been proposed, inducing inflammatory cytokines and collaborating with infectious parasites to activate the inflammasome in macrophages. Inhibiting this pathway by impeding ROS could present new possibilities for designing anti-disease remedies where pathology is driven by oxidative stress-induced inflammation (Ty et al., 2019). As indicated by these findings, the highest levels of ROS in *B. rodhaini*-infected mice might have adversely affected the host, leading to erythrocyte lysis, contributing to the pathology of *B. rodhaini*.

There are certain limitations in this study. Immunohistochemistry analysis of the spleen and immunophenotyping of immune cells in blood, which could have substantiated the splenic cell population results, were not conducted in this research. Additionally, the involvement of ROS in erythrocyte lysis needs confirmation. Considering the potential adverse effects of ROS on the kidneys, it is essential to investigate how this organ is affected during babesiosis. Addressing these gaps in future studies would provide a more accurate and comprehensive understanding of the immune mechanisms involved during co-infection, aiding in the development of effective vaccines in the future.

1.5 Summary

The undertaken study illustrated that, at specific time points in the acute stage of co-infection, the initiation of the innate immune response by *B. microti* diminished *B. rodhaini* parasitemia, ultimately ensuring the survival of co-infected mice. The results unveiled that *B. microti* negatively influenced the adaptive immune response by reducing populations of splenic B and

T cells, a phenomenon reflected in the compromised humoral immunity against both parasites. Consequently, a prevalence of Th1 immune response was observed, with IL-10 and IFN-γ emerging as pivotal contributors to the pathology associated with *B. rodhaini*.

Table 1.1. Antibody panel used for sorting antibody-tagged splenocytes.

Immune cell population	Anti-mouse antibody markers	Fluorophore	Antibody dilution (vol/vol µL)	Manufacturer (catalog no.)
Total leukocytes	CD45	FITC	0.5/200	BioLegend (147709)
T lymphocytes	CD3	PE/Cyanine7	1/200	BioLegend (100219)
B lymphocytes	CD19	Brilliant Violet 421™	1/200	BioLegend (115537)
Macrophages	F4/80	PE	1/200	BioLegend (123109)
Natural killer cells	CD49b	PerCP-Cy5.5	1/200	BioLegend (108915)
Dendritic cells	CD11c	Brilliant Violet 510 ™	1/200	BioLegend (117337)

1   **Table 1.2.** Estimated total count and percentage of immune cell populations.

Group	Immune cell marker	Total count[*]	Percentage	Group	Immune cell marker	Total count[*]	Percentage
Br	CD45	15,176		bm/br4	CD45	38,385	
	F4/80	1,604	10.57		F4/80	5,009	13.05
	CD11c	2,000	13.19		CD11c	6,360	16.57
	CD19	2,929	19.30		CD19	4,291	11.18
	CD3	4,184	27.57		CD3	8,625	22.47
	CD49b	1,199	7.91		CD49b	4,265	11.11
Bm	CD45	14,682		bm/br6	CD45	15,868	
	F4/80	2,525	17.20		F4/80	2,456	15.48
	CD11c	1,220	8.31		CD11c	1,903	11.99
	CD19	4,174	28.43		CD19	3,083	19.43
	CD3	4,352	29.64		CD3	2,034	12.82
	CD49b	1,321	9.00		CD49b	1,254	8.79
Naive	CD45	35,605					
	F4/80	2,642	7.42				
	CD11c	367	1.03				
	CD19	13,252	37.22				
	CD3	17,201	48.31				
	CD49b	1,264	3.55				

2   [*]Estimated numbers obtained from the mean percentage of immune cell populations.
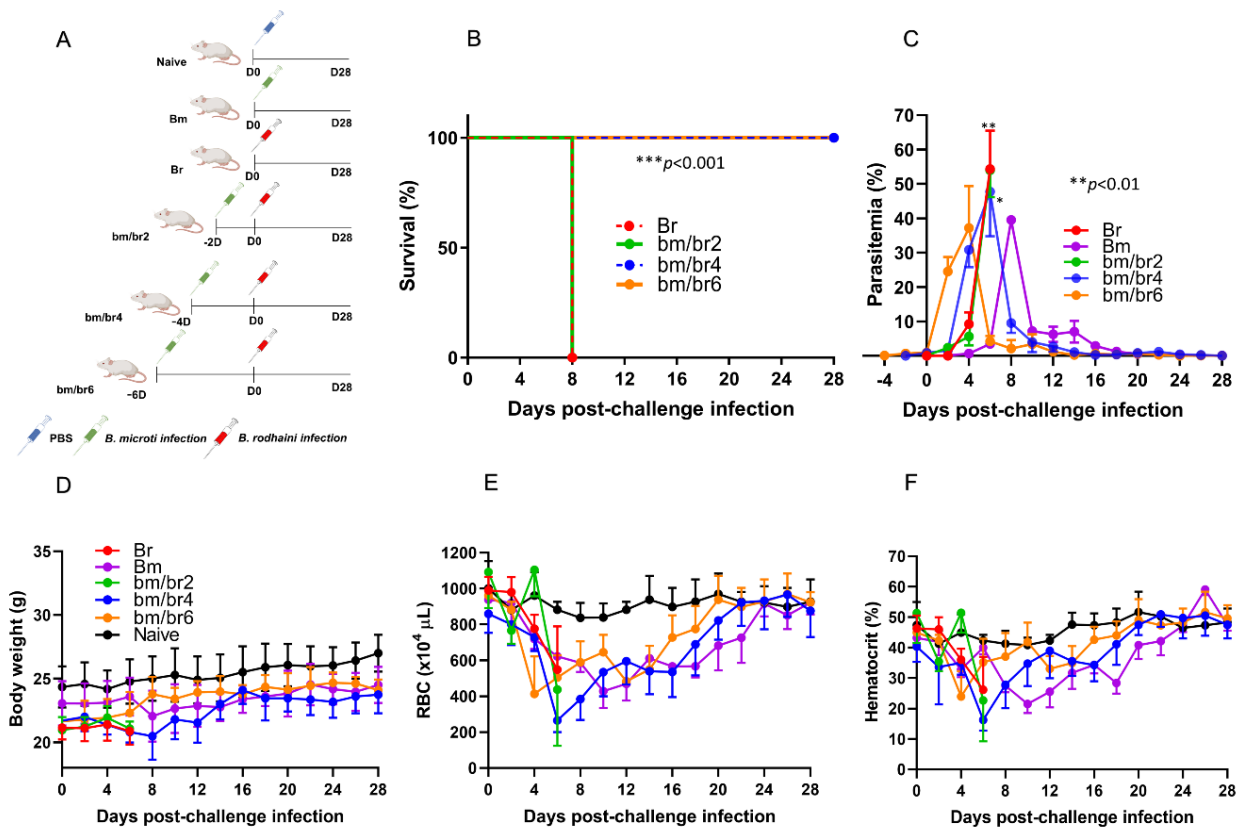
Figure 1.1. The course of *B. rodhaini* challenge infection in BALB/c mice undergoing acute *B. microti* infection. Test BALB/c mice were initially infected with *B. microti* and then challenge infected with *B. rodhaini* at different time points (on days 2, 4, 6) post-primary infection. **(A)** Overall experimental plan. **(B)** Survival curve, **(C)** course of parasitemia, **(D)** body weight, **(E)** red blood cell (RBC) count, and **(F)** hematocrit values were monitored for 28 days after challenge infection. Mean percent parasitemia, body weight, RBC, and hematocrit values were calculated from individual values taken from all surviving mice at each specific time point. Results are expressed as the mean values ± standard deviation (SD) of six mice (n=6). Ordinary one-way analysis of variance (ANOVA) with Tukey's test was used for the comparison of parasitemia between Br and co-infected groups, while the Kaplan-Meier non-parametric model was used for the survival analysis. Asterisks indicate statistical significance (*$P < 0.05$; **$P < 0.01$; ***$P < 0.001$).
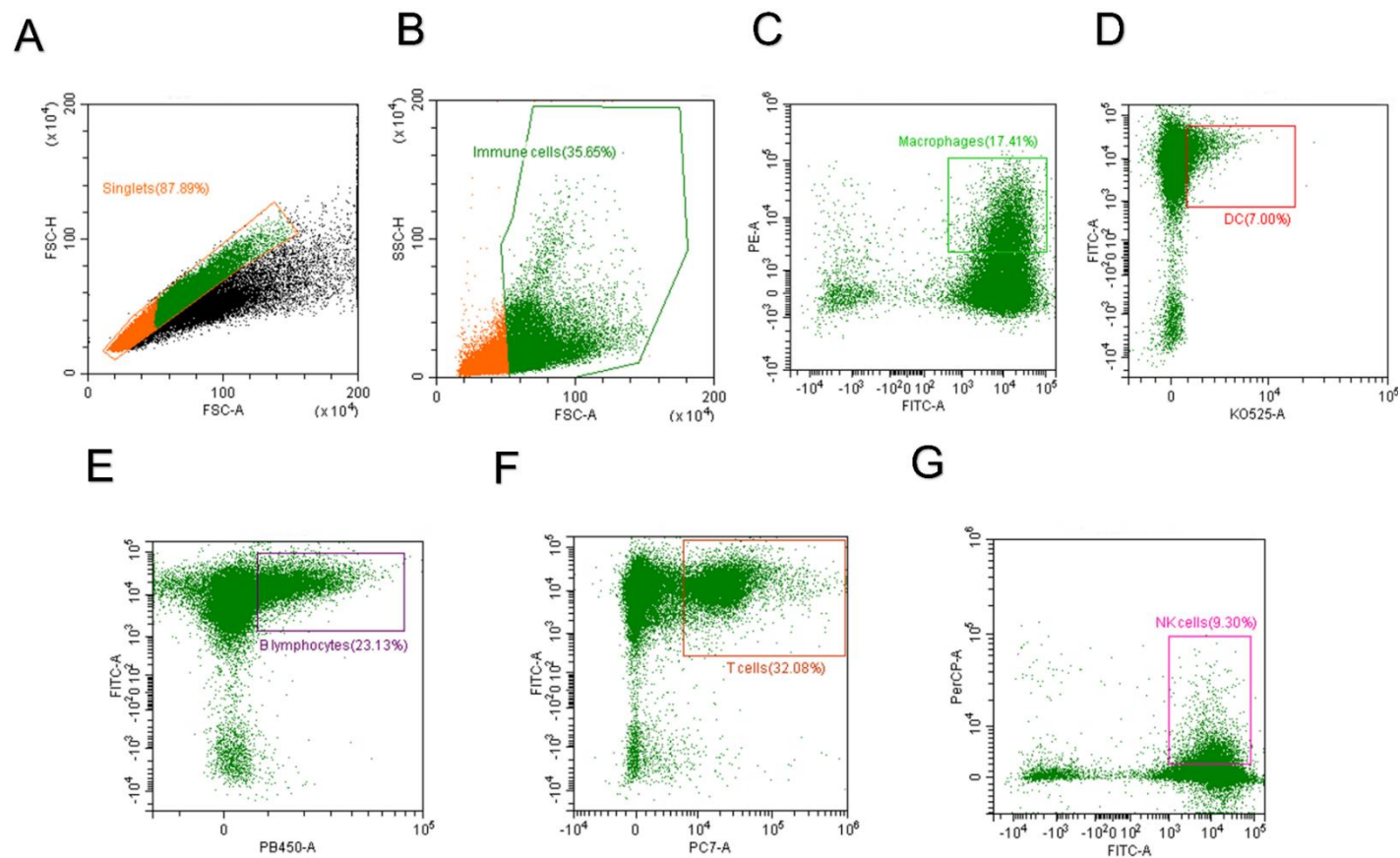
Figure 1.2. Gating scheme for fluorescence-activated sorting (FACS) analysis of immune cells. A total of 50,000 events were analyzed. Each panel is a representative image of gating for (A) singlets, (B) CD45+ (immune cells), (C) CD45+ F4/80+ (macrophages), (D) CD45+ CD11c+ (dendritic cells), (E) CD45+ CD19+ (B lymphocytes), (F) CD45+ CD3+ (T cells), and (G) CD45+ CD49b+ (natural killer cells).
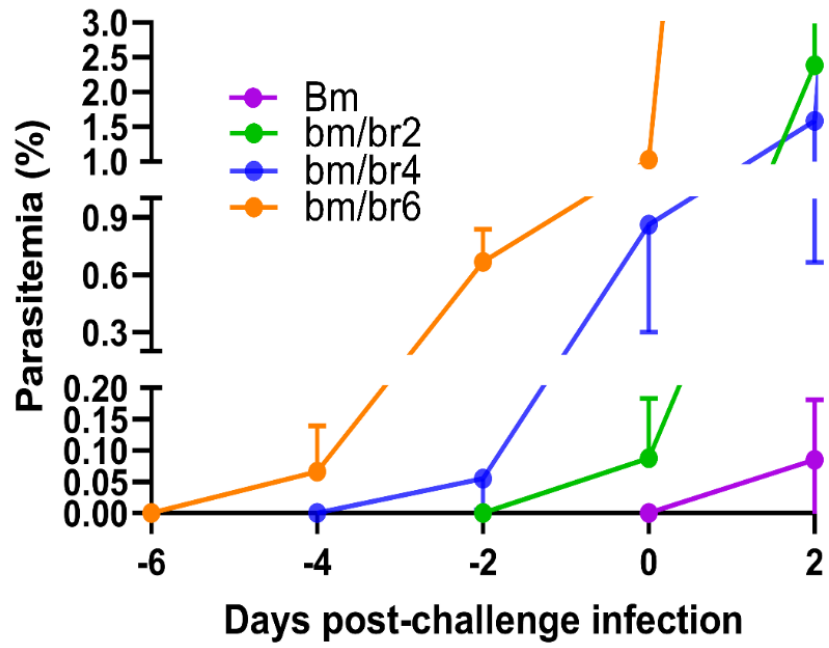
Figure 1.3. *Babesia microti* parasitemia levels in co-infected (bm/br2, bm/br4, and bm/br6) groups prior to challenge infection with *B. rodhaini* and parasitemia of Bm group
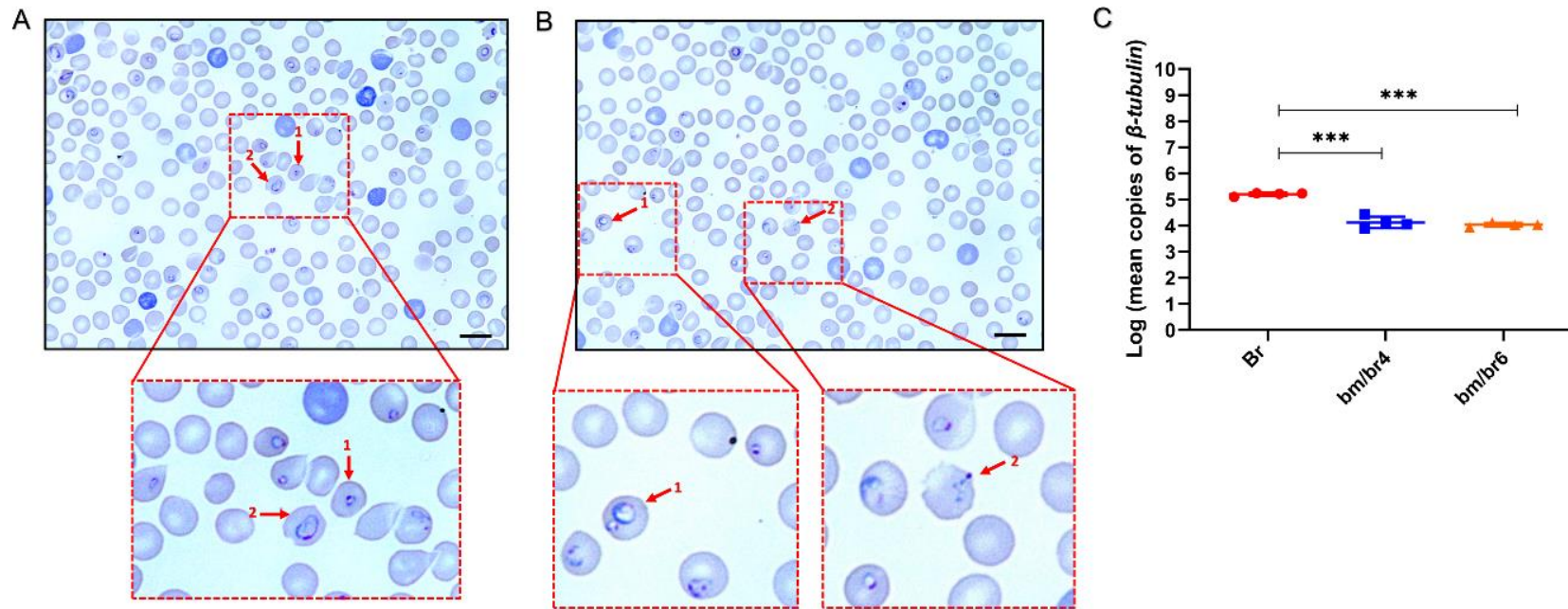
Figure 1.4. Giemsa-stained thin blood smear showing **(A)** 1, *B. microti*; 2, *B. rodhaini* infecting mouse erythrocytes and **(B)** 1, *B. microti* and *B. rodhaini* infecting the same erythrocyte; 2, crisis form of *Babesia*. Bars represent 10 μm. **(C)** Mean copy numbers of *B. rodhaini β-tubulin* in mouse DNA samples (n=4 per group at day 4 post-challenge infection) were transformed to log values. Individual values are the mean of duplicate samples. Log values were analyzed using one-way ANOVA and Tukey's multiple comparison post-hoc test; ***$P<0.001$.
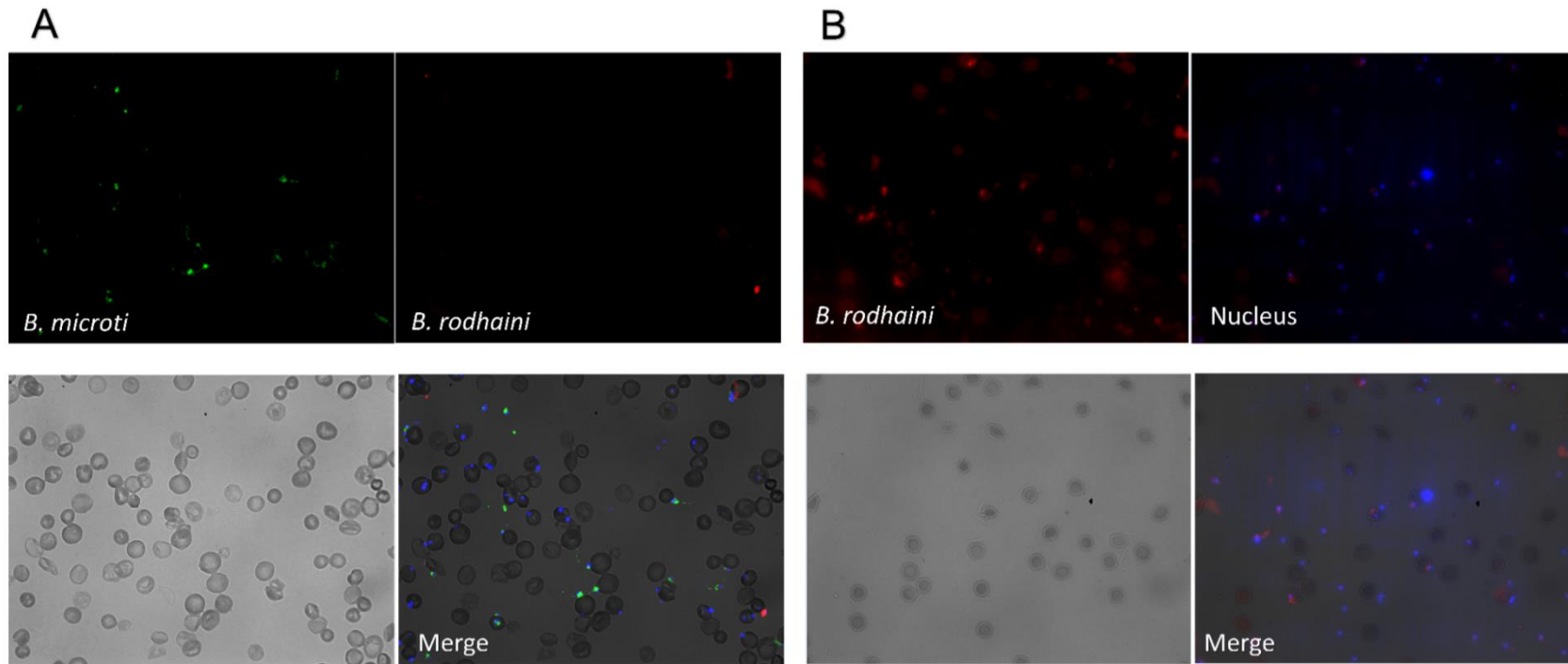
Figure 1.5. Immunofluorescence microscopy images of blood smears from **(A)** co-infected mouse challenged at day 4 post-primary *B. microti* infection and **(B)** mouse with *B. rodhaini* infection only. Alexa Fluor® 594-conjugated goat anti-rabbit IgG (green) and Alexa Fluor® 488-conjugated anti-mouse IgG (red) were used as parasite markers.
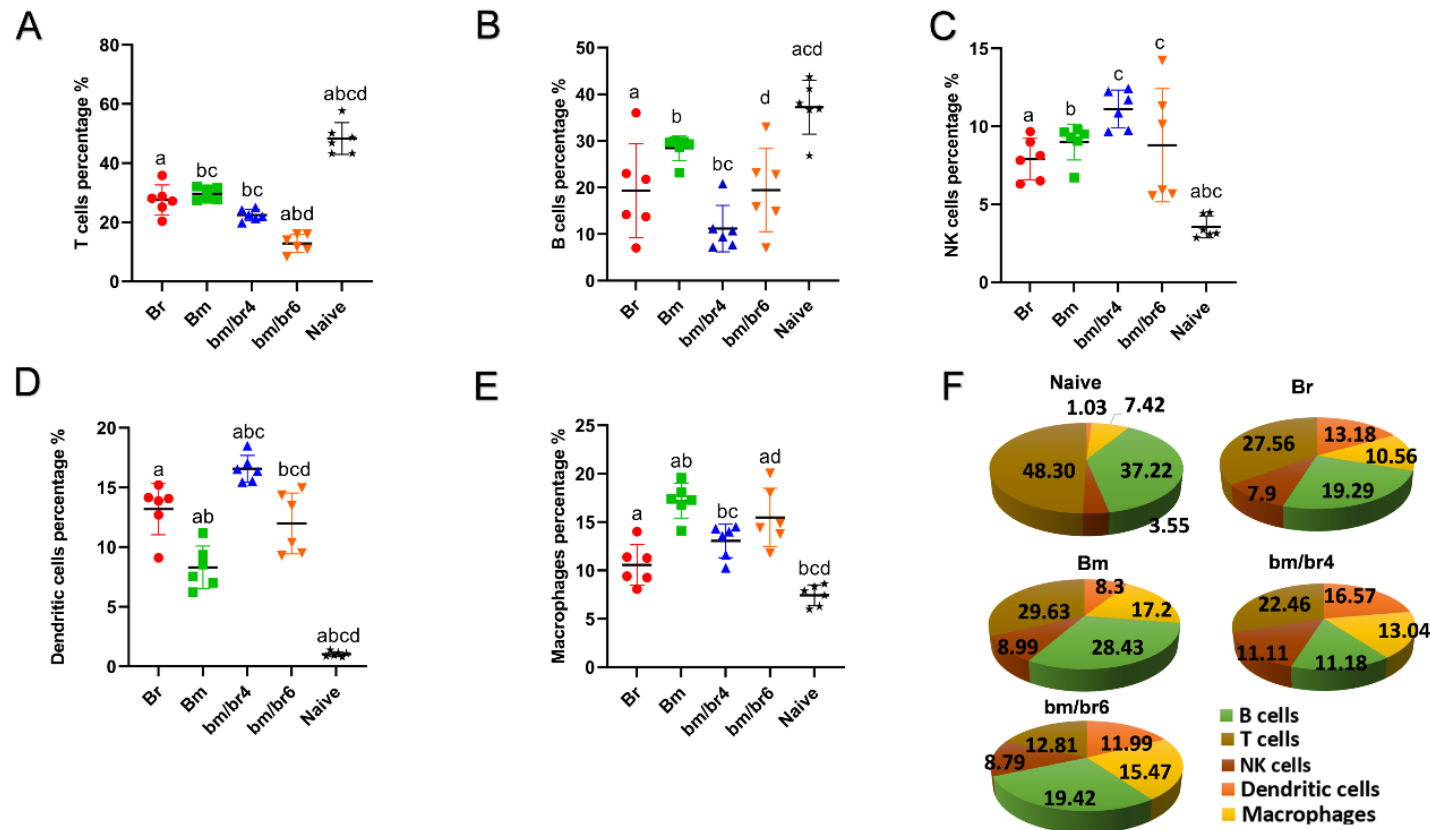
Figure 1.6. Fluorescence-activated sorting (FACS) analysis of splenic immune cells of mice at day 6 post-challenge infection. Percentage population of each cell type is presented as mean ± SD: **(A)** CD45$^+$CD3$^+$ cells (T cells), **(B)** CD45$^+$CD19$^+$ cells (B cells), **(C)** CD45$^+$CD49b$^+$ cells (natural killer cells), **(D)** CD45$^+$CD11c$^+$ cells (dendritic cells), and **(E)** CD45$^+$F4/80$^+$ cells (macrophages). **(F)** Pie chart representing the population composition of T cells, B lymphocytes, NK cells, dendritic cells, and macrophages in Naive, Br, Bm, bm/br4, and bm/br6 groups. Different letters denote significant differences between groups.
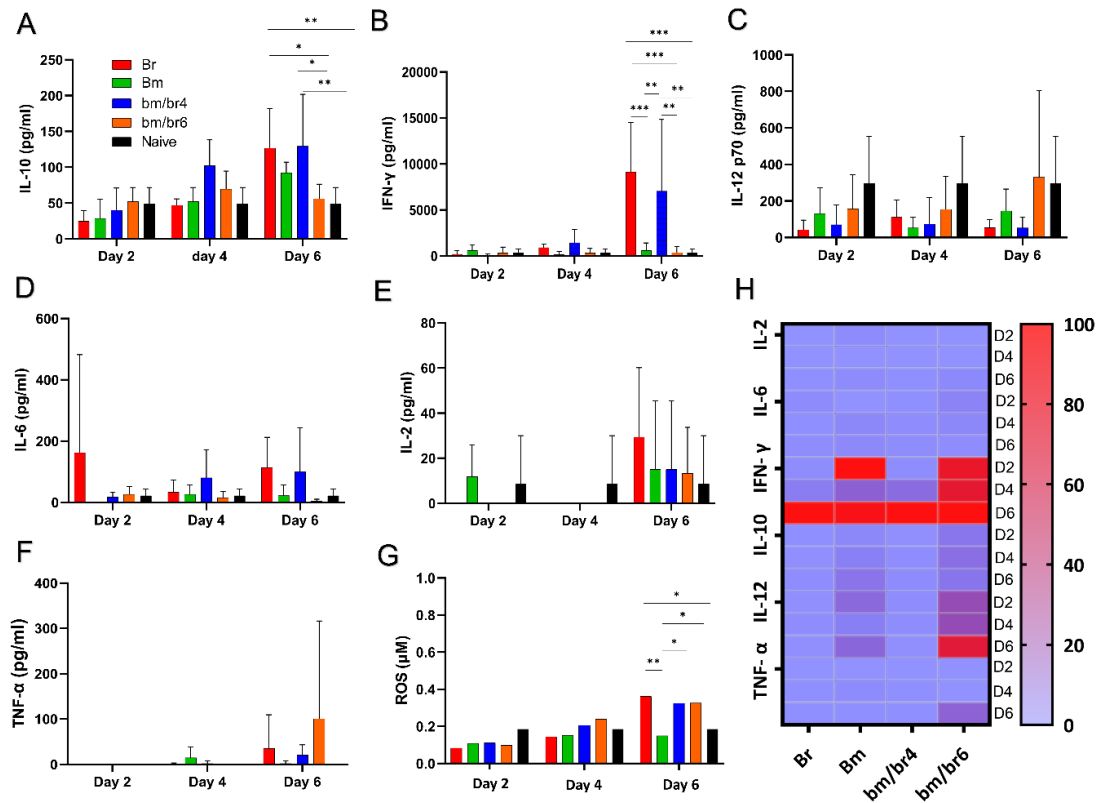
27

Figure 1.7. The kinetics of serum cytokines of protected and susceptible mice after *B. rodhaini* challenge infection. Test mice were initially infected with *B. microti* and challenge infected with *B. rodhaini* on days 4 and 6. On day 6 post-challenge infection, serum was collected from all groups and levels of (**A**) IL-10, (**B**) IFN-γ, (**C**) IL-12p70, (**D**) IL-6, (**E**) IL-2, and (**F**) TNF-α were measured. (**G**) ROS levels were determined by measuring serum levels of H_2O_2. (**H**) Heatmap showing the progression of secretion of the six cytokines at timepoints day 2 (reference), 4, 6 pci. The results are expressed as means ± SD. Ordinary one-way analysis of variance (ANOVA) with Tukey's test was used for the statistical analysis. Asterisks indicate statistical significance (*$P< 0.05$; **$P< 0.01$; ***$P< 0.001$).
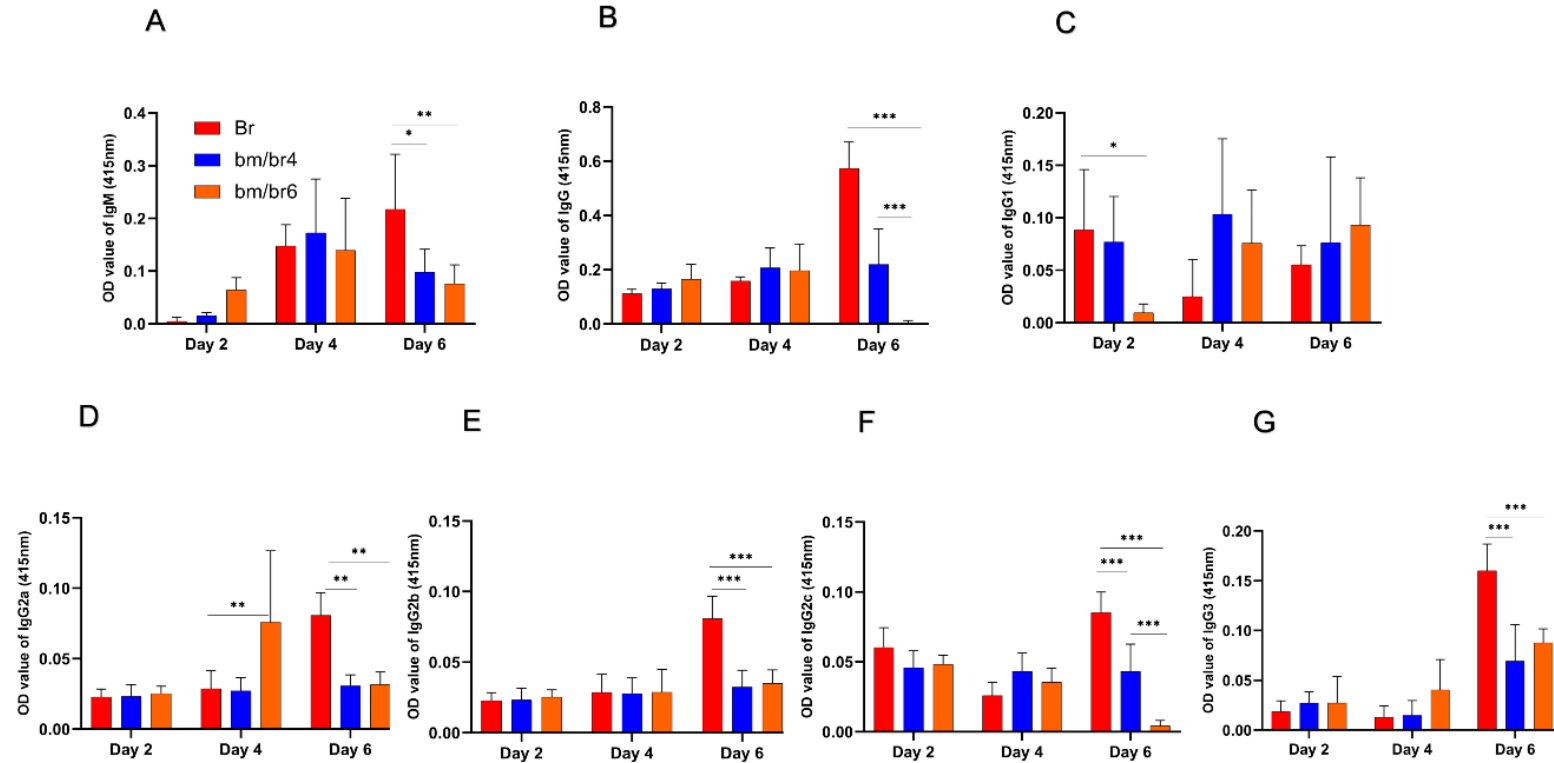
Figure 1.8. Kinetics of serum antibodies specific to *B. rodhaini* after challenge infection. The production of **(A)** IgM, **(B)** IgG, **(C)** IgG1, **(D)** IgG2a, **(E)** IgG2b, **(F)** IgG2c, and **(G)** IgG3 in mice after challenge infection with *B. rodhaini* was determined in Br mice and *B. rodhaini* and *B. microti* co-infected groups (bm/br4 and bm/br6 mice). Detection of IgGs and IgM was performed on days 2, 4, and 6. For the detection of serum antibodies against *B. rodhaini*, rBrP26 protein was used as the detection antigen in ELISA assays. The results are expressed as mean values ± the SD for six mice. Ordinary one-way analysis of variance (ANOVA) with Tukey's test was used for the statistical analysis. Asterisks indicate statistical significance (*$P< 0.05$; **$P< 0.01$; ***$P< 0.001$).
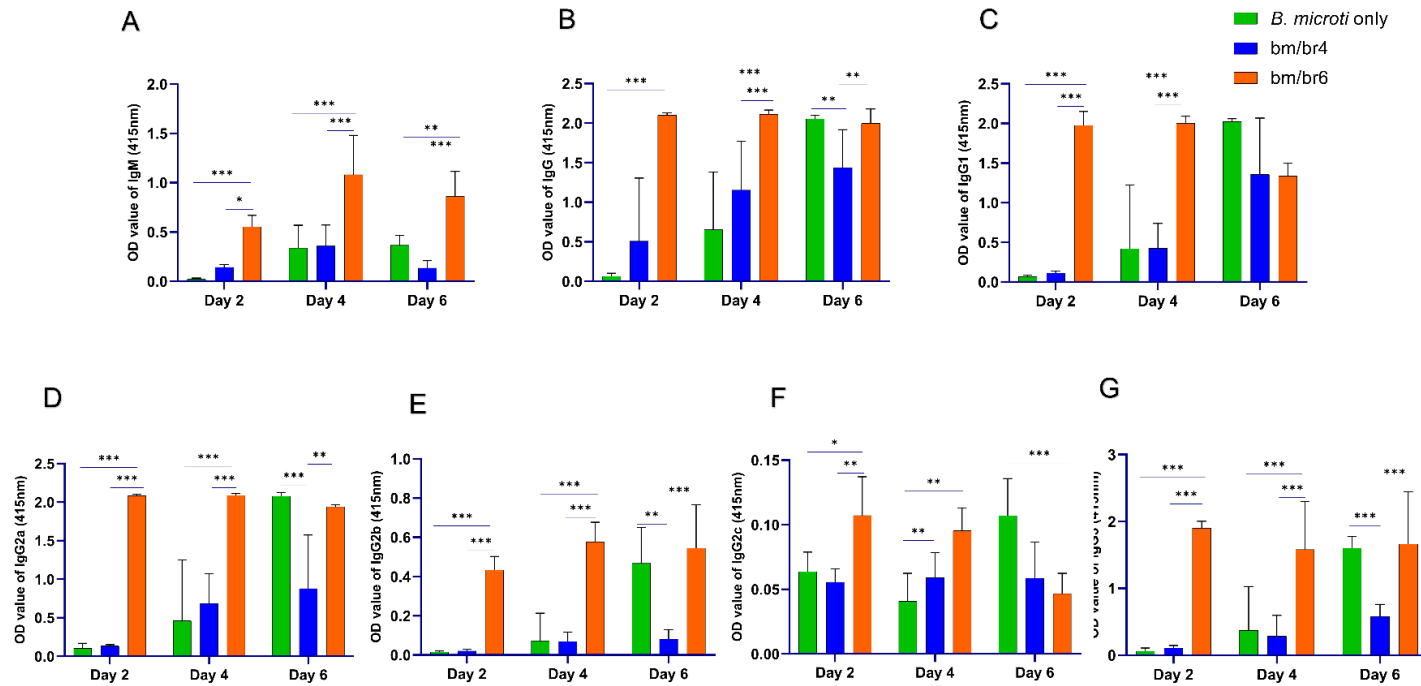
Figure 1.9. Kinetics of serum antibodies specific to *B. microti* after *B. rodhaini* challenge infection. The production of **(A)** IgM, **(B)** IgG, **(C)** IgG1, **(D)** IgG2a, **(E)** IgG2b, **(F)** IgG2c, and **(G)** IgG3 in mice after challenge infection with *B. rodhaini* was determined. Control mice (*B. microti* only infection) and *B. rodhaini* and *B. microti* co-infected groups (bm/br4 and bm/br6 mice). Detection of IgGs and IgM was performed in mice at days 2, 4 and 6 in all groups. For detection of serum antibodies against *B. microti* rBmP32 protein was used as detection antigen in ELISA assays. The results are expressed as mean values ± the SD for six mice. Asterisks indicate statistical significance (*$P< 0.05$; **$P< 0.01$; ***$P< 0.001$).
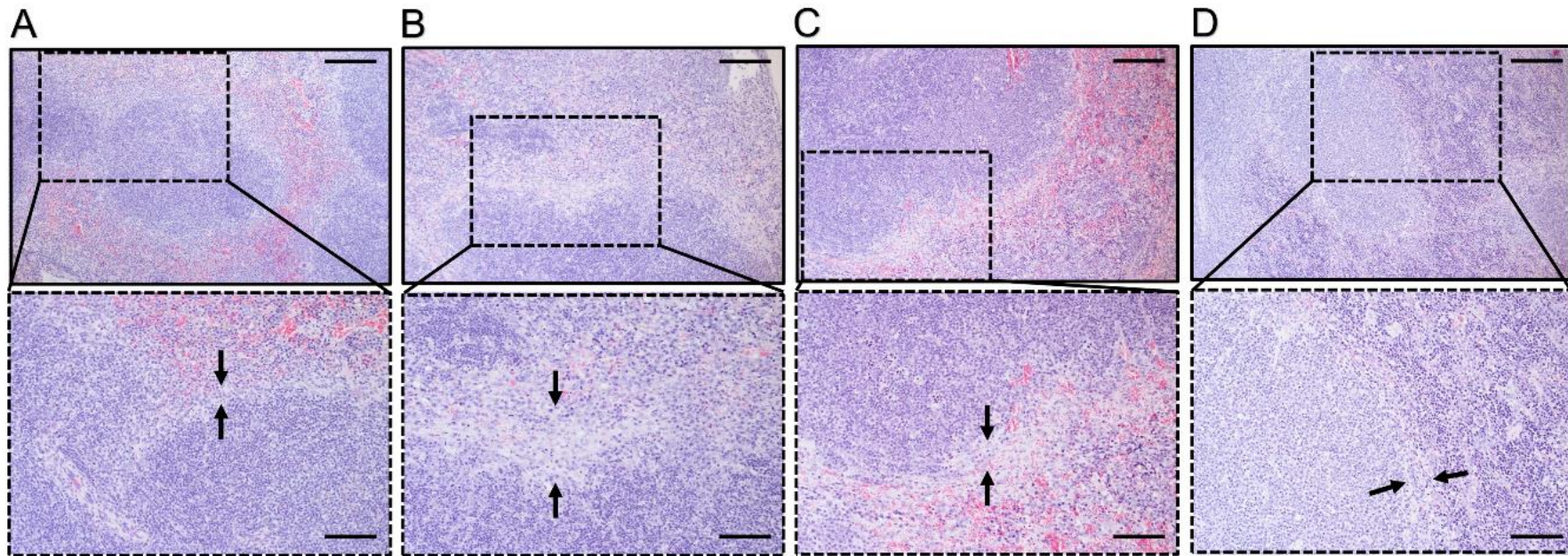
Figure 1.10. Histopathological analysis of the spleen depicting the impact of *B. microti*, *B. rodhaini*, and co-infection on the spleen compared to uninfected mice. Sections collected on day 6 post-challenge infection were stained with H & E, 100× and 200×. Black arrowheads indicate the variations in the marginal zone relative to (A) Naive mouse group. Erosion of the marginal zone in terms of loss of cellularity was found to be more pronounced in (B) Br mice compared to (C) bm/br4, and (D) bm/br6 mice. Bars in upper and lower images represent 200 and 100 μm, respectively.

Chapter 2

***Babesia microti* alleviates disease manifestations caused by *Plasmodium berghei* ANKA in murine co-infection model of complicated malaria**

2.1 Introduction

In spite of numerous endeavors to eradicate malaria, it remains widespread in numerous nations, causing over 200 million instances of infection annually. The World Malaria Report of 2022 estimated approximately 619,000 deaths attributable to malaria. Predictions suggest a rise in the geographic spread of malaria in tropical regions due to climate change (Cella et al., 2019). The causative agent for malaria is the intracellular parasite *Plasmodium*, which infiltrates the host through the bite of an infected carrier, *Anopheles* mosquitoes (Sanches-Vaz et al., 2019). Five different *Plasmodium* species affect humans, with *Plasmodium falciparum* being notably lethal, leading to a spectrum of clinical symptoms ranging from asymptomatic to severe manifestations of the disease (Mishra & Newton, 2009; Hunt et al., 2006). The term "severe malaria" encompasses various syndromes in humans, including acute respiratory distress (pulmonary edema), hyperparasitemia, severe anemia, liver dysfunction, acute renal failure, hypoglycemia, multiorgan failure, and ultimately, cerebral malaria (CM), with a mortality rate ranging from 15% to 20% (Dondorp et al., 2000; De Oca et al., 2013). In adults, pulmonary edema, acute renal failure, and jaundice are common occurrences, while children frequently experience anemia, hypoglycemia, and convulsions (Dondorp et al., 2000). Malaria-associated hematological changes involve anemia, thrombocytopenia, and disseminated intravascular coagulopathy. Complicated malaria often manifests liver involvement, presenting clinical symptoms such as jaundice, liver enlargement, and elevated levels of liver enzymes, including aspartate and alanine transaminases (Al-Salahy et al., 2016). Cerebral malaria, known for its catastrophic consequences (Ghazanfari et al., 2018), predominantly affects children under the age of 5, with morbidity and mortality rates ranging from 15% to 20%. Even if children survive this threat, they may suffer lifelong neurological sequelae (Pais et al., 2022). Currently, there is no cure for cerebral malaria, emphasizing the crucial need to explore host and parasite interactions to comprehend the pathogenesis for the development of novel therapeutic interventions (Mineo et al., 2013; Briquet et al., 2015).

The utilization of *Plasmodium berghei* ANKA infection in C57BL/6J mice has been

acknowledged as an experimental model for cerebral malaria (ECM), replicating most of the pathologies observed in complicated malaria (De Oca et al., 2013). The characteristic feature of human cerebral malaria (HCM) is the infiltration of infected red blood cells (iRBCs) in the brain and lung microvasculature. Despite the association of iRBC-endothelium interaction with malaria severity, the infiltration of iRBC by *P. berghei* ANKA remains incompletely characterized (El-Assaad et al., 2013). Several other pathophysiological aspects of severe malaria remain elusive (Dondorp et al., 2000). To effectively combat malaria, a deeper understanding of its pathogenesis is imperative (Mawson, 2013; Junaid et al., 2017). The establishment of a successful therapeutic strategy against this ailment is yet to be achieved. Therefore, unraveling the mechanism of protection against *Plasmodium* infection is crucial (Yoneto et al., 1999). Intriguingly, protection against malaria can also be conferred by previous parasite infections. Co-infection mouse models have demonstrated instances of cross-protection between *Babesia* and *Plasmodium* (Miyagami et al., 1987; Efstratiou et al., 2020). Babesiosis, an underexplored tick-transmitted zoonotic disease, is caused by the intraerythrocytic parasite *Babesia*, predominantly *Babesia microti*, resulting in a malaria-like disease that can be asymptomatic (Elton et al., 2019; Homer et al., 2000). Immunity to *Babesia* spp. can be established by the host post-infection, with both cell-mediated and humoral immunity playing roles in protection against babesiosis (Homer et al., 2000; Elton et al., 2019). Instances of mixed infection with *B. microti* and other pathogens are on the rise, where *Babesia* parasites themselves act as immunomodulators (Lobo et al., 2013; Swanson et al., 2023).

There is a shortage of information regarding co-infections and their implications for health (McArdle et al., 2018). Co-infections with certain pathogens can hinder the diagnosis of diseases. A more profound understanding of the influence of co-infections on the host's immune response and the outcomes of diseases will enhance both diagnosis and the development of innovative clinical interventions (Mabbott, 2018). The initial case of co-infection involving both *Plasmodium* and *Babesia* parasites in humans was documented in 1983 (Vermeil et al., 1983). Instances of co-infections with *Babesia* spp. and *Plasmodium* spp. have been reported in regions where malaria is endemic (Ahn, 2010; Zhou et al., 2013; Na et al., 2014; Gabrielli et al., 2016). In mice, *B. microti* has effectively provided cross-immunity against *Plasmodium* spp. (Cox, 1972; Zivkovic et al., 1984). Additional instances of cross-protection have been observed between *B. microti* and *P. vinckei* (Cox, 1978), *P. berghei* ANKA and *P. berghei* NK65 XAT (Miyagami et al., 1987), and *P. berghei* XAT (Pb XAT) and *P. berghei* NK65 (Pb NK65)

(Niikura et al., 2008). *B. microti* has also demonstrated protective effects against *P. cynomolgi* (Van Duivenvoorde et al., 2010) and *P. chabaudi* (Efstratiou et al., 2020) infections. The sequestration of infected red blood cells (iRBCs) in various organs through cytoadherence has not been observed in *Babesia* yet. While antibodies appear to play a minor role in resolving these iRBCs, macrophages contribute not only to resolving both infections but also to providing cross-protection against these parasites (Djokic et al., 2021).

However, there is a lack of information regarding the immunology of co-infections, and the inhibitory effect of babesiosis on malaria is not fully understood (Efstratiou et al., 2020).

The development of a malaria vaccine stands as a primary goal in biomedical research. RTS,S is a subunit vaccine derived from the circumsporozoite protein (CSP) of *P. falciparum* (Nunes-Cabaço et al., 2022). Nevertheless, RTS,S does not confer protection against other malaria parasites, specifically *P. vivax*, *P. ovale*, *P. malariae*, and *P. knowlesi* (Venkatesan, 2022). Protein subunit and/or DNA-based vaccines have shown limited efficacy and disappointing outcomes so far (Douradinha et al., 2008). An alternative type of vaccine is the whole-organism vaccine. Immunization using complete irradiated sporozoites is one of the most effective vaccinations against the same parasite strains, providing 100% protection. However, irradiated sporozoites exhibit reduced efficacy when faced with different parasite strains. Unlike liver-stage vaccines, the application of a blood-stage genetically attenuated malaria parasite (GAP) is not yet available for human use. Nevertheless, there are advantages to employing whole-pathogen vaccines. For instance, whole organism vaccines encompass the complete spectrum of parasite proteins, whereas subunit vaccines typically consist of only one or a few specific target proteins. Consequently, if the primary malaria parasite undergoes a mutation in the gene targeted by the subunit vaccine, the vaccine is susceptible to losing its effectiveness. In contrast, a whole-organism vaccine will maintain its stability against single gene mutations (Imai et al., 2020).

There is a pressing need for a vaccine capable of providing cross-protection against various plasmodial species, including *P. falciparum* and *P. vivax*. Such a vaccine would yield significant economic, safety, and manufacturing advantages. Nonetheless, cross-species immunity in malaria, particularly concerning the protection offered by live attenuated whole-organism-based approaches, has been overlooked in recent decades. Regrettably, none of the documented instances of human co-infections have succeeded in identifying the pathogens

beyond the species level. Consequently, the impact of the genetic background of pathogens on subsequent pathogenicity remains unknown (Efstratiou et al., 2020). In conclusion, it is crucial to thoroughly investigate and evaluate the potential for inducing cross-species immunity by employing the whole-organism approach in the development of malaria vaccines. Given this objective, future research is necessary to explore the immunological mechanisms responsible for initiating and sustaining cross-protection through the utilization of heterologous parasites (Douradinha et al., 2008).

It is important to note, that co-infection involving *B. microti* Peabody mjr, a human isolate, and *P. berghei* ANKA using the C57BL/6J murine model has not been explored to date. Based on the aforementioned information, I hypothesized that the primary infection of *B. microti* during the acute stage might impact the susceptibility of mice to *P. berghei* ANKA challenge infection. Therefore, in the pursuit of unraveling the host immune mechanisms and enhancing our understanding of host-parasite interactions in a co-infection model, the present study was conducted. Herein, I shed light on the immune dynamics and various aspects of disease manifestations in a co-infection disease model tailored for complicated malaria.

2.2 Materials and methods

Experimental animals

To analyze co-infection and experimental cerebral malaria (ECM), 5 weeks old female, C57BL/6J mice were bought from CLEA, Japan. To avoid any discrepancy that may arise due to the effect of testosterone, female mice were used (Djokic et al., 2019).

Parasite maintenance and experimental design

Cryostabilates of *B. microti* (Peabody mjr) were obtained from the cell bank whereas, *Plasmodium berghei* ANKA was provided by Nagasaki University with support in part by National BioResource Project (NBRP), MEXT, Japan. After thawing the frozen stabilates, mice were intraperitoneally inoculated to passage and were maintained for experiments. One group of mice (n= 6) was infected by intraperitoneal injection with 10^8 *B. microti*-infected red blood cells (iRBCs). The research was performed to investigate the influence of a non-lethal *B. microti* primary infection on a consequent lethal *P. berghei* infection. One group of mice (n=

6) was infected by intraperitoneal injection with 10^8 *B. microti*-infected red blood cells (iRBCs). Then, the same group was challenge infected with 10^3 *P. berghei*-infected RBCs at day 7 (henceforth mentioned as Bm/PbA7; n=6). Likewise, one more group (n= 6) was intraperitoneally inoculated with 10^3 *P. berghei*-infected RBCs only (henceforth mentioned as PbA) (n= 6) and an additional group with *B. microti*-infected RBCs only (henceforth mentioned as Bm) (n= 6).

A series of experiments was undertaken to probe the effects of co-infection. Preliminary experiments were conducted to optimize the infection dose. Out of the four doses tested ($10^2, 10^3, 10^4, 10^5$ iRBCs), the minimum infection dose of 10^3 iRBCs was selected for *P. berghei* infection. Similarly, for *B. microti* infection, two doses were evaluated during the preliminary trial, and out of those, 10^8 iRBCs was selected as the primary infection dose (Mordue & Wormser, 2019) (Figure 2.1). After preliminary experiments, the initial study was executed with four groups including, *B. microti*-infected group (Bm), co-infected group (Bm/PbA7), a control group (PbA), and a Naïve mouse group (injected with PBS) in a quest to investigate the progression of parasitemia, ECM signs, and other parameters. The subsequent trial was conducted including co-infected (Bm/PbA7), control (PbA), and Naïve groups (n=5) wherein the extent of blood-brain barrier (BBB) disruption and the integrity of the vascular endothelial barrier in the lungs were assessed using the Evans blue assay. Another trial was conducted with Bm, PbA, Bm/PbA7, and Naïve mouse groups (n=5) to determine the parasite burden in tissues and the host immune response against infections. At the end, mice were again infected according to the aforementioned experimental design for performing the histopathological analysis.

Monitoring mice for parasitemia and hematological parameters

Regular monitoring of mice was done, and parameters including parasitemia, and body weight were recorded. RBCs and hematocrit (HCT) values were measured by Celltac Alpha MEK-6550K (Nihon Kohden) (Li et al., 2012). To determine the parasitemia percentage, thin blood smears were made, after staining with Giemsa, the percent parasitemia was assessed from 10^3 iRBCs after examining under $100 \times$ oil immersion Eclipse E200 microscope (Nikon, Tokyo, Japan). As we assessed the parasitemia using blood smears, it was challenging to differentiate

the levels of parasitemia specifically for *Babesia* and *Plasmodium* parasites in Bm/PbA7 mice. Consequently, we presented the combined parasitemia levels as an overall representation.

Assessment of experimental cerebral malaria (ECM) and survival rates

Mice were monitored daily for survival rates, and symptoms were recorded for the development of ECM by the use of the rapid murine coma and behavior scale (RMCBS) score, as explained by (Carroll et al., 2010). When the RMCBS score was ≤5/20, mice were categorized as exhibiting ECM symptoms (Sanches-Vaz et al., 2019).

Use of flow cytometry to determine the immunophenotype of organs

In a new trial, brain, liver, lungs, kidney and spleen were harvested aseptically, weighed and photographed at day 8 post-challenge infection from Bm/PbA7 mice (day 15 post-primary infection), at day 8 from PbA, Bm, and Naïve mice (n=5) following *P. berghei*, *B. microti* and PBS inoculation respectively. For single cell suspension, PBS was used for spleen and digest solution was used for rest of the organs (Liu et al., 2020). Then, organs were cut and triturated to make single cell suspension. Ground spleen tissues were strained a in 50 µm tube through a 70 µM nylon sterile cell strainer, whereas other organ tissues were incubated in digest solution for 1 h at 37°C. After digestion, the rest of the organ tissues were strained as described earlier. Single-cell suspensions of liver, lungs, kidney, and spleen were washed with PBS by centrifugation at 375 × g for 5 min at 4°C and RBCs were lysed with 1× ACK lysis buffer (Gibco, Massachusetts, USA) for 5 min at 25°C. After lysis was stopped by adding cold PBS, centrifugation was performed at 375 × g for 5 min at 4°C, 2 mL cell staining buffer (CSB, BioLegend, California, USA) was used to resuspend the cell pellet and kept at 4°C until the next step. Cell suspension of brain tissues was processed differently. The strained brain tissue suspension was washed with PBS and the pellet was resuspended with 8 mL of 40% Percoll (Cytiva, Tokyo, Japan). Then, 5 mL of 80% Percoll was taken into a round bottom tube and 8 mL of 40% Percoll was layered on top of it. After centrifugation at 1,578 × g for 20 min at 25°C with low acceleration (acceleration 1) and no brake, the middle interface layer was collected and transferred into a new tube containing 10 mL PBS. Later, centrifugation was carried out at 375 × g for 5 min at 4°C, and 2 mL CSB was used to resuspend the pellet. Two

antibody panels were used for each sample and approximately one million cells were reconstituted in CSB (Table 2.1-2.2). After Fc block was performed by resuspending the reconstituted cells with 70 µL CSB containing CD16/CD32 monoclonal antibody (Invitrogen, Massachusetts, USA) at 4°C for 25 min. Later, staining of samples was carried out, wherein the cells were labeled with fluorophore-tagged, marker antibodies for each type of immune cell and incubated at 4°C for 30 min in the dark. Then, samples were fixed with 4% paraformaldehyde (PFA) solution for 15 mins and washed two times with CSB and centrifuged at 375 × g for 5 min at 4°C. Finally, 200 µL CSB was used to resuspend the cells. Above mentioned protocol was described by (Rico et al., 2021). Sorting of stained and fixed cells was conducted by employing the CytoFLEX flow cytometer (Beckman Coulter, California, USA) and data were carefully evaluated by CytExpert 2.4 software (Beckman Coulter, California, USA) (Figure 2.2). The representative of the cell sorting strategy is shown in Figure 2.3, followed according to (Bayne & Vonderheide, 2013).

Evaluation of organ damage by histopathology

After harvesting the organs from experimental groups (n=1), the fixation of tissues was done in 4% paraformaldehyde, followed by dehydration in graded alcohol, and embedding in paraffin. Next, 5 μm thick slices were made. Subsequently, the sections were deparaffinized, and stained using hematoxylin & eosin (H & E). Eventually, the sections were mounted on MGK-S with coverslips. Changes in tissue histology were examined by the histopathologist in a blinded manner, by utilizing a Microphot-FX from Nikon, and images were captured using a Digital Sight DS-5M camera also from Nikon.

Quantification of serum cytokine levels

All groups of mice (Bm, PbA, Bm/PbA7, and Naïve n=5), were exsanguinated by withdrawing the blood from the heart at day 8 post-primary infection or day 8 pci with *P. berghei*. Later, the serum was collected by centrifugation at 1500 × g for 15 mins at 4°C. To detect and quantify serum cytokines, commercial enzyme-linked immunosorbent assay (ELISA) kits (Thermo Fisher Scientific, Massachusetts, USA) were used, and the assay was performed according to the manufacturers` guidelines and methods. To detect the cytokine levels in serum samples, 1:100 dilution was made in PBS. The MULTISKAN SkyHigh plate reader (Thermo Fisher

Scientific) was employed to determine the optical density. The serum cytokines (IFN-γ, TNF-α, IL-2, IL-6, IL-10, IL-12p70) were quantified by extrapolating the standard curves.

Preparation of *P. berghei* ANKA lysate

Previously established protocol by (Kim et al., 2022) was used to prepare *P. berghei* ANKA crude antigen. Concisely, *P. berghei* infected-blood was withdrawn intracardially when the parasitemia was more than 30%. Collected blood was centrifuged at 3,000 × g for 5 min and lysed chemically. For lysing, 0.15% saponin in PBS was mixed with equal volume of pelleted RBCs at room temperature for 5 mins. Followed by centrifugation, the pelleted parasites were washed 3 times with 1× PBS and re-suspended in 1× PBS. Released parasites were subjected to mechanical disruption by 2 cycles of sonication for 30 seconds, at 40% amplitude. Protein quantity of the lysate was measured by Pierce™ BCA Protein assay kit (Thermo Fisher Scientific, USA). The lysate was. kept at −20 °C and later used as coating agent for ELISA plates.

Determination of humoral immunity

To assess the humoral immune response, antibodies against *B. microti* and *P. berghei* were measured by ELISA. We had sera from Bm, PbA, Bm/PbA7, and Naïve mice (n=5) collected at day 8 pci. Co-infected mouse serum was detected for antibodies against each parasite. A previously described protocol was followed to measure the antibody response. In brief, either 50 μL *P. berghei* lysate or GST-fused rBmP32 antigen was used to coat microtiter plates (Nunc, Roskilde, Denmark) and kept at 4°C overnight. Washing was performed with 0.05% Tween 20-PBS (PBST) and blocking with 3% skim milk in PBS for 1 h at 37°C. After washing, the plates were incubated with 50 μL of 1:100 diluted serum samples in a blocking solution for 1 h at 37°C. While the samples were put in incubation, goat anti-mouse-Immunoglobulin HRP-conjugated secondary antibody (IgG, IgG1, Ig2a, IgG3, and IgM) were prepared. Secondary antibodies were diluted in a blocking solution to a concentration of 1:4,000. After incubation with diluted mouse serum, plates were washed 6 times. Then, incubated for 1 h at 37°C with secondary antibody and again washed for 6 times. Finally, plates were incubated with tetramethylbenzidine (TMB) substrate for 1 h at room temperature (RT) to detect bound antibodies. Absorbance values were read at 415 nm using the MULTISKAN SkyHigh plate

reader (Thermo Fisher Scientific). To ensure the consistency of results and avoid any discrepancy, triplicates of each sample were used.

Absolute Quantification of *P. berghei* Parasites

At day 8 pci, organs were harvested and blood was collected from mouse groups (PbA and Bm/PbA7; n=5). DNA was extracted from tissues and blood using NucleoSpin® Tissue Kit (Takara, Japan), and QIAamp® DNA Blood Mini Kit (Qiagen, Hilden, Germany), respectively, adhering to the directions specified by the manufacturer. The DNA was eluted to a final volume of 100 µL. To quantify the parasites, a pair of specific primers (F: 5`-AAGCATTAAATAAAGCGAATACATCCTTAC-3`; R: 5`GGAGATTGGTTTTGACGTTTATGTG-) was used to amplify a part of the 18S rRNA gene (134 bp) of *P. berghei* (Baptista et al., 2010). A final volume reaction of 10 µL was run in duplicates, composed of 5 µL 1 × PowerUp™ SYBR™ Green Master Mix (Applied Biosystems, Massachusetts, USA), 0.8 µM primers, 1 uL DNA, and 2.4 uL UltraPure™ DNase/RNase-free water (Thermo Fisher Scientific). The cycling regimen employed was 50 °C for 2 min, 95 °C for 2 min, 40 cycles of 95 °C for 15 sec and 60 °C for 45 sec, with a dissociation stage. The reactions were run in the QuantStudio™ 5 Real-time PCR System water (Thermo Fisher Scientific). Serially diluted standards prepared from plasmids served as reference samples. Gene copy values were derived from the average quantified cycle values of the replicates relative to the obtained values from the standards. Values were converted to their corresponding log values followed by statistical analysis.

Evans Blue Assay for Assessment of the BBB Disruption and Lungs Vascular Integrity

To measure the disruption of BBB in C57BL/6 mouse groups (n=5), either single infected or challenge-infected with *P. berghei* ANKA and in Naïve, we followed the previously stated protocol by (Baptista et al., 2010). Concisely, 200 µL of 2% Evans blue (EB) in PBS was injected intravenously (iv) in the mouse tail after the onset of clinical symptoms of ECM. One group of Naïve mice was injected with PBS as the negative control to distinguish morphology. One hour later, mice were euthanized and perfused with PBS. Harvested brains and lungs were weighed, photographed, and kept in 2 ml formamide (Merck, New Jersey, USA) for 48 h at 37°C to recover the Evans blue dye from the tissue. The extent of BBB and lung damage was assessed by measuring the absorbance at 620 nm. Evans blue concentration was quantified by

calculations using a standard curve.

Statistical Analyses

GraphPad Prism 8 software (GraphPad Prism, California, USA) was used for statistical analyses of all data. To make a comparison among groups, ordinary one-way analysis of variance (ANOVA) followed by post hoc Tukey's multiple-comparisons test and two-tailed unpaired student t-test was used. A P-value less than 0.05 was considered significant at a 95% confidence interval.

2.3 Results

Extended survival of co-infected mice with *B. microti* primary infection against *P. berghei* deadly challenge

In this investigation, Bm/PbA7 mice exhibited prolonged survival compared to PbA mice. All PbA mice succumbed to the infection by day 12, as depicted in Figure 2.4A, whereas Bm/PbA7 mice survived until day 21 and ultimately perished at day 22 post-challenge infection (pci). Notably, PbA mice displayed clinical signs such as piloerection, shivering, convulsions, seizures, and coma, while co-infected mice managed to survive without manifesting any overt signs of experimental cerebral malaria (ECM) (Figure 2.4B). These findings clearly indicate that although complete survival was not achieved, the primary infection with *B. microti* conferred immunity, enabling co-infected mice to survive for a more extended period compared to PbA mice.

Parasitemia and hematologic indices during acute stage of *B. microti* and *P. berghei* co-infection

Throughout the experiment, the levels of parasitemia were monitored through Giemsa-stained blood smears. The curves illustrated in "Figure 2.4C" were utilized to compare parasitemia levels among the three groups. This comparison unveiled that at day 0 of post-challenge infection, the Bm/PbA7 mice exhibited a parasitemia level of 32.5%, resulting from a prior *B. microti* infection. Subsequently, the parasitemia declined by day 6 post-challenge infection (pci) (equivalent to day 13 post-primary infection), only to peak again. This subsequent increase in parasitemia was attributed to the *P. berghei* challenge-infection. It is crucial to acknowledge that the observed parasitemia reflects combined parasitemia caused by both

Babesia and *Plasmodium* parasites. Notably, co-infected mice displayed the highest parasitemia (38%), while the peak parasitemia in PbA mice was 32.47%. In the case of Bm mice, the peak parasitemia level reached 36.39% and was observed on day 8 post-infection (pi) (Figure 2.4C). The body weights of the Bm mice indicated transient loss that was subsequently recovered after the resolution of parasitemia. In PbA mice, a drastic weight loss was observed from the initial weight (20.058 g) to the final weight (14.887 g) before their demise. In contrast, co-infected mice exhibited a gradual decline in weight from (16.98 g) to (14 g) (Figure 2.4D). Furthermore, all groups developed anemia, with Bm and Bm/PbA7 mice experiencing particularly intense anemia, evidenced by lower-than-normal RBCs and hematocrit indices. Prior to the day of death, Bm/PbA7 mice displayed severe anemia, whereas hematologic parameters were rehabilitated and sustained until day 28 pci in Bm mice (Figures 2.4E and 2.4F). Our findings substantiate that the escalation in blood parasites hastened the breakdown of infected red blood cells (iRBCs) and reduced hematologic indices, leading to anemia.

Immune microenvironment in the spleen, brain, liver, lungs, and kidneys of mice

The aforementioned vital organs were investigated using flow cytometry to elucidate the dynamics of immune cell populations. The objective was to explore the impact of co-infection on immune cell dynamics during the early stages of infection, thereby elucidating the role of innate immunity in this study. Spleen, brain, liver, lungs, and kidneys were aseptically extracted, and after processing the samples, data were collected (Figure 2.5). While the brain of PbA mice exhibited the lowest population of NK cells, DCs, and macrophages, the populations of CD4+ and CD8+ T cells significantly increased compared to the other groups (Figure 2.5B). Co-infected mice showed a significantly higher number of B cells than PbA mice (Figure 2.5A). There were notable differences in the macrophage population between PbA and Bm/PbA7 mice. In co-infected mice, macrophages were the predominant immune cells in all probed organs compared to PbA mice. Particularly, macrophages were significantly higher in co-infected (5.36%) spleen compared to PbA (0.13%) mouse spleen (Figure 2.5A). Among all organs, the liver had the greatest percentage of macrophages in all the groups: 2.56%, 7.41%, 6.67%, and 13.27% in PbA, Bm, Bm/PbA7, and Naïve mice, respectively (Figure 2.5C). PbA mice exhibited a comparatively low immune cell population in kidneys and lungs than Bm/PbA7 mice (Figures 2.5D and 2.5E). In summary, the percentages of B cells, CD4+ and CD8+ T cells, macrophages, NK cells, and DCs varied among all groups, with the spleen of PbA mice having the lowest immune cell population (except for CD8+ cells), and Bm/PbA7

being comparatively higher (Table 2.3).

The interplay between pro-inflammatory and anti-inflammatory cytokines might drive the outcome of *B. microti* and *P. berghei* co-infection in mice

In an effort to comprehend the cytokine interplay in mice, the serum levels of cytokines (IFN-γ, TNF-α, IL-6, IL-12p70, IL-2, IL-10) (Figure 2.6G) were assessed. Co-infected mice displayed diminished levels of pro-inflammatory cytokines (IFN-γ, TNF-α, IL-12p70), while the anti-inflammatory cytokine (IL-10) exhibited an elevation during the acute phase of co-infection (Figure 2.6). Although the reduction in the level of IL-12p70 did not reach statistical significance, it is noteworthy that PbA mice demonstrated a slightly higher level compared to co-infected mice: 58.7 pg/ml in PbA mice and 57.5 pg/ml in Bm/PbA7 mice, respectively. Our results suggested a protective role of IL-10 against ECM, as co-infected mice had significantly higher levels of IL-10 compared to PbA mice (Figure 2.6F). Additionally, the absence of early IFN-γ secretion led to fatal infection, as significantly elevated levels of IFN-γ were observed in PbA mice at day 8 post-infection (pi) (Figure 2.6A) compared with Bm/PbA7 mice. Relatively higher levels of TNF-α and IL-12p70 were observed in PbA mice, although a significant difference was not noted in the levels of IL-12p70 (Figure 2.6B and 2.6D). In PbA mice, the serum level of TNF-α was enhanced compared to other groups (Figure 2.6B). Elevated levels of IL-6 (Figure 2.6C) and IL-2 (Figure 2.6E) were also observed in mice with *P. berghei* infection. Overall, these findings indicate that IL-10, IFN-γ, and TNF-α are pivotal cytokines, where high levels of IFN-γ and TNF-α contribute to the lethality of the disease, and IL-10 acts as a protective factor during *B. microti* and *P. berghei* co-infection.

Modification of humoral response during *B. microti* and *P. berghei* co-infection

Subsequently, the objective was to verify whether the surge in B and T cells corresponded to the species-specific antibody response (Figure 2.5). To achieve this, antibodies targeting *B. microti* and *P. berghei* (Figure 2.7) were assessed on day 8 post-cerebral infection (pci). For singly infected mice, day 8 pci represented 8 days post-infection, while for co-infected mice, denoted day 14 post-*B. microti* primary infection, coinciding with day 8 pci at the time of serum collection. Consequently, co-infected mice exhibited prominent IgG-specific antibody responses against *B. microti* (Figure 2.7A). Although the levels of IgM in singly infected Bm

and PbA mice were elevated compared to co-infected mice, this difference did not reach statistical significance (Figure 2.7E and 2.7J). The production of specific antibodies against *P. berghei* was comparable between co-infected and PbA mice. Our findings suggested that there was minimal disparity in serum antibody production between PbA and co-infected mice. In summary, our results indicated that mice during the acute stage of infection displayed a diminished humoral immune response.

Alterations in structure of organs during acute stage of *Babesia* co-infection

In H & E-stained spleen sections, Naïve mice exhibited typical, normal histology with well-defined red and white pulps (Figure 2.8C). In spleens infected with *P. berghei* ANKA, the demarcation between red and white pulps became indistinct due to the accumulation of immune cells in the red pulp. Conversely, in co-infected spleens, the formation of the marginal zone made the white pulp more discernible (Figure 2.8C). In the livers of Naïve mice, a normal structure featuring liver lobules with a well-organized arrangement of hepatocyte plates was evident (Figure 2.8A). This arrangement and morphology of hepatocytes were severely compromised in livers infected with *P. berghei* ANKA, whereas in the livers of co-infected mice, these features appeared normal (Figure 2.8A). The lungs of Naïve mice displayed an intact and typical structure with normal histology, characterized by pulmonary alveoli separated by thin septa (Figure 2.8B). Lungs infected with *P. berghei* ANKA exhibited severe and moderate interstitial pneumonia, accompanied by interstitial thickening. This abnormality was mitigated in co-infected lungs (Figure 2.8B). Overall, these observations suggest that co-infection alleviated disease manifestations in the spleen, liver, and lungs of mice.

B. microti* primary infection reduces subsequent tissue sequestration of *P. berghei

The findings of flow cytometry indicated a potential role of innate immune cells in conferring protective immunity (Figure 2.5). Similarly, qPCR outcomes underscored the defensive function of innate immune cells against *P. berghei* infiltration in various organs, as evidenced by the reduced *P. berghei* burden in tissues such as the liver, spleen, kidneys, lungs, and brain. To investigate whether the exacerbated manifestation of severe disease in PbA mice resulted from the accumulation of *P. berghei*-infected red blood cells (iRBCs) in organs, qPCR analysis was conducted on DNA extracted from the brain, liver, lungs, spleen, kidneys, and blood of

PbA and co-infected mice at day 8 post-infection (pci) (Figure 2.9). Our results demonstrated a direct correlation between tissue injury extent (Figure 2.8) and *P. berghei* sequestration in the tissues, with a significantly lower *P. berghei* burden in the liver, spleen, kidneys, lungs, and brain of co-infected mice (Figure 2.9A-2.9E). Interestingly, mouse blood exhibited the opposite trend, with a higher parasite load in co-infected mice compared to PbA mice (Figure 2.9F). The increased *P. berghei* load in the organs of PbA mice, as compared to co-infected mice, emphasized the protective immune response preventing the sequestration of a high load of iRBCs in co-infected mice. The lower parasite burden in the liver, spleen, kidney, lung, and brain of co-infected mice correlated with the prevention of tissue injury (Figure 2.9A-2.9E). These findings were statistically significant.

Disruption of BBB and lungs vascular permeability is concomitant with ECM in PbA mice

The disruption of the blood-brain barrier (BBB) and increased vascular permeability in the lungs were concurrent with experimental cerebral malaria (ECM) in PbA mice. To confirm that co-infected mice survived longer without ECM, the integrity of the BBB and changes in lung vascular endothelial barrier function were assessed by measuring Evans blue infiltration in respective tissues. As expected, co-infected mice exhibited intact BBB and lungs vascular endothelial barriers, while in PbA mice, the BBB became more permeable with the onset of ECM (Figure 2.10A and 2.10B). A notably higher extravasation of Evans blue was observed in PbA mice compared to co-infected mice (Figure 2.10C). Overall, results suggest that the severity of cerebral malaria, characterized by compromised BBB integrity due to *P. berghei* infection, substantially decreased in co-infected mice. Additionally, the function of the lung vascular endothelial barrier was impaired in PbA mice compared to co-infected mice, as indicated by the higher infiltration of Evans blue dye (Figure 2.10D).

2.4 Discussion

This study was conducted to examine co-infections and to determine their potential involvement in the onset or evasion of complicated malaria and associated pathologies. Previous studies in mice have reported evidence of pathology in the brain, liver, lung, and

spleen, along with instances of anemia and parasite sequestration in tissues (Briquet et al., 2015). The outcomes of this research revealed modifications in disease progression and immune responses within a mouse co-infection model. In Bm/PbA7 mice, elevated parasitemia at day 0 of the challenge infection, attributed to *B. microti*, was deemed advantageous for the early activation of innate immunity. Additionally, *P. berghei* has preference for reticulocytes, a factor believed to contribute to the elevated parasite burden leading to severe anemia and vice versa (Thakre et al., 2018). Ultimately, Bm/PbA7 mice were observed to succumb to infection due to anemia. The sequestration of *Plasmodium* in tissues is thought to benefit the parasite by evading recognition and clearance of infected red blood cells (iRBCs) by macrophages in the spleen (Lagassé et al., 2016). This sequestration of iRBCs is evidently associated with pulmonary pathology in the murine model (Franke-Fayard et al., 2005; Lovegrove et al., 2008). The infection of hepatocytes by *Plasmodium* sporozoites can lead to congestion, sinusoidal blockage, and cellular inflammation (Al-Salahy et al., 2016). Our results also indicated a proportional relationship between the intensity of malaria-induced lung pathologic features and the increased levels of iRBC sequestration, aligning with the findings of Lagassé et al. (2016).

The observed organ damage in PbA mice, including the brain, liver, and lungs, stemmed from diminished microcirculatory blood flow resulting from structural and functional alterations of infected red blood cells (iRBCs) (Dondorp et al., 2000). Therefore, the insufficiency of antimalarial immunity by *Plasmodium* may be elucidated by the evasion of the immunological defenses through infiltration into organs and reduced immunogenicity (Dondorp et al., 2000). A notable feature of severe malarial syndrome is the significantly increased parasite loads compared to individuals with uncomplicated malaria. This suggests that the parasite load plays a crucial role in the development of brain, lung, and liver diseases during malaria (Bagot et al., 2002; Haque et al., 2011; Strangward et al., 2017). Despite higher peripheral parasitemia in Bm/PbA7 mice, our qPCR results indicated less sequestration of *P. berghei* in the brain, liver, lungs, spleen, and kidneys compared to PbA mice. This observation might account for the prolonged survival and evasion of severe malaria in Bm/PbA7 mice compared to PbA mice.

Macrophages have been identified as pivotal cell types involved in the host immune response against malaria infections. In addition to their role in phagocytosing infected red blood cells (iRBCs), they influence the surrounding tissue environment by releasing both pro-inflammatory and anti-inflammatory cytokines (Ozarslan et al., 2019). Mice lacking

macrophages displayed more malaria complications, such as disruption in the blood-brain barrier (BBB) and increased vascular permeability in the lungs (Gupta et al., 2016). These studies strongly suggest the crucial role of macrophages in immunity against malaria, emphasizing that their activation can modulate the disease outcome. However, the mechanisms governing their activation remain unknown. With a few exceptions, the populations of innate immune cells (including B cells, NK cells, DCs, and macrophages) in PbA mice organs declined, while those in co-infected mice organs increased (Table 2.3). Despite *Plasmodium*-induced immunosuppression (Millington et al., 2007), mice with primary *B. microti* infection appear to evade the immunosuppressive effect of *Plasmodium* in co-infected mice. Therefore, depending on the organ, the innate immune response determines the course of infection. This clarifies the prolonged survival and partial protection of co-infected mice, as they were exposed to a *Plasmodium*-like parasite to activate the first line of defense. There is consensus that the presence of CD8+ T cells and sequestration of infected red blood cells in the brain are crucial for the progression of experimental cerebral malaria (ECM). The activation of brain endothelial cells could lead to the phagocytosis of the pathogen and the presentation of antigens to CD8+ T cells. This, in turn, might initiate the killing of endothelial cells through the perforin pathway by CD8+ T cells, ultimately resulting in BBB breakdown (Baptista et al., 2010).

Additional studies have emphasized that the presence of CD8+ T and CD4+ T cells in the brain is a distinctive feature of cerebral pathology (Grau et al., 1986; Belnoue et al., 2002). Liver damage occurs in experimental cerebral malaria (ECM) before the manifestation of neurological symptoms. Consequently, the liver is considered a significant reservoir of CD8+ T cells during the symptomatic stages of ECM (Haque et al., 2011). In alignment with our flow cytometric and qPCR analyses, PbA mice exhibited significantly higher infiltration of CD8+ T cells in the brain, liver, and lungs, while co-infected mice displayed reduced infiltration of CD8+ T cells and infected red blood cells (iRBCs). Therefore, both the parasite burden and CD8+ T cells play crucial roles in exacerbating multiorgan injury in PbA mice.

Alterations in the balance between pro-inflammatory and anti-inflammatory responses can significantly influence the disease outcome (Beiting, 2014). The secretion of IL-10 stands out as a crucial characteristic of tissue-resident macrophages (Gupta et al., 2016; Kumar et al., 2019). Malaria complications are enhanced in the absence of macrophages (Ozarslan et al., 2019). Stimulation of B cells or infection with *B. microti* leads to the production of IL-10, with the numbers of IL-10-producing B cells increasing with *B. microti* infection (Jeong et al.,

2012). In the context of malaria, IL-10 production serves to protect tissues from injury. It exerts its anti-inflammatory effects by suppressing the secretion of pro-inflammatory cytokines and by reducing the expression of MHC-II molecules on antigen-presenting cells (APCs) (Sanni et al., 2004; Couper et al., 2008; Kumar et al., 2019). An insufficient pro-inflammatory response may lead to uncontrolled parasite replication, while an excessive pro-inflammatory response can result in tissue injury. In summary, cytokine findings illustrated the protective role of IL-10 against experimental cerebral malaria (ECM) (Freitas Do Rosario & Langhorne, 2012). The FACS data corroborate these results, as evidenced by the significant decrease in B cell and macrophage populations in PbA mice, leading to a reduction in IL-10 production, whereas B cell and macrophage populations increased in co-infected mice, accompanied by a simultaneous rise in IL-10 cytokine levels.

The early release of IFN-γ has been identified as a protective factor against experimental cerebral malaria (ECM) (King & Lamb, 2015), while the absence of timely IFN-γ release can result in lethality (Stevenson & Riley, 2004). IL-10 serves to inhibit the excessive secretion of IFN-γ and TNF-α during *B. microti* infection (Djokic et al., 2018), simultaneously enhancing the immune response to eradicate the parasite (Trinchieri, 2007; Couper et al., 2008; Redpath et al., 2014). Malaria pathology has been linked to the overproduction of IFN-γ and IL-12 (Engwerda et al., 2002). In a separate investigation, protected mice exhibited minimal levels of IFN-γ and TNF-α, along with an increased concentration of IL-10 following *P. chabaudi* challenge infection. The cytokine outcomes suggest that the protection afforded by *B. microti* against *P. berghei* is attributed to the absence of elevated levels of IFN-γ, TNF-α, and IL-12p70. In contrast, these cytokine levels peaked in PbA mice compared to co-infected mice. A potential mechanism through which pro-inflammatory mediators such as TNF-α and IFN-γ induce tissue pathology is by upregulating adhesion molecules like ICAM-1, VCAM-1, and P-selectin on endothelial cells, leading to the accumulation of leukocytes and infected red blood cells (iRBCs). This implies that the sequestration of iRBCs and leukocytes may play a pathogenic role (Bagot et al., 2002; Claser et al., 2019).

This study has some limitations. One constraint is the absence of a green fluorescent protein (GFP) parasite, which would have allowed us to distiguish the impact of co-infection solely on PbA parasitemia. Furthermore, the use of a GFP parasite would have facilitated the convenient visualization and tracking of the parasite's location and behavior within tissues. Another aspect that warrants exploration is the influence of co-infection on the prepatent period. In contrast to

a previous investigation (Efstratiou et al., 2020) demonstrating 100% cross-protection by *B. microti* against lethal *P. chaubadi*, our study indicates that primary infection with *B. microti* is associated with mitigating disease manifestations in complicated malaria compared to a sole infection with *P. berghei*. Given that co-infected mice did not exhibit complete cross-protection, it is imperative to investigate other factors that might enhance the immune response and further fortify the host defense. To validate the protective role of macrophages in controlling and resisting infections, it is essential to transfer bone marrow-derived macrophages (BMM) from naive mice to co-infected mice. This approach will help determine whether co-infected mice exhibit enhanced survival and improved recovery from parasitemia compared to PbA mice that did not receive BMM. Further exploration is also necessary to unravel the contribution of distinct macrophage subtypes, such as M1 and M2, in orchestrating the balance between pro- and anti-inflammatory cytokines, a phenomenon hypothesized to facilitate the cross-protection.

2.5 Summary

In this study, a murine co-infection model of severe malaria was utilized. The research findings revealed that primary *B. microti* infection extended the survival of co-infected mice and mitigated the severity of the disease compared to *P. berghei* control mice. Additionally, the immune cell compositions in the liver, lungs, kidneys, brain, and spleen of all experimental groups of mice were quantified and compared, providing a detailed insight into the immune microenvironment within organs. These results suggest that innate immunity is crucial for cross-protection, with macrophages appearing to play a role in conferring immunity in co-infected mice. Alongside the higher parasite burden in the organs, a substantial population of CD8+T cells was linked to organ damage. Co-infected mice exhibited reduced levels of pro-inflammatory cytokines (such as IFN-γ, TNF-α, IL-12p70), contrasting with the elevated levels of the anti-inflammatory cytokine IL-10 in mouse serum, indicating a protective function of IL-10 against complicated malaria. Further investigation is necessary to explore the malaria-suppressing effects of *Babesia*, aiming to gain a better understanding and develop novel therapeutic tools to combat malaria.

Table 2.1. Antibody panel 1 used for FACS analyses

Immune cells	Anti-mouse antibody markers	Fluorophore	Antibody dilution (vol/vol μL)	Manufacturer (catalog no.)
Total leukocytes	CD45	FITC	0.5/200	BioLegend (147709)
T lymphocytes	CD3	PE/Cyanine7	1/200	BioLegend (100219)
B lymphocytes	CD19	Brilliant Violet 421™	1/200	BioLegend (115537)
Natural killer cells	CD49b	PerCP/Cyanine5.5	1/200	BioLegend (108915)
CD4 cells	CD4	PE	1/200	BioLegend (100408)
CD8 cells	CD8a	Brilliant Violet 510™	1/200	BioLegend (100751)

Table 2.2. Antibody panel 2 used for FACS analyses

Immune cells	Anti-mouse antibody markers	Fluorophore	Antibody dilution (vol/vol µL)	Manufacturer (catalog no.)
Total leukocytes	CD45	FITC	0.5/200	BioLegend (147709)
Macrophages	F4/80	PE	1/200	BioLegend (123109)
Dendritic cells	CD11c	Brilliant Violet 510 ™	1/200	BioLegend (117337)

Table 2.3. Percentage of immune cell populations in test organs.

ORGANS	IMMUNE CELLS%	PbA	BM	BmPbA7	Naïve
Spleen	B lymphocytes	54.688	53.463	59.760	62.256
	CD8	13.332	10.207	10.280	10.886
	CD4	16.967	21.680	17.144	23.338
	NK cells	1.042	3.203	7.490	6.734
	Dendritic cells	2.794	2.113	2.932	5.762
	Macrophages	0.138	6.433	5.366	8.134
Brain	B lymphocytes	12.642	12.304	13.100	12.496
	CD8	44.378	3.982	15.048	3.602
	CD4	12.034	1.962	10.220	5.966
	NK cells	0.348	0.988	0.504	1.079
	Dendritic cells	0.028	0.030	0.048	1.116
	Macrophages	0.078	0.780	0.705	2.020
Liver	B lymphocytes	17.622	16.464	23.154	24.776
	CD8	24.602	23.838	14.050	10.506
	CD4	11.068	11.200	14.474	9.640
	NK cells	1.954	12.360	2.956	7.176
	Dendritic cells	3.748	5.200	4.076	6.750
	Macrophages	2.560	7.416	6.676	13.270
Lung	B lymphocytes	6.290	24.538	13.610	14.598
	CD8	26.794	22.856	27.012	38.860
	CD4	7.398	10.700	4.148	11.918
	NK cells	5.054	3.142	5.168	1.796
	Dendritic cells	1.432	11.501	1.204	1.846
	Macrophages	0.322	4.882	4.480	2.884
Kidney	B lymphocytes	10.072	14.152	12.598	30.958
	CD8	11.496	22.274	28.270	4.456
	CD4	8.578	12.200	13.108	9.782
	NK cells	7.272	3.374	3.360	3.788
	Dendritic cells	7.544	4.500	3.924	2.070
	Macrophages	0.506	3.646	3.725	0.840
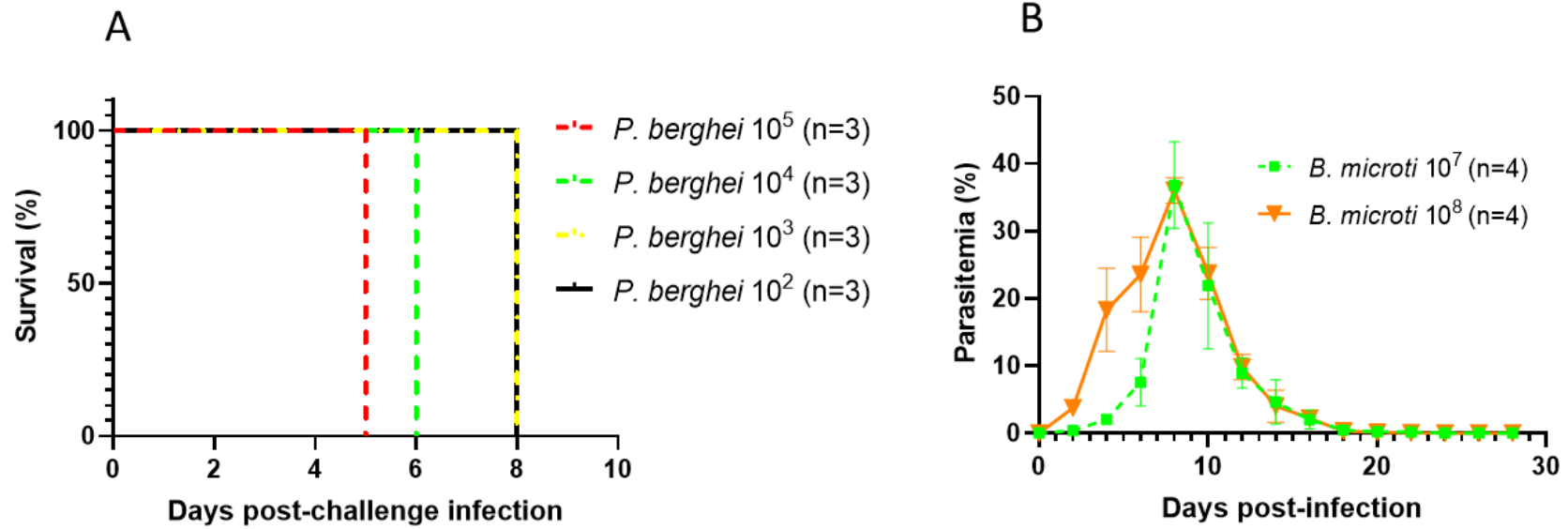
Figure 2.1. Results of preliminary trials. (A) Out of the four doses (10^2, 10^3, 10^4, 10^5), 10^3, was selected for *P. berghei* infection. (B) For *B. microti* infection, two doses (10^7, 10^8) were used in the preliminary trial, and out of those, 10^8 was selected for primary infection.
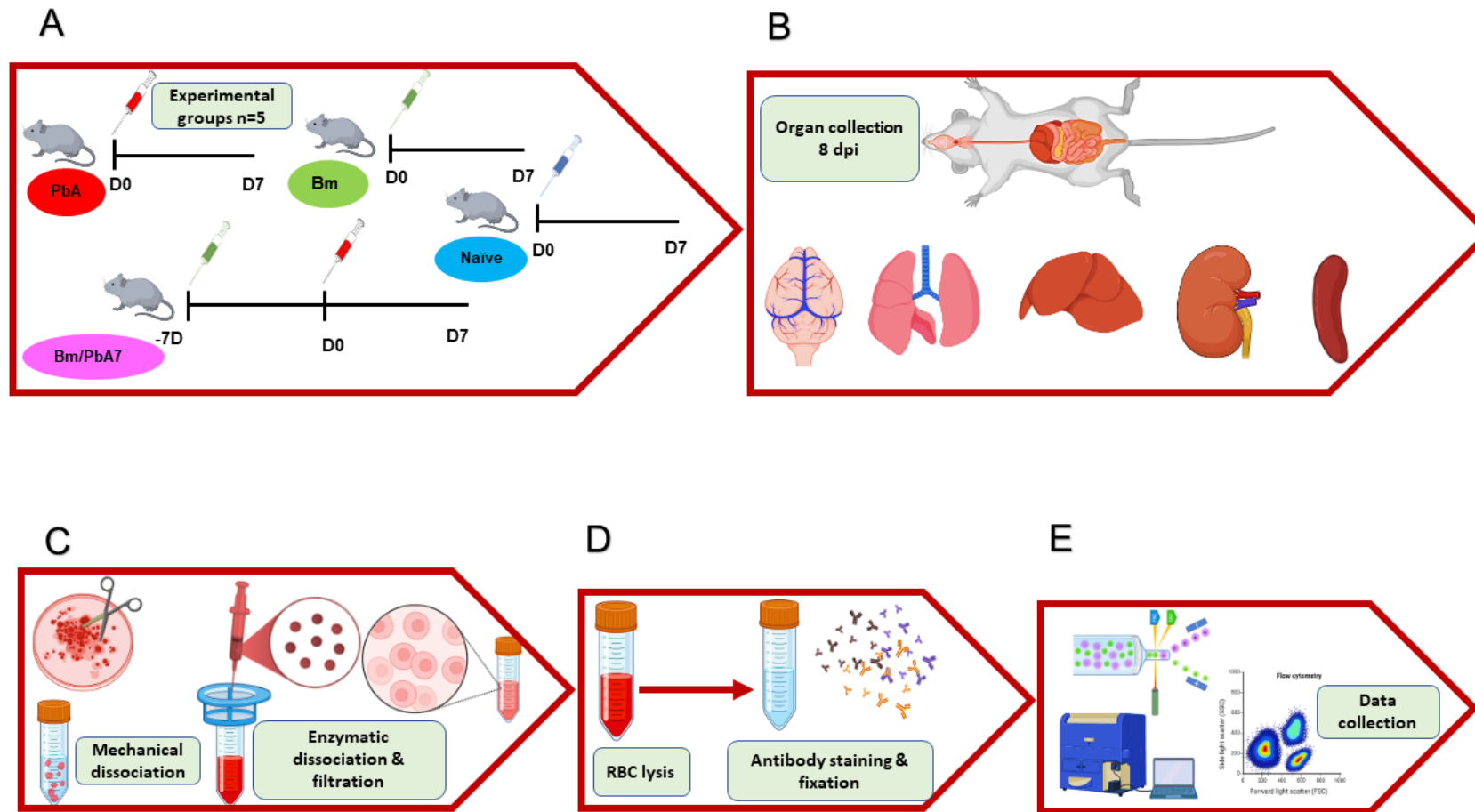
Figure 2.2. Figure showing processes involved in performing FACS. (A) Overall experiment design, (B) Organ harvest at day 8 post challenge-infection (pci) from all groups (PbA, Bm, Bm/PbA7 and naïve, (C) Mechanical and enzymatic dissociation followed by filtration, (D) RBC lysis, antibody staining, and fixation, (E) Data collection by flow cytometer and analysis of data.
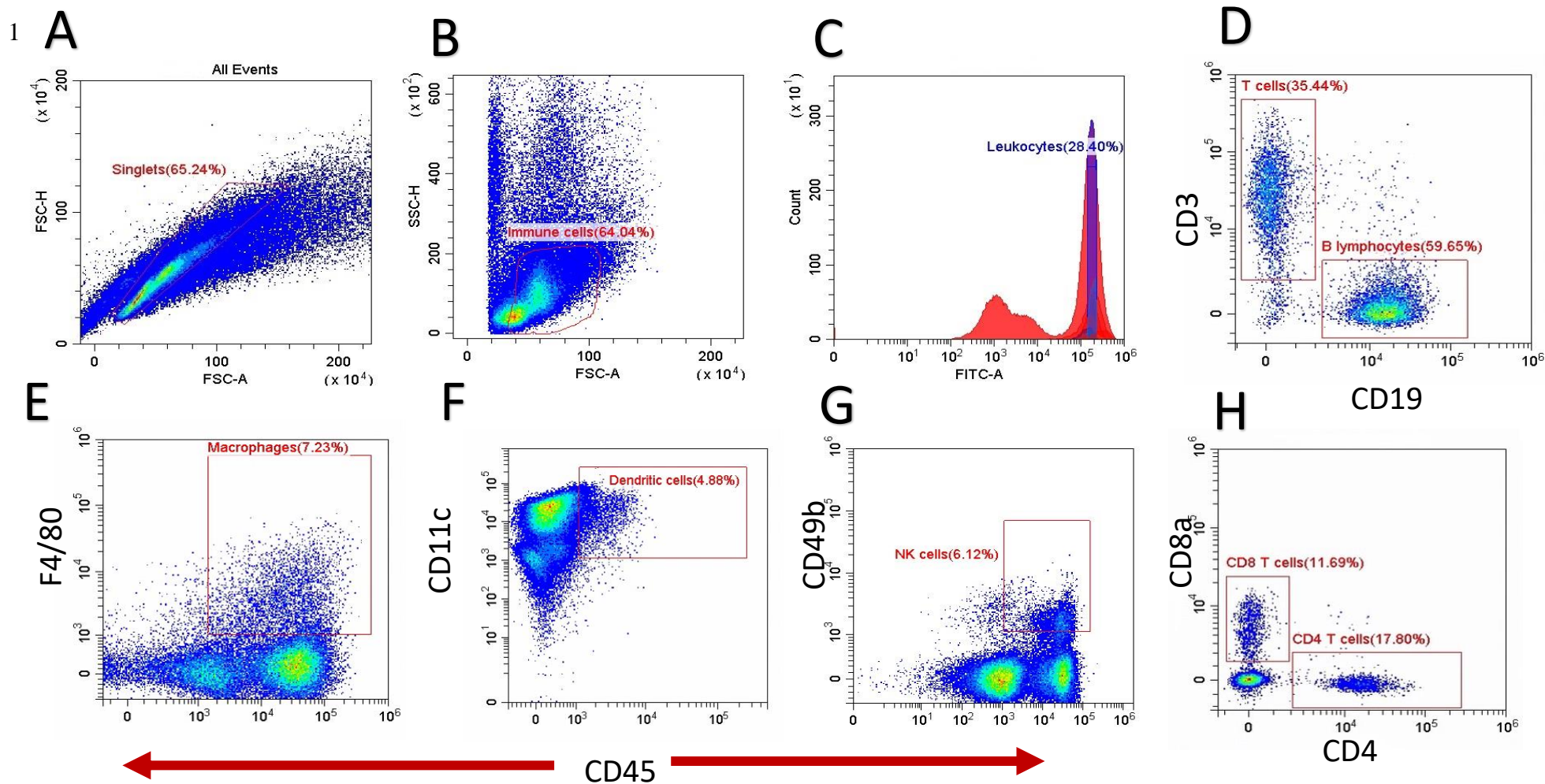
Figure 2.3. Gating scheme for fluorescence-activated sorting (FACS) analysis of immune cells. A total of 50,000 events were analyzed. Each panel is a representative image of gating for (A) singlets, (B) CD45^{+} (immune cells), (C) CD45^{+} leukocytes, (D) CD45^{+} CD3^{+} (T cells), CD19^{+} (B cells), (E) CD45^{+} F4/80^{+} (macrophages), (F) CD45^{+} CD11c^{+} (dendritic cells), (G) CD45^{+} CD49b^{+} (natural killer cells), and (G) CD45^{+} CD8a^{+} (CD8 T cells), CD45^{+} CD4^{+} (CD4 T cells).
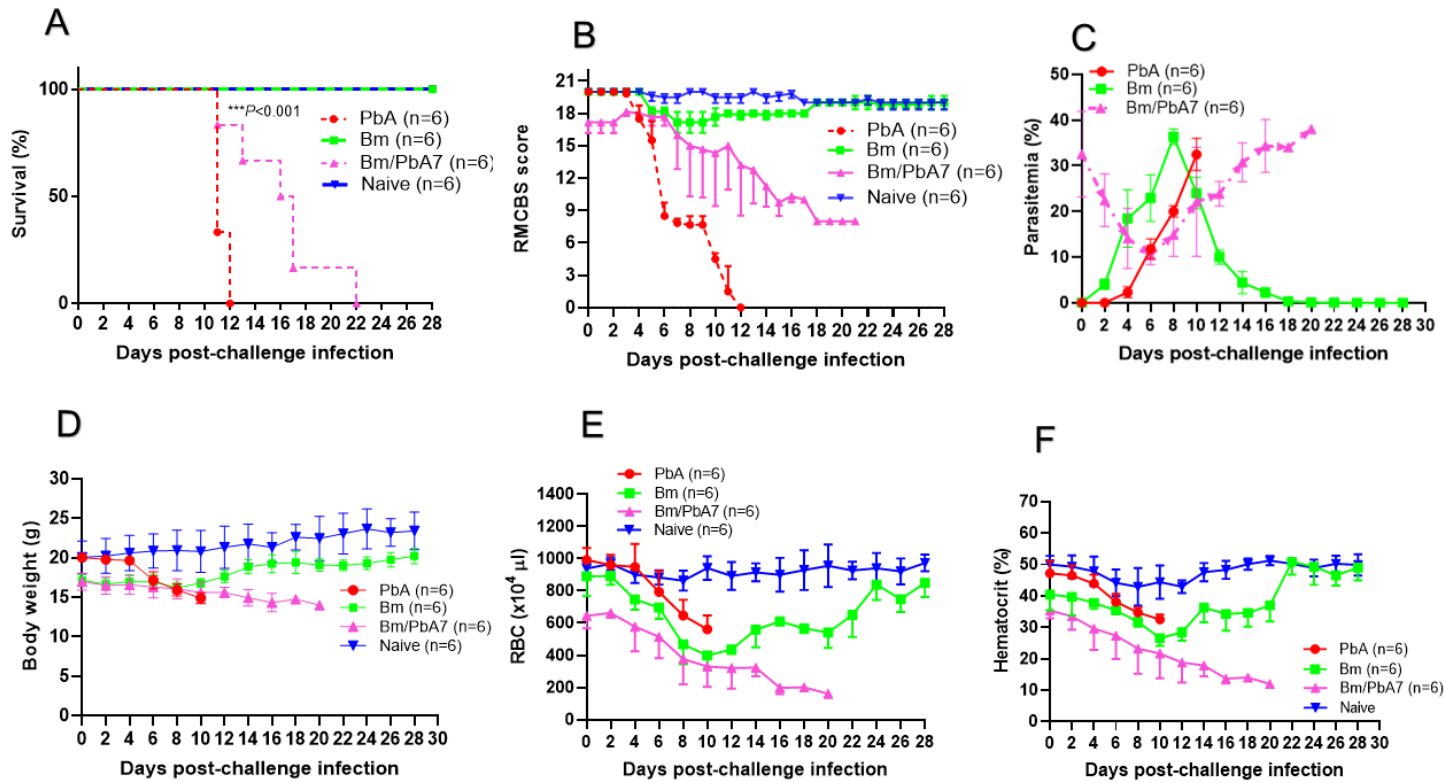
Figure 2.4. Monitoring the course of disease in C57BL/6J mice in Bm, PbA7, Bm/PbA7, and Naïve mice groups (n=6). In the first trial test mice were initially infected with *B. microti* and then challenge infected with *P. berghei* at day 7 post-primary infection. (A) Survival curve, (B) RMCBS score, (C) course of parasitemia, (D) body weight, (E) red blood cell (RBC) count, and (F) hematocrit values were monitored until PbA and Bm/PbA7 mice died and for 28 days for Bm and Naïve mice. Mean percent parasitemia, body weight, RBC, and hematocrit values were calculated from individual values taken from all surviving mice at each specific time point. Results are expressed as the mean values ± standard deviation (SD) of six mice (n = 6). Ordinary one-way analysis of variance (ANOVA) with Tukey's test was used for the comparison of parasitemia between Br and co-infected groups, Two-way ANOVA followed by Tukey`s multiple comparison test was used for the analysis of clinical score, whereas for the survival analysis the Kaplan-Meier non-parametric model was used. Asterisks indicate statistical significance (*$P < 0.05$; **$P < 0.01$; ***$P < 0.001$).
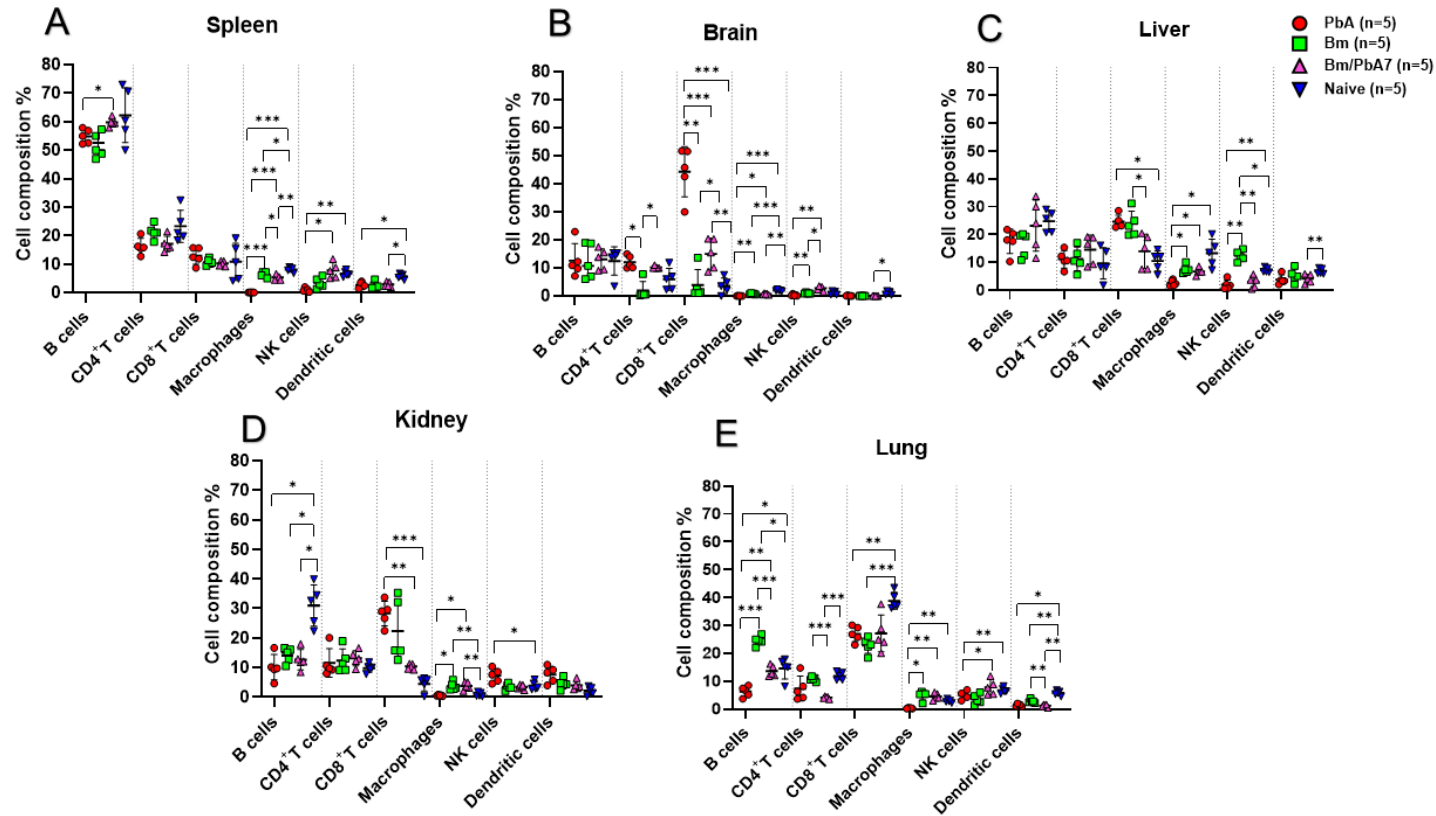
Figure 2.5. A subsequent trial conducted to perform immunophenotyping of different types of immune cells in mice spleen, brain, liver, kidney and lungs at day 8 post-challenge infection based upon surface markers by FACS. (A) Spleen (B) Brain, (C) Liver, (D) Kidney, and (E) Lungs in PbA, Bm, Bm/PbA7, and Naïve mice (n=5). Markers used were CD45+ CD3+ cells (T cells), CD45+ CD19+ cells (B cells), CD45+ CD49b+ cells (natural killer cells), CD45+ CD11c+cells (dendritic cells), and CD45+ F4/80+ cells (macrophages). Analysis of variance (ANOVA) followed by post hoc Tukey's multiple comparison test. The percentage population of each cell type is presented as mean ± SD. Asterisks indicate statistical significance (* $P < 0.05$; ** $P < 0.01$; *** $P < 0.001$).
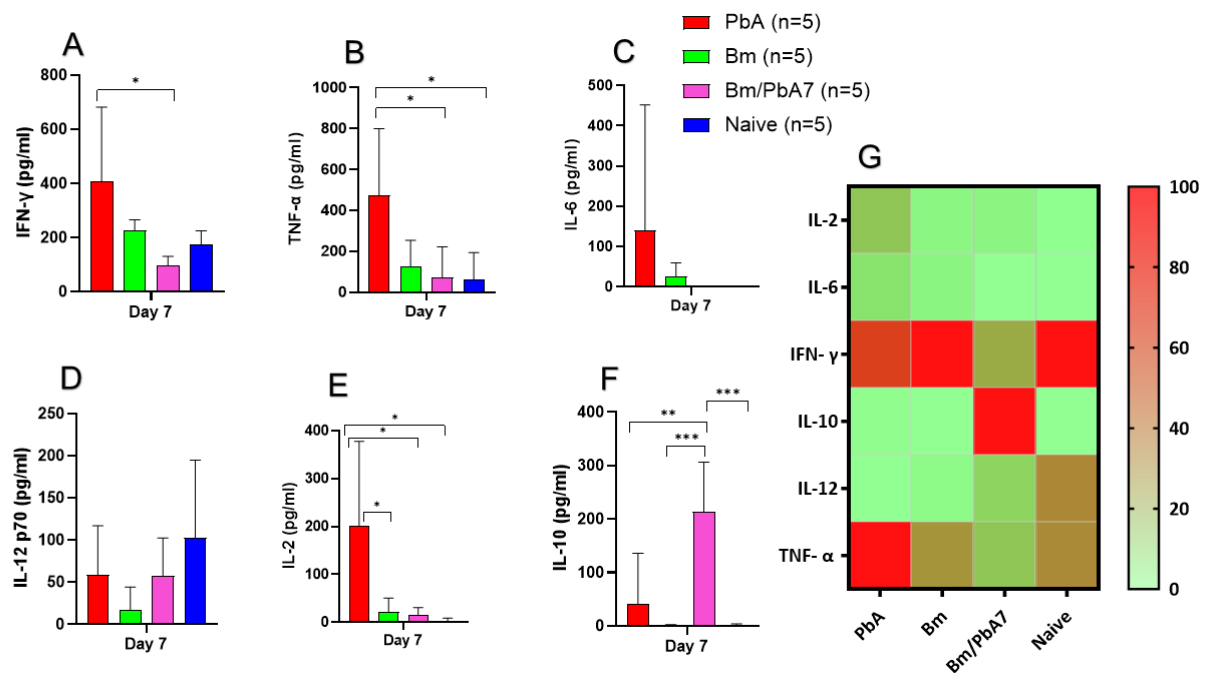
Figure 2.6. The kinetics of serum cytokines of experimental PbA, Bm, Bm/PbA7, Naïve mice groups (n=5). Test C57BL/6J mice were initially infected with B. microti and then challenge infected with *P. berghei* at day 8 post-primary infection. Serum was collected from all groups at day 8 pci and levels of (A) IFN- g, (B) TNF-a, (C) IL-6, (D) IL-12p70, (E) IL-2, and (F) IL-10 were measured. (G) Heatmap representing the progression of secretion of the six cytokines. The results are expressed as means ± SD. Ordinary one-way analysis of variance (ANOVA) with Tukey's test was used for the statistical analysis. Asterisks denote statistical significance ($*P < 0.05$; $**P < 0.01$; $***P < 0.001$).
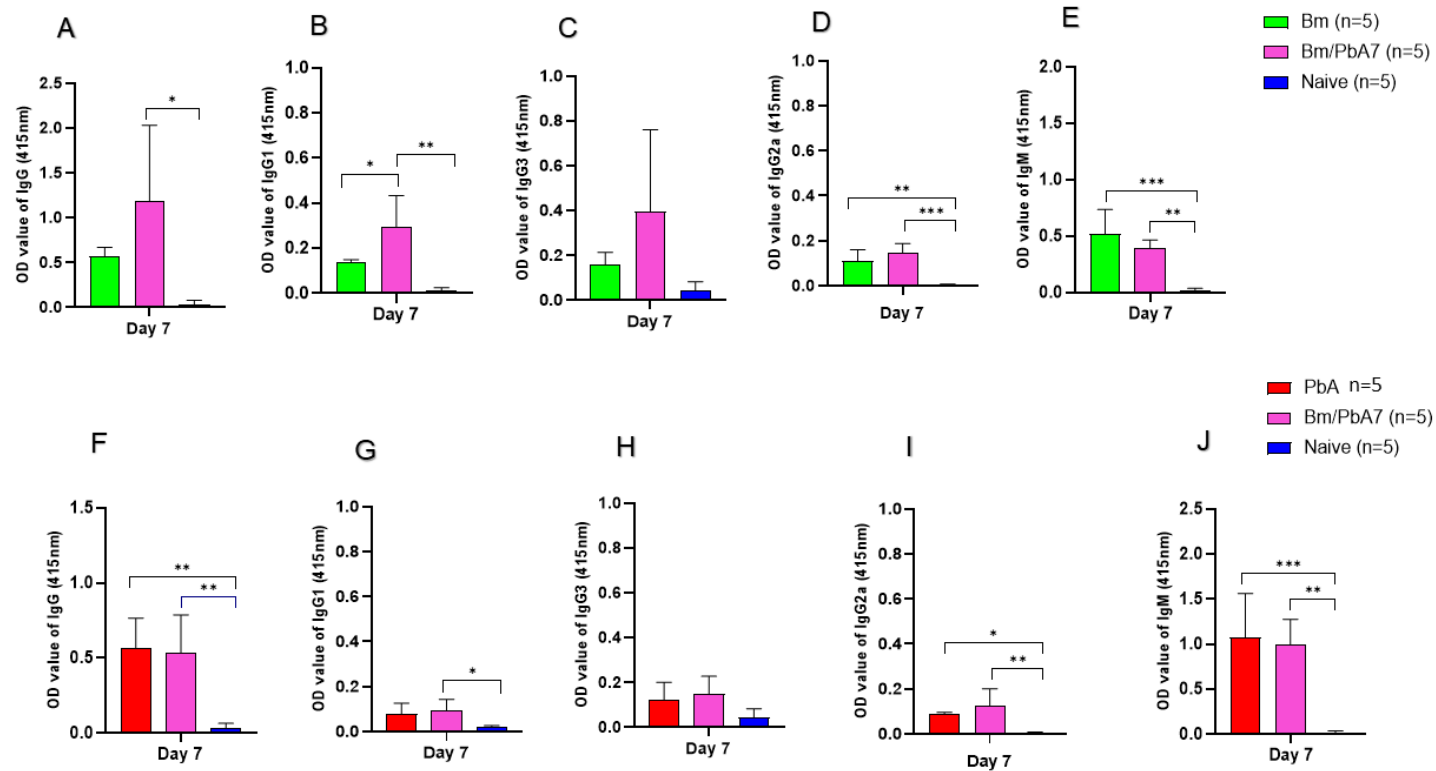
Figure 2.7. The dynamics of serum antibodies against *B. microti* and *P. berghei* in Bm, PbA mice, Bm/PbA7, and Naïve mice groups (n=5). The production of (A), IgG (B), IgG1 (C), IgG3 (D), IgG2a and (E), IgM showed B. microti-specific while (F), IgG (G), IgG1 (H), IgG3 (I), IgG2a and (J), IgM showed *P. berghei*-specific antibodies in mice serum collected at day 8 pci post-challenge infection. Results of ELISA indicated a significant increase in the specific antibodies in the serum of co-infected mice. Ordinary one-way analysis of variance (ANOVA) with Tukey's test was used for the statistical analysis. Asterisks indicate statistically significant differences (*, $P < 0.05$; **, $P < 0.005$; ***, $P < 0.0001$. The results are expressed as mean values ± the SD for five mice.
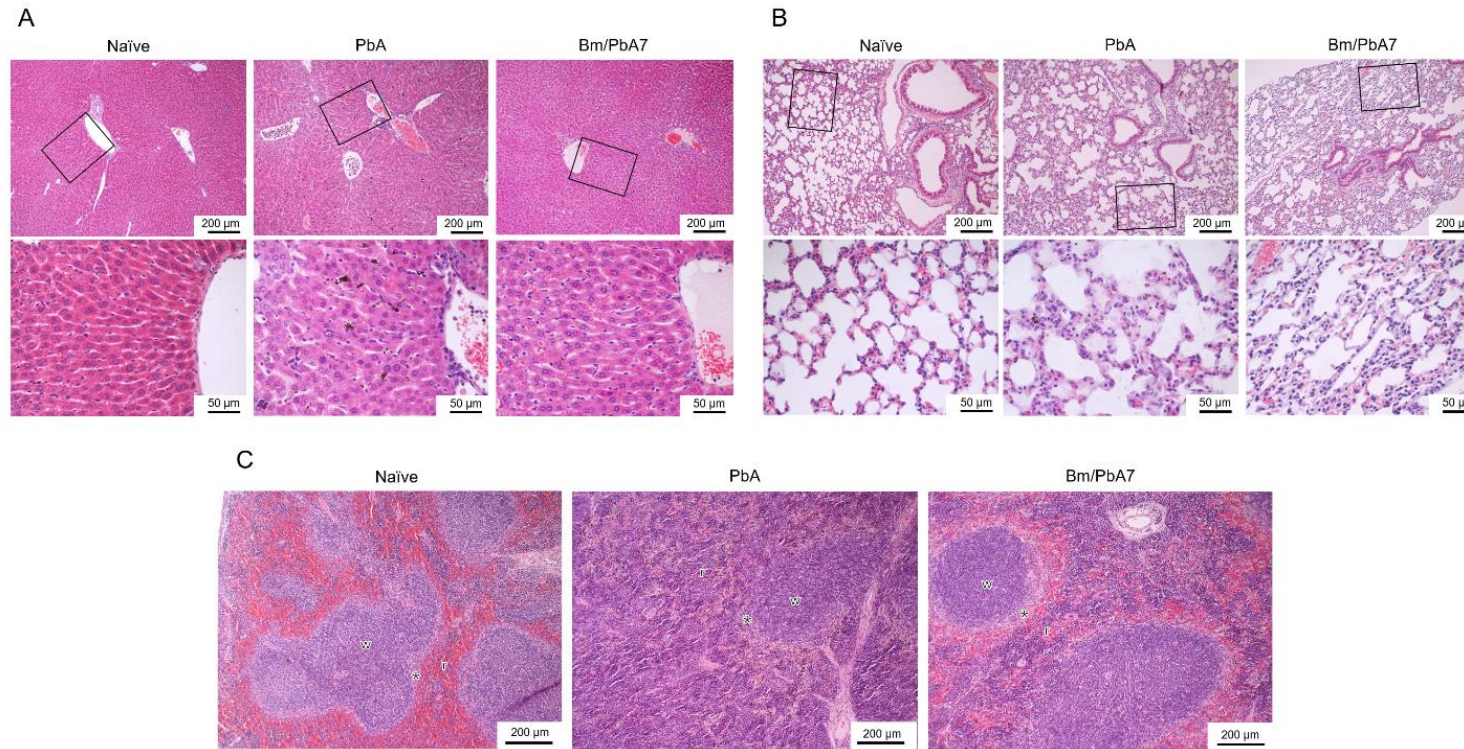
Figure 2.8. Histopathological analysis of the (A) liver, (B) lung, and (C) spleen depicting the impact of *P. berghei* and Bm/PbA7 mice compared to Naïve mice (n=1). Sections of 5 μm thickness were collected and stained with H & E. Black boxes indicate (A) Naïve mice showed liver lobules with an orderly arrangement of hepatocyte plates. This arrangement and morphology of hepatocytes were severely damaged in PbA mice livers, in Bm/PbA7 mice morphology was normal. (B) Lung of Naïve mice had intact structure, containing pulmonary alveoli separated by thin septa. PbA mice showed severe and moderate interstitial pneumonia, with the thickening of the interstitium. Mild abnormality was seen in the Bm/PbA7 mice. (C) Naïve mice spleen showed distinct red (r) and white (w) pulps, PbA mice indicated the blurred boundary between red and white pulp because of repletion of immune cells in the red pulp. In Bm/PbA7 mice spleen, the marginal zone (*) distinguished by the white pulp clearly.
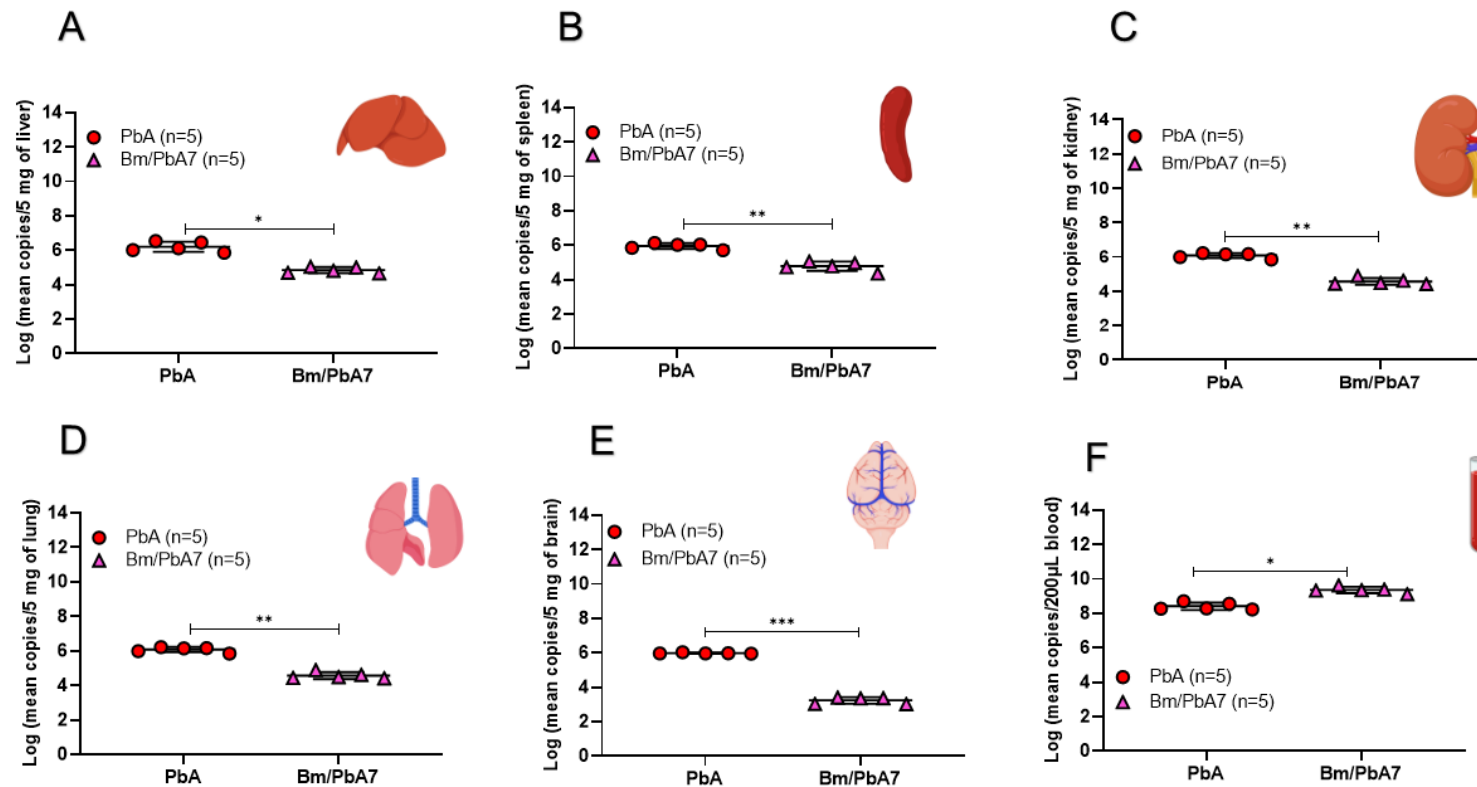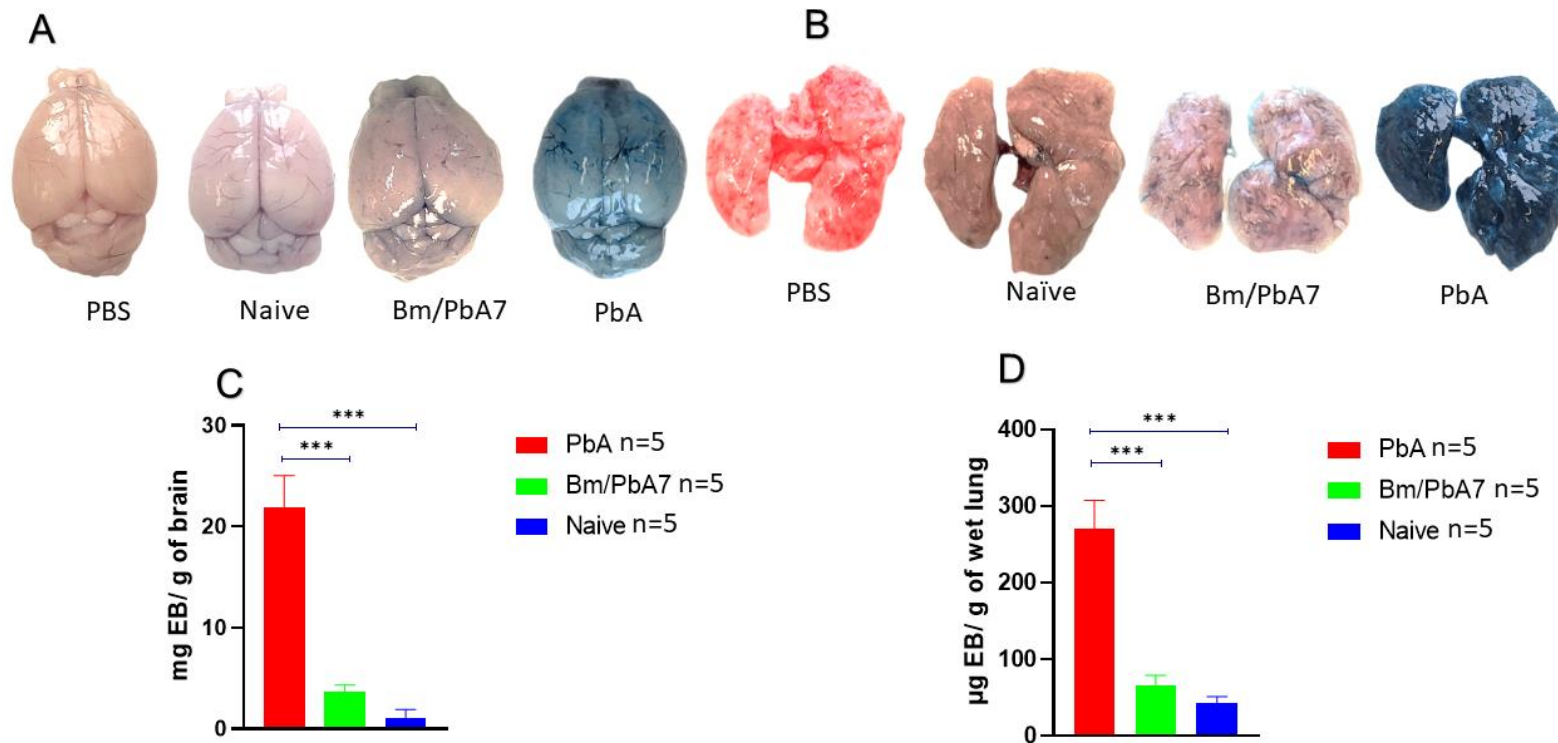
Figure 2.9. Measure of *P. berghei* burden in mice (A) Liver (B) Spleen, (C) Kidney, (D) Lung, (E) Brain, and (E) Blood of PbA and Bm/PbA7 mice (n=5). Mean copy numbers of *P. berghei* 18S in mouse DNA samples (n = 5 per group at day 8 post-challenge infection) were transformed to log values. Bm/PbA7 mice have less sequestration of *P. berghei* in organs than PbA mice. Individual values are the mean of duplicate samples. Log values were analyzed using one-way ANOVA and Tukey's multiple comparison post hoc test; ***$P < 0.001$.

Figure 2.10. Second trial was conducted employing PbA, Bm/PbA7 and Naïve mice (n=5). Following the protocol as described in the method section harvested brains and lungs from mice were weighed, and photographed. The morphology and color of the (A) brain (B) lungs. The amount of Evans blue dye that infiltrated the (C) brain and (D) lungs was measured. Co-infected mice showed less extravasation of Evans blue dye in the brain and lungs as compared to the PbA mice. Analysis of variance (ANOVA) followed by post hoc Tukey's multiple comparison test. Results are expressed as means ± SD. Asterisks indicate statistical significance (*$P < 0.05$; **$P < 0.01$; ***$P < 0.001$).

General discussion

In the realm of parasitic diseases, co-infections can be particularly challenging to unravel due to their potential to elicit complex and intertwined immune responses. This complexity is exemplified in the co-infection of rodents with two protozoan parasites: *Babesia* and *Plasmodium*. Two separate research projects have been conducted to investigate co-infections involving both *Babesia* and *Plasmodium* parasites and their impact on disease outcomes, immune responses, and related pathologies, as well as the potential for cross-protection against severe malaria.

In the first study, the immune mechanisms responsible for protection against *Babesia* and the consequences of co-infections were explored to examine the impact of *B. microti* acute co-infection on *B. rodhaini*. The findings of this study demonstrated that *B. microti* primary infection had a mitigating effect on parasitemia peaks while exacerbating anemia in *B. rodhaini*-challenged mice. In contrast, mice infected solely with *B. rodhaini* exhibited a rapid increase in parasitemia and exacerbated anemia (Wang et al., 2016). These results validated the previously established cross-protection observed during chronic *B. microti-B. rodhaini* co-infections and elucidated that this phenomenon commences at a specific point during the acute stage co-infection. The role of mature erythrocytes in curtailing parasitemia was also highlighted (Li et al., 2012). A decline in antibody production during the acute co-infection phase was observed in the results, consistent with findings from a previous study (Li et al., 2012). Previous *B. microti-B. rodhaini* co-infection studies did not address dynamics of the spleen in co-infected models. Spleen disorganization and splenomegaly are known to occur during human and murine malaria infections, driven by innate immune activation, monocytic cell expansion, and the removal of infected red blood cells (RBCs) (Weiss, 1989; Weiss et al., 1989; Villeval et al., 1990). These structural alterations, especially in the germinal centers of the spleen, can affect antibody responses during malaria and influence the development of immunity (Cadman et al., 2008). *B. microti* infection activates macrophages early in the infection, which helps control parasite replication (Terkawi et al., 2015). Studies have shown that *B. microti* can confer immunity against other *Babesia* and *Plasmodium* infections, primarily through macrophages (Li et al., 2012; Efstratiou et al., 2020). The results of this study support these findings, with a significant increase in the macrophage population in splenocytes during co-infection (Li et al., 2012; Djokic et al., 2018a). Additionally, histopathology

observations confirmed the impact on spleen structure. However, B and T cell populations decreased during co-infection, consistent with previous studies (Djokic et al., 2018a; Djokic et al., 2019). This highlights the role of innate immunity during the acute phase of *Babesia* co-infection in mouse models. IFN-γ and IL-10, classic double-edged sword cytokines, were found to have varying levels in cross-protected mice compared to control mice (Li et al., 2012). The study showed that elevated IL-10 levels may have contributed to relatively lower levels of IFN-γ and TNF-α in co-infected mice, affecting the outcome (Li et al., 2012). The consequence of IL-10 production depends on the timing, location, and the cell type producing it (Kumar et al., 2019). Lower IFN-γ production during co-infection may have contributed to reduced parasitemia and increased survival (Li et al., 2012). High ROS levels in *B. rodhaini*-infected mice may have contributed to erythrocyte lysis, leading to severe pathology (Li et al., 2012). The role of oxidative stress and ROS during malaria remains a subject of debate, with oxidative stress potentially exerting both protective and pathophysiological effects (Percário et al., 2012). These findings contribute to our understanding of the host's immune response during co-infection and highlight the complex interplay of various factors that can influence the outcome of *Babesia* infections.

The second study aimed to explore the impact of co-infections on the development and evasion of severe malaria and related pathologies. Evidence of pathological changes in various organs, anemia, and tissue-sequestration of parasites in mice has been documented (Briquet et al., 2015). This research highlighted the modification of disease outcomes and immune responses in a mouse co-infection model. The Bm/PbA7 mice exhibited high parasitemia levels at the onset of *B. microti* infection, which was believed to activate innate immunity early. *P. berghei*, known for its preference for reticulocytes, resulted in an increased parasite burden and, consequently, severe anemia. The sequestration of *Plasmodium* in tissues, particularly the lungs, was associated with pulmonary pathology. The infection of hepatocytes by *Plasmodium* sporozoites led to congestion, sinusoidal blockage, and cellular inflammation (Al-Salahy et al., 2016).

The intensity of malaria-induced lung pathology was proportional to the levels of iRBC sequestration. Organ damage observed in PbA mice, including in the brain, liver, and lungs, was attributed to diminished microcirculatory blood flow caused by structural and functional changes in iRBCs (Dondorp et al., 2000). This allowed the parasites to evade the host's immune

response by infiltrating organs and reducing immunogenicity. Higher parasite loads were associated with the development of brain, lung, and liver diseases during malaria (Bagot et al., 2002; Haque et al., 2011; Strangward et al., 2017). Notably, the qPCR results indicated lower sequestration of *P. berghei* in co-infected mice's organs compared to PbA mice, explaining the prolonged survival and reduced severity of malaria in co-infected mice. Macrophages were identified as crucial cells in the host's immune response against malaria infections, involved in phagocytosis and cytokine release. Mice lacking macrophages experienced more malaria complications, indicating the critical role of macrophages in immunity (Gupta et al., 2016). Co-infected mice exhibited increased innate immune cell populations compared to PbA mice, suggesting that the innate immune response determined the outcome of infection, depending on the organ. This provides insight into the mechanisms modulating macrophage activation (Ozarslan et al., 2019). In the context of cerebral malaria, CD8+ T cells and iRBC sequestration in the brain were essential for the progression of experimental cerebral malaria (ECM). Brain endothelial cells activated CD8+ T cells, leading to BBB disruption (Baptista et al., 2010). Higher infiltration of CD8+ T cells in the brain, liver, and lungs was observed in PbA mice compared to co-infected mice, explaining the multi-organ injury in PbA mice (Grau et al., 1986; Belnoue et al., 2002; Haque et al., 2011). The balance between pro-inflammatory and anti-inflammatory responses played a crucial role in determining disease outcomes. IL-10 production by tissue-resident macrophages protected against tissue injury in malaria. A low pro-inflammatory response allowed unrestrained parasite replication, while an excessive pro-inflammatory response led to tissue damage. The cytokine results indicated that IL-10 protected against ECM, while high levels of pro-inflammatory cytokines, such as IFN-γ and IL-12, were associated with pathology (Trinchieri, 2007; Couper et al., 2008; Redpath et al., 2014).

Overall, these two studies provide comprehensive insights into the complexities of co-infections involving *Babesia* and *Plasmodium* parasites. They highlight the interplay between the parasites, the immune responses of the host, and the resulting disease outcomes. The findings emphasize the potential for cross-protection, the influence of parasite load, the importance of macrophages, and the delicate balance between pro- and anti-inflammatory responses. These insights are critical for understanding the mechanisms of co-infections and could inform the development of more effective strategies for managing and preventing these debilitating diseases in the future.

General summary

Babesiosis and malaria are two significant vector-borne diseases that cause high morbidity and mortality, particularly in immunocompromised individuals. Babesiosis causes high morbidity and mortality in immunocompromised individuals. Previous studies suggested that lethal *Babesia rodhaini* and *Plasmodium* infection in murine can be evaded by *Babesia microti* primary infection via activated macrophage-based immune response. On the other hand, malaria remains one of the most significant health issues worldwide, accounting for 2.6% of the total global disease burden, and efforts to eliminate this threat continue. Key focus of global research is to develop an efficient and long-term immunity to this disease via vaccination or therapeutic approach, and innovative strategies would enable us to achieve this target. This study aimed to investigate the immune dynamics and pathology associated with acute co-infection of these two diseases in murine models.

Chapter 1 focused on the interaction between two species of *Babesia*, *Babesia microti*, and *Babesia rodhaini*, of different pathogenicity. This study was planned to investigate the immune dynamics and pathology associated with acute co-infection of these two diseases in murine models. Female wild-type BALB/c mice were used to investigate the dynamics of *Babesia* infections. *Babesia microti* (Munich strain) and *Babesia rodhaini* (Australia strain) stabilates were utilized for intraperitoneal infections. Mice were infected with *B. microti* and subsequently challenged with *B. rodhaini* at different time points. Parasitemia, body weight, hematocrit values, and survival rates were monitored regularly. Immunofluorescence microscopy and flow cytometry were employed to assess the immune response and cell populations. Spleen histopathological analysis examined tissue changes, and serum cytokines and antibody responses were quantified. Absolute quantification of *B. rodhaini* parasites was performed using real-time PCR. These comprehensive methods shed light on the interactions and immune responses in co-infections of *Babesia* parasites. It was found that primary infection with *B. microti* during the chronic stage of *B. rodhaini* infection resulted in significantly attenuating parasitemia and conferring immunity against the challenge infection. This attenuation was marked by a decrease in splenic B and T cells, a reduction in antibody levels, and a decline in humoral immunity. Interestingly, increased populations of macrophages and natural killer cells were observed, suggesting their subtle role in protection. The cytokines IFN-γ and IL-10 were found to be major players in the lethality caused by *B. rodhaini* infection.

Even a two-day delay in challenge infection had a significant impact on the resulting pathology. Oxidative stress in the form of reactive oxygen species also contributed to disease severity. Histopathological examination revealed differences in the spleen's marginal zone between *B. rodhaini* infection and co-infection. Further research is needed to investigate the roles of various immune cell subtypes in the protection of co-infected hosts.

Chapter 2 aimed to understand the impact of acute *B. microti* Peabody mjr and *Plasmodium berghei* ANKA co-infection on the consequence of complicated malaria in the C57BL/6J mouse model of malaria. In the conducted research, mice were divided into several groups, including *B. microti*-infected (Bm), co-infected (Bm/PbA7), *P. berghei*-infected (PbA), and a Naïve control group. Parasitemia, body weight, RBCs, and hematocrit, were regularly monitored. Survival rates and experimental cerebral malaria (ECM) were assessed. Flow cytometry was used to determine the immunophenotype of various organs. Pathological features were examined for the extent of tissue damage. Serum cytokine levels were quantified, and humoral immunity was evaluated through ELISA. Absolute quantification of *P. berghei* parasites was performed by qPCR. The Evans Blue assay assessed blood-brain barrier disruption and lung vascular integrity. These methods allowed for a comprehensive investigation of the impact of co-infection on the immune response and pathology in the murine models of babesiosis and malaria. Bm/PbA7 mice survived longer than PbA mice. All the PbA mice succumbed to infection within day 12. It was established that acute *B. microti* infection activated immunity which was otherwise suppressed by *P. berghei*. The immunosuppressive tissue microenvironment was counteracted as evidenced by the enhanced immune cell population in co-infected mice, in contrast to *P. berghei*-infected control mice. Parasite sequestration in the brain, liver, lung, and spleen of co-infected mice was significantly decreased and tissue injury was ameliorated. Meanwhile, the serum levels of IFN-γ, TNF- α, and IL-12p70 were reduced while the secretion of IL-10 was promoted in co-infected mice. Eventually, co-infected mice showed an extended rate of survival. Hereby, the principal cytokines associated with the severity of malaria by *P. berghei* infection were TNF- α, IFN-γ, and IL-12p70. Moreover, it was evident from our flow cytometry results that innate immunity is crucial against *P. berghei* infection. This study recommended further investigations to shed light on the effects of babesiosis in suppressing malaria with the goal of developing *Babesia*-based therapy against malaria.

In conclusion, these studies explore the immune responses and pathological features of co-infection with *Babesia* and *Plasmodium*. The results of this research shed light on potential strategies for mitigating the impact of these diseases, characterized by innate immunity being crucial in providing protection and macrophages at the frontline of protection. These findings warrant future research to explore the potential of using *Babesia*-based therapy to suppress babesiosis and malaria and improve survival rates with the aim of developing novel therapeutic tools to control these diseases.

和文要約

バベシア症とマラリアは、特に免疫不全の人に高い罹患率と死亡率を示す2つ
の重要なベクター媒介性疾患である。 バベシア症は、免疫不全の人に高い罹患率と
死亡率を示す。以前の研究では、マウスにおける致死性の *Babesia rodhaini* 感染は、
感染の慢性期に活性化されたマクロファージに基づく免疫反応を介して *B. microti* の
一次感染によって回避できることが示唆されている。一方で、マラリアは依然とし
て世界で最も重大な健康問題の一つであり、世界全体の疾病の 2.6% を占めており、
この脅威を排除する取り組みが続けられている。世界的な研究の主な焦点は、ワク
チン接種または治療アプローチを通じてこの病気に対する効率的制御法を開発する
ことであり、革新的な戦略によりこの目標の達成を可能とする。この研究は、マウ
スモデルにおけるこれら2つの疾患の急性同時感染に関連する免疫動態と病理を調査
することを目的として行われた。

第 1 章では、2 種のバベシア間の相互作用に焦点を当て、*B. microti* (ミュンヘ
ン株) と *B. rodhaini* (オーストラリア株) の安定系統を腹腔内感染に利用した。雌の野
生型 BALB/c マウスを *B. microti* に感染させ、その後、さまざまな時点で *B. rodhaini*
を感染させた。 感染率、体重、ヘマトクリット値、生存率の定期的なモニタリング
を行った。免疫蛍光顕微鏡法とフローサイトメトリーにより、免疫応答と細胞集団
を評価した。 脾臓の組織病理学的分析により組織変化を検査し、血清サイトカイン
と抗体反応を定量化した。リアルタイム PCR により *B. rodhaini* 定量化が行われた。
これらの包括的な方法は、バベシア原虫の同時感染における相互作用と免疫応答に
焦点を当てる。*B. rodhaini* 感染の慢性期における *B. microti* の一次感染により、感染
率が大幅に軽減し、攻撃感染に対する免疫が付与されることが判明した。この弱毒
化は、脾臓の B 細胞および T 細胞の減少、抗体レベルの低下、および体液性免疫の

低下によって特徴付けられる。興味深いことに、マクロファージとナチュラルキラー細胞の集団の増加が観察され、防御におけるそれらのな役割が示唆された。サイトカイン IFN-γ および IL-10 は、*B. rodhaini* 感染によって引き起こされる致死率に主要な要因となる。活性酸素種の形での酸化ストレスも疾患の重症化に寄与する。組織病理学的検査により、*B. rodhaini* 感染と同時感染では脾臓の辺縁領域に違いがあることが明らかになった。同時感染した宿主の防御におけるさまざまな免疫細胞サブタイプの役割を調査するには、さらなる研究が必要となる。

　　第 2 章では、C57BL/6J マウスモデルにおける急性 *B. microti* (Peabody mjr) と *Plasmodium berghei* ANKA の同時感染が複雑性マラリアに及ぼす影響の理解を目的とした。マウスを、*B. microti* 感染 (Bm)、同時感染 (Bm/PbA7)、*P. berghei* 感染 (PbA)、およびナイーブ対照グループを含むいくつかのグループに分けた。感染率、体重、赤血球、ヘマトクリット、免疫細胞集団の定期的なモニタリングを行った。生存率と実験的脳マラリア (ECM) を評価した。さまざまな臓器の免疫表現型を決定するためフローサイトメトリーを利用した。組織の損傷を調べるために組織病理学を行った。血清サイトカインレベルを定量化し、ELISA によって体液性免疫を評価した。*P. berghei* の絶対定量を qPCR によって実行した。エバンスブルーアッセイでは、血液脳関門の破壊と肺血管の不整合を評価した。これらの方法により、バベシア症とマラリアのマウスモデルにおける免疫応答と病理に対する同時感染の影響を包括的に調査することが可能となった。急性 *B. microti* 感染は、*P. berghei* によって抑制されていた免疫を活性化した。同時感染したマウスの免疫細胞集団は増強され、脳、肝臓、肺、脾臓における寄生虫の隔離が減少し、組織損傷が減少した。サイトカイン分析により、TNF-α、IFN-γ、IL-12p70 が *P. berghei* 感染によるマラリアの重症度に関連する主要なサイトカインであることが示された。自然免疫、特にマクロファージは、

P. berghei 感染に対する防御において重要な役割を果たした。

　　結論として、これらの研究は、バベシアとプラスモディウムの同時感染の免疫応答と病理学的特徴の調査を行った。これらの発見は、バベシア症とマラリアを抑制し、最終的には生存率を改善し、これらの疾患を制御するための新しい治療ツールを開発するために、有意義な基礎データを提供するものと考えられる。

Acknowledgements

My academic journey has been an incredible odyssey, filled with profound moments, transformative experiences, and enduring friendships. I extend my heartfelt appreciation to those whose support, guidance, and inspiration have been instrumental in shaping this endeavor. My journey to doctoral studies was illuminated in 2017 when I joined the JICA program at OBIC. On one unforgettable day, during one of the breaks in my training for the JICA Cattle Management course, I had the privilege of meeting Prof. Xuan Xuenan, whose benevolence and wisdom set the stage for a remarkable journey. His mentorship transcended the boundaries of academia, offering me invaluable support and wisdom. Even before formally becoming my supervisor, he guided me with such grace that I was able to secure the highly competitive Embassy-sponsored MEXT scholarship, turning a cherished dream into reality.

My gratitude to Prof. Xuan Xuenan knows no bounds, for he has not only been my supervisor but also a beacon of wisdom and mentorship. He embodies excellence both as a dedicated researcher and a distinguished educator. His encouragement allowed me to focus on intensive Japanese language studies before starting my research, a crucial foundation for my life in Japan. I am grateful to him for providing me with the opportunity to work in his distinguished laboratory and for becoming a guiding light in my life in Japan. Under his guidance, I had the privilege of not only conducting research but also participating in a multitude of academic and cultural activities that enriched my doctoral experience. His profound insights and wealth of knowledge have been instrumental in my growth as a researcher and an individual. His enduring encouragement and the opportunities he provided, allowed me to flourish in myriad ways, facilitating my academic and personal development. I am profoundly fortunate to have a supervisor who not only believed in my potential but also nurtured it with dedication and kindness.

My journey through the vast realms of knowledge was further enriched by the wisdom and guidance of my co-supervisors, Prof. Nishikawa Yoshifumi and Prof. Igarashi Makoto. Their scholarly counsel, advice and constructive comments have been instrumental in shaping my research. I extend my appreciation to all the researchers at NRCPD including Prof. Kawazu Shin-ichiro, Prof. Inoue Noboru, Prof. Yokoyama Naoaki, Prof. Suzuki Hiroshi, Associate Prof. Umemiya-Shirafuji Rika, Associate Prof. Fukumoto Shinya, Associate Prof. Asada Masahito

and Assistant Prof. Suganuma Keisuki for their invaluable professional engagements and for cultivating NRCPD into a hub of literary and scholarly excellence. I am sincerely thankful to Associate Prof. Kondoh Daisuke for his indispensable and prompt assistance in histopathology, which was instrumental in the successful completion of this research.

The generosity of the Ministry of Education, Culture, Sports, Science, and Technology (MEXT) in funding my research and making my life in Japan comfortable cannot be overstated. My heartfelt appreciation goes to MEXT for their support. My doctoral odyssey commenced with the earnest study of the Japanese language at Hokkaido University, and for this, I am eternally grateful. I extend my heartfelt appreciation to my Japanese language teachers, including Yamashita sensei, Suzuki sensei, Yakata sensei, Yoshida sensei, and Morioka sensei. Their dedication and expertise not only unlocked the doors to communication but also facilitated my immersion in the rich tapestry of Japanese culture.

It is said that anyone who teaches you even a single word is your teacher. In this spirit, I am indebted to my fellow labmates, past and present, for their collective knowledge and support. I acknowledge my esteemed seniors, Dr. Ehab Mosad, Dr. Mingming Liu, Dr. Hassan Hakimi, Dr. Abdelbaset, Dr. Hanan, Dr. Taniguchi, Dr. Tuvshee, and Dr. Ali Raza, whose guidance and invaluable insights have been the pillars of my research journey. I also extend my gratitude to the dedicated staff of the National Research Center for Protozoan Diseases (NRCPD) Mr. Habaguchi san, Ms. Ai Shindo san, Ms. Kanomata san, Ms. Fujioka san for their tireless support and cooperation to carry out research smoothly. To the devoted staff of the International Office, and Admissions and Educational Affairs section, including Chiba san, Hara san, Hattori san, Shizuka san, Nishida san and Ishiyama san who provided me with prompt support and assistance and made the transition to life in Japan seamless, I offer my sincere thanks. I express my gratitude to the entire faculty at OUAVM, with special acknowledgment to Associate Prof. Marshall Smith, a scholarly gem, whom I had the privilege of getting acquainted with during my time as a JICA participant. His profound scholarly engagements, support, and mentorship have played a pivotal role in shaping my academic journey. I will never forget my kind friends, Maki Ishiwata and Pooh, for always being there for me. You are a true example of 'a friend in need is a friend indeed!'. My friends, Chisako, Airi, Shingo, Kazuko, and Sara, I am thankful for your support, invaluable help and the laughter we shared.

In moments of challenge and triumph, my family, mom, sister and brother have been my anchor.

I am deeply thankful to my mother, who has been my persistent source of strength, my rock, and my forever constant. This dissertation is dedicated to my late father, whose absence is felt acutely, yet whose memory has been an enduring source of inspiration. I know he would have been overjoyed to witness this milestone, and his spirit continues to illuminate my path. Finally, I am always thankful to the one and only God for guiding my path and bestowing me with the strength, wisdom, and relentless determination to pursue my dreams. I am profoundly thankful for the blessings and opportunities that have illuminated my journey thus far.

With a heart full of appreciation and humility, once again, I express my heartfelt thanks to all those who have played a role, however small or significant, in my academic and personal journey. This dissertation is a testament to the collective effort and support that have made this moment possible. Thank you and may God's grace continue to shine upon us all!

<div align="center">

اَلْحَمْدُ لِلّٰهِ

</div>

References

Aguilar-Delfin I, Wettstein PJ, Persing DH (2003). Resistance to acute babesiosis is associated with interleukin-12- and gamma interferon-mediated responses and requires macrophages and natural killer cells. Infect Immun, 71(4), 2002–2008. doi: 10.1128/IAI.71.4.2002-2008.2003

Ahmed J (2002). The role of cytokines in immunity and immunopathogenesis of piroplasmoses. Parasitol Res, 88, S48–S50. doi: https://doi.org/10.1007/s00436-001-0573-4

Ahn MH (2010). Imported parasitic diseases in Korea. Infect Chemother, 42, 271. doi: 10.3947/ic.2010.42.5.271

Al-Salahy M, Shnawa B, Abed G, Mandour A, and Al-Ezzi A (2016). Parasitaemia and its relation to hematological parameters and liver function among patients malaria in Abs, Hajjah, Northwest Yemen. Interdiscip Perspect Infect Dis, 2016, 1–5. doi: 10.1155/2016/5954394

Bayne LJ, Vonderheide RH (2013). Multicolor flow cytometric analysis of immune cell subsets in tumor-bearing mice. Cold Spring Harb Protoc, 2013, pdb-prot077198. doi:10.1101/pdb.prot077198

Bagot S, Idrissa Boubou M, Campino S, Behrschmidt C, Gorgette O, Guénet JL, Guénet, J.-L., Penha-Gonçalves C, Mazier D, Pied S, & Cazenave P-A (2002). Susceptibility to experimental cerebral malaria induced by *Plasmodium berghei* ANKA in inbred mouse strains recently derived from wild stock. Infect Immun, 70, 2049–2056. doi: 10.1128/IAI.70.4.2049-2056.2002

Baptista, FG, Pamplona, A, Pena, A C, Mota, MM, Pied, S, and Vigário, AM (2010). Accumulation of *Plasmodium berghei*-infected red blood cells in the brain is crucial for the

development of cerebral malaria in mice. Infect Immun, 78, 4033–4039. doi: 10.1128/IAI.00079-10

Beiting DP (2014). Protozoan parasites and type I interferons: a cold case reopened. Trends Parasitol, 30, 491–498. doi: 10.1016/j.pt.2014.07.007

Belnoue E, Kayibanda M, Vigario AM, Deschemin J-C, Rooijen NV, Viguier M, Snounou G, & Rénia, L (2002). On the pathogenic role of brain-sequestered αβ CD8+ T cells in experimental cerebral malaria. J Immunol, 169, 6369–6375. doi: https://doi.org/10.4049/jimmunol.169.11.6369

Briquet S, Lawson-Hogban N, Boisson B, Soares M P, Péronet R, Smith L, Ménard R, Huerre M, Mécheri S, & Vaquero C (2015). Disruption of parasite hmgb2 gene attenuates *Plasmodium berghei* ANKA pathogenicity. Infect Immun, 83, 2771–2784. doi: 10.1128/IAI.03129-14

Bloch EM, Kumar S, Krause PJ (2019). Persistence of *Babesia microti* infection in humans. Pathogens, 8, 102. doi:10.3390/pathogens8030102

Borggraefe I, Yuan J, Telford SR, 3rd, Menon S, Hunter R, Shah S, Spielman A, Gelfand JA, Wortis HH, & Vannier, E (2006). *Babesia microti* primarily invades mature erythrocytes in mice. Infect Immun, 74, 3204–3212. doi: 10.1128/IAI.01560-05

Bock R, Jackson L, De Vos A, & Jorgensen W (2004). Babesiosis of cattle. Parasitol, 129(S1), S247–S269. doi: https://doi.org/10.1017/S0031182004005190

Bonnet SI, & Nadal C (2021). Experimental infection of ticks: an essential tool for the analysis of *Babesia* species biology and transmission. Pathogens, 10(11), 1403. doi: https://doi.org/10.3390/pathogens10111403

Brown H, Turner G, Rogerson S, Tembo M, Mwenechanya J, Molyneux M, & Taylor T (1999). Cytokine expression in the brain in human cerebral malaria. J Infect Dis, 180(5), 1742–1746. doi: https://doi.org/10.1086/315078

Bronte V, Pittet MJ (2013). The spleen in local and systemic regulation of immunity. Immunity, 39, 806–818. doi:10.1016/j.immuni.2013.10.010

Cadman ET, Abdallah AY, Voisine C, Sponaas A-M, Corran P, Lamb T, Brown D, Ndungu F, Langhorne J (2008). Alterations of splenic architecture in malaria are induced independently of Toll-Like Receptors 2, 4, and 9 or MyD88 and may affect antibody affinity. Infect Immun, 76, 3924–3931. doi:10.1128/IAI.00372-08

Carroll RW, Wainwright MS, Kim K-Y, Kidambi T, Gómez ND, Taylor T, & Haldar, K (2010). A rapid murine coma and behavior scale for quantitative assessment of murine cerebral malaria. PLoS ONE, 5, e13124. doi: 10.1371/journal.pone.0013124

Cella W, Baia-da-Silva DC, Melo GCD, Tadei WP, Sampaio VDS, Pimenta P, Lacerda MVG, & Monteiro WM (2019). Do climate changes alter the distribution and transmission of malaria? Evidence assessment and recommendations for future studies. Rev Soc Bras Med Trop, 52, e20190308. doi: 10.1590/0037-8682-0308-2019

Chen Z, Quan L, Huang A, Zhao Q, Yuan Y, Yuan X, Shen Q, Shang J, Ben Y, Qin FX-F, & Wu A (2018). seq-ImmuCC: Cell-centric view of tissue transcriptome measuring cellular compositions of immune microenvironment from mouse RNA-Seq data. Front Immunol, 9, 1286. doi: 10.3389/fimmu.2018.01286

Claser C, Nguee SYT, Balachander A, Wu Howland S, Becht E, Gunasegaran B, Hartimath SV, Lee AWQ, Theng Theng Ho J, Bing Ong C, Newell EW, Goggi J, Guan Ng L, Renia L (2019). Lung endothelial cell antigen cross-presentation to CD8+T cells drives malaria-associated lung injury. Nat Commun, 10, 4241. doi: 10.1038/s

Couper KN, Blount DG, & Riley EM (2008). IL-10: the master regulator of immunity to infection. J Immunol, 180(9), 5771–5777. doi: 10.4049/jimmunol.180.9.5771

Cox FEG (1972). Protective heterologous immunity between *Plasmodium atheruri* and other *Plasmodium* spp. and *Babesia* spp. in mice. Parasitol, 65, 379–387. doi:10.1017/S0031182000044000

Cox FEG (1978). Heterologous immunity between piroplasms and malaria parasites: the simultaneous elimination of *Plasmodium vinckei* and *Babesia microti* from the blood of doubly infected mice. Parasitology, 76, 55–60. doi: 10.1017/S0031182000047387

Centers for Disease Control and Prevention (CDC) (2012). Babesiosis surveillance-18 states, 2011. MMWR Morb Mortal Wkly Rep, 61, 505-509. PMID: 22785341

Cesta MF (2006). Normal structure, function, and histology of the spleen. Toxicol Pathol, 34, 455–465. doi: doi.org/10.1080/01926230600867743

Chiou SP, Kitoh K, Igarashi I, Takashima Y (2014). Generation of monoclonal autoantibodies from *Babesia rodhaini*-infected mice. J Vet Med Sci, 76, 1281–1284. doi:10.1292/jvms.14-0095

Clark IA (2001). Heterologous immunity revisited. Parasitol, 122, S51–S59. doi:10.1017/S0031182000017340

Clark IA (2007). The advent of the cytokine storm. Immunol Cell Biol, 85, 271–273. doi: 10.1038/sj.icb.7100062

Clark IA, Alleva LM, Budd AC, Cowden WB (2008). Understanding the role of inflammatory cytokines in malaria and related diseases. Travel Med Infect Dis, 6, 67–81. doi: 10.1016/j.tmaid.2007.07.002

Clark IA, Wills EJ, Richmond, Joan E, Allison, AC (1975). Immunity to intra-erythrocytic protozoa. Lancet, 306, 1128–1129. doi: 10.1016/S0140-6736(75)91010-7

Clawson ML, Paciorkowski N, Rajan TV, La Vake C, Pope C, La Vake M, Wikel SK, Krause PJ, Radolf JD (2002). Cellular immunity, but not gamma interferon, is essential for resolution of *Babesia microti* infection in BALB/c mice. Infect Immun, 70, 5304–5306. doi: 10.1128/IAI.70.9.5304-5306.2002

Cox FEG (2001). Concomitant infections, parasites and immune responses. Parasitol, 122, S23–S38. doi: 10.1017/S003118200001698X

Cox FEG, Young AS (1969). Acquired immunity to *Babesia microti* and *Babesia rodhaini* in mice. Parasitol, 59, 257–268. doi: 10.1017/S0031182000069997

Crutcher JM, Stevenson MM, Sedegah M, Hoffman, SL (1995). Interleukin-12 and malaria. Res Immunol, 146, 552–559. doi:10.1016/0923-2494(96)83031-8

D'Andrea A, Rengaraju M, Valiante NM, Chehimi J, Kubin M, Aste M, Chan SH, Kobayashi M, Young D, Nickbarg E, et al. (1992). Production of natural killer cell stimulatory factor (interleukin 12) by peripheral blood mononuclear cells. J Exp Med, 176, 1387–1398. doi: 10.1084/jem.176.5.1387

De Oca MM, Engwerda C, and Haque A (2013). *Plasmodium berghei* ANKA (PbA) infection of C57BL/6J mice: a model of severe malaria. Methods Mol Biol, 1031, 203–213. doi: 10.1007/978-1-62703-481-4_23

Dondorp AM, Kager PA, Vreeken J, and White NJ (2000). Abnormal blood flow and red blood cell deformability in severe malaria. Parasitol Today, 16, 228–232. doi: 10.1016/S0169-4758(00)01666-5

Douradinha B, Mota MM, Luty AJF, and Sauerwein RW (2008). Cross-species immunity in malaria vaccine development: two, three, or even four for the price of one? Infect Immun, 76, 873–878. doi: https://doi.org/10.1128/IAI.00431-07

Dobrescu I, de Camargo TM, Gimenez AM, Murillo O, Amorim KNDS, Marinho CRF, Soares IS, Boscardin SB, Bargieri DY (2020). Protective immunity in mice immunized with *P. vivax* MSP119-based formulations and challenged with *P. berghei* expressing PvMSP119. Front Immunol, 11, 28. doi: https://doi.org/10.3389/fimmu.2020.00028

Djokic V, Akoolo L, Parveen N (2018a). *Babesia microti* infection changes host spleen architecture and is cleared by a Th1 immune response. Front Microbiol, 9, 1–11. doi: 10.3389/fmicb.2018.00085

Djokic V, Primus S, Akoolo L, Chakraborti M, Parveen N (2018b). Age-related differential stimulation of immune response by *Babesia microti* and *Borrelia burgdorferi* during acute phase of infection affects disease severity. Front Immunol, 9, 2891. doi: 10.3389/fimmu.2018.02891

Djokic V, Akoolo L, Primus S, Schlachter S, Kelly K, Bhanot P, Parveen N (2019). Protozoan parasite *Babesia microti* subverts adaptive immunity and enhances Lyme disease severity. Front Microbiol, 10, 1596. doi: 10.3389/fmicb.2019.01596

Djokic V, Rocha SC, Parveen N (2021). Lessons learned for pathogenesis, immunology, and disease of erythrocytic parasites: *Plasmodium* and *Babesia*. Front Cell Infect Microbiol, 11, 685239. doi: 10.3389/fcimb.2021.685239

Dvoraková HM, Dvorácková M (2007). Babesiosis, a little known zoonosis. Epidemiol Mikrobiol Imunol, 56, 176–180. PMID: 18072299

Efstratiou A, Galon EMS, Wang G, Umeda K, Kondoh D, Terkawi MA, Kume A, Liu M, Ringo AE, Guo H, Gao Y, Lee SH, Li J, Moumouni PFA, Nishikawa Y, Suzuki H, Igarashi I, Xuan X (2020). *Babesia microti* confers macrophage-based cross-protective immunity against murine malaria. Front Cell Infect Microbiol, 10, 193. doi: 10.3389/fcimb.2020.00193

El-Assaad F, Wheway J, Mitchell AJ, Lou J, Hunt NH, Combes V, et al (2013). Cytoadherence of *Plasmodium berghei*-infected red blood cells to murine brain and lung microvascular endothelial cells in vitro. Infect Immun, 81, 3984–3991. doi: 10.1128/IAI.00428-13

Elton CM, Rodriguez M, Ben Mamoun C, Lobo CA, and Wright GJ (2019). A library of recombinant *Babesia microti* cell surface and secreted proteins for diagnostics discovery and reverse vaccinology. Int J Parasitol, 49, 115–125. doi: 10.1016/j.ijpara.2018.10.003

Engwerda CR, Mynott TL, Sawhney S, De Souza JB, Bickle QD, Kaye PM (2002). Locally up-regulated lymphotoxin α, not systemic tumor necrosis factor α, is the principal mediator of murine cerebral malaria. J Exp Med, 195, 1371–1377. doi: 10.1084/jem.20020128

Franke-Fayard B, Janse CJ, Cunha-Rodrigues M, Ramesar J, Büscher P, Que I, Löwik C, Voshol PJ, den Boer MA, van Duinen SG, Febbraio M, Mota MM, Waters AP (2005). Murine malaria parasite sequestration: CD36 is the major receptor, but cerebral pathology is unlinked

to sequestration. Proc Natl Acad Sci, 102, 11468–11473. doi: https://doi.org/10.1073/pnas.0503386102

Freitas do Rosario AP, and Langhorne J (2012). T cell-derived IL-10 and its impact on the regulation of host responses during malaria. Int J Parasitol, 42, 549–555. doi: 10.1016/j.ijpara.2012.03.010

Gabrielli S, Totino V, Macchioni F, Zuñiga F, Rojas P, Lara Y, Roselli M, Bartoloni A, Cancrini G (2016). Human babesiosis, Bolivia, 2013. Emerg Infect Dis, 22, 1445–1447. doi: 10.3201/eid2208.150195

Ghazanfari N, Mueller SN, and Heath WR (2018). Cerebral malaria in mouse and man. Front Immunol, 9, 2016. doi: 10.3389/fimmu.2018.02016

Golub R, Tan J, Watanabe T, Brendolan A (2018). Origin and immunological functions of spleen stromal cells. Trends Immunol, 39, 503–514. doi: 10.1016/j.it.2018.02.007

Grau GE, Piguet PF, Engers HD, Louis JA, Vassalli P, Lambert PH (1986). L3T4+ T lymphocytes play a major role in the pathogenesis of murine cerebral malaria. J Immunol, 137, 2348–2354

Gupta P, Lai SM, Sheng J, Tetlak P, Balachander A, Claser C, Renia L, Karjalainen K, Ruedl C (2016). Tissue-resident CD169+ macrophages form a crucial front line against *Plasmodium* infection. Cell Rep, 16, 1749–1761. doi: 10.1016/j.celrep.2016.07.010

Gray J, Zintl A, Hildebrandt A, Hunfeld K-P, Weiss L (2010). Zoonotic babesiosis: Overview of the disease and novel aspects of pathogen identity. Ticks Tick Borne Dis, 1, 3–10. doi: 10.1016/j.ttbdis.2009.11.003

Haque A, Best SE, Amante FH, Ammerdorffer A, de Labastida F, Pereira T, Ramm GA, Engwerda CR (2011). High parasite burdens cause liver damage in mice following *Plasmodium berghei* ANKA infection independently of CD8+ T cell-mediated immune pathology. Infect Immun, 79, 1882–1888. doi: 10.1128/IAI.01210-10

Hensel JA, Khattar V, Ashton R, and Ponnazhagan S (2019). Characterization of immune cell subtypes in three commonly used mouse strains reveals gender and strain-specific variations. Lab Invest, 99, 93–106. doi: 10.1038/s41374-018-0137-1

Hildebrandt A, Gray JS, Hunfeld K-P (2013). Human babesiosis in Europe: What clinicians need to know. Infection, 41, 1057–1072. doi: 10.1007/s15010-013-0526-8

Homer MJ, Aguilar-Delfin I, Telford SR, Krause, PJ, Persing, DH (2000). Babesiosis. Clin Microbiol Rev, 13, 451–469. doi: 10.1128/CMR.13.3.451

Hunt NH, Golenser J, Chan-Ling T, Parekh S, Rae C, Potter S, Medana IM, Miu J, & Ball HJ (2006). Immunopathogenesis of cerebral malaria. Int J Parasitol, 36(5), 569–582. doi: https://doi.org/10.1016/j.ijpara.2006.02.016

Hunt NH, & Grau GE (2003). Cytokines: accelerators and brakes in the pathogenesis of cerebral malaria. Trends Immunol, 24(9), 491–499. doi: https://doi.org/10.1016/S1471-4906(03)00229-1

Igarashi I, Suzuki R, Waki S, Tagawa Y, Seng S, Tum S, Omata Y, Saito A, Nagasawa H, Iwakura Y, Suzuki N, Mikami T, Toyoda Y (1999). Roles of CD4+ T cells and gamma interferon in protective immunity against *Babesia microti* infection in mice. Infect Immun, 67, 4143–4148. doi: 10.1128/IAI.67.8.4143-4148.1999

Inoue N, Omata Y, Igarashi I, Saito A, Claveria FG, Suzuki N (1994). *Babesia rodhaini* and *Babesia microti*: Cross-immunity and cross-antigens. J Protozool Res, 4, 98-104. doi: 10.32268/jprotozoolres.4.3_98

Imai T, Suzue K, Ngo-Thanh H, Shimokawa C, & Hisaeda H (2020). Potential and limitations of cross-protective vaccine against malaria by blood-stage naturally attenuated parasite. Vaccine, 8, 375. doi: https://doi.org/10.3390/vaccines8030375

Jeong Y-I, Hong S-H, Cho S-H, Lee W-J, Lee S-E (2012). Induction of IL-10-producing CD1dhighCD5+ regulatory B cells following Babesia microti-infection. PLoS One, 7, e46553. doi: 10.1371/journal.pone.0046553

Junaid QO, Khaw LT, Mahmud R, Ong KC, Lau YL, Borade PU, Liew JWK, Sivanandam S, Wong KT, Vythilingam I (2017). Pathogenesis of *Plasmodium berghei* ANKA infection in the gerbil (Meriones unguiculatus) as an experimental model for severe malaria. Parasite, 24, 38. doi: https://doi.org/10.1051/parasite/2017040

Johnson WC, Cluff CW, Goff WL, Wyatt CR (1996). Reactive oxygen and nitrogen intermediates and products from polyamine degradation are babesiacidal in vitro. Ann N Y Acad Sci, 791, 136–147. doi: 10.1111/j.1749-6632.1996.tb53520.x

Kawabuchi T, Tsuji M, Kuwahara S, Nishida A, Shimofurutachi T, Oka H, Ishihara C (2005). Isolation of a human erythrocyte-adapted substrain of *Babesia rodhaini* and analysis of the merozoite surface protein gene sequences. J Vet Med Sci, 67, 901–907. doi: 10.1292/jvms.67.901

King T, Lamb T (2015). Interferon-γ: The Jekyll and Hyde of malaria. PLoS Pathog, 11, e1005118. doi: 10.1371/journal.ppat.1005118

Kim MJ, Chu KB, Lee SH, Kang HJ, Yoon KW, Ahmed MA, Quan FS (2022). Recombinant vaccinia virus expressing *Plasmodium berghei* apical membrane antigen 1 or microneme protein enhances protection against *P. berghei* infection in mice. Trop Med Infect Dis, 7, 350. doi: 10.3390/tropicalmed7110350

Kjemtrup AM & Conrad PA (2000). Human babesiosis: An emerging tick-borne disease. Int J Parasitol, 30, 1323–1337. doi: 10.1016/S0020-7519(00)00137-5

Knapp KL & Rice NA (2015). Human coinfection with *Borrelia burgdorferi* and *Babesia microti* in the United States. J Parasitol Res, 2015, 1–11. doi: 10.1155/2015/587131

Koch O, Rockett K, Jallow M, Pinder M, Sisay-Joof F, Kwiatkowski D (2005). Investigation of malaria susceptibility determinants in the IFNG/IL26/IL22 genomic region. Genes Immun, 6, 312–318. doi: 10.1038/sj.gene.6364214

Krause PJ (2019). Human babesiosis. International Journal for Parasitology, 49(2), 165–174. https://doi.org/10.1016/j.ijpara.2018.11.007

Kumar R, Ng S, Engwerda C (2019). The role of IL-10 in malaria: A double-edged sword. Front Immunol, 10, 229. doi: 10.3389/fimmu.2019.00229

Lacerda-Queiroz N, Riteau N, Eastman RT, Bock KW, Orandle MS, Moore IN, Sher A, Long CA, Jankovic D, Su XZ (2017). Mechanism of splenic cell death and host mortality in a *Plasmodium yoelii* malaria model. Sci Rep, 7, 10438. doi: 10.1038/s41598-017-10776-2

Lagassé HA, Anidi IU, Craig JM, Limjunyawong N, Poupore AK, Mitzner W, Scott AL (2016). Recruited monocytes modulate malaria-induced lung injury through CD36-mediated clearance of sequestered infected erythrocytes. J Leukoc Biol, 99, 659–671. doi: 10.1189/jlb.4HI0315-130RRR

Liu Z, Gu Y, Shin A, Zhang S, Ginhoux F (2020). Analysis of myeloid cells in mouse tissues with flow cytometry. STAR Protoc, 1, 100029. doi: https://doi.org/10.1016/j.xpro.2020.100029

Leiby DA (2011). Transfusion-transmitted *Babesia* spp.: Bull's-eye on *Babesia microti*. Clin Microbiol Rev, 24, 14–28. doi: 10.1128/CMR.00022-10

Leitner WW, Haraway M, Pierson T, Bergmann-Leitner ES (2020). Role of opsonophagocytosis in immune protection against malaria. Vaccines, 8, 264. doi: 10.3390/vaccines8020264

Li J, Galon EM, Guo H, Liu M, Li Y, Ji S, Zafar I, Gao Y, Zheng W, Adjou Moumouni PF, Rizk MA, Tumwebaze MA, Benedicto B, Ringo AE, Masatani T, Xuan X (2021). PLK:Δgra9 live attenuated strain induces protective immunity against acute and chronic toxoplasmosis. Front Microbiol, 12, 619335. doi: 10.3389/fmicb.2021.619335

Li Y, Terkawi MA, Nishikawa Y, Aboge GO, Luo Y, Ooka H, Goo YK, Yu L, Cao S, Sun Y, Yamagishi J, Masatani T, Yokoyama N, Igarashi I, Xuan X (2012). Macrophages are critical for cross-protective immunity conferred by *Babesia microti* against *Babesia rodhaini* infection in mice. Infect Immun, 80, 311–320. doi: 10.1128/IAI.05900-11

Lobo CA, Cursino-Santos JR, Alhassan A, Rodrigues M (2013). *Babesia*: An emerging infectious threat in transfusion medicine. PLoS Pathog, 9, e1003387. doi: 10.1371/journal.ppat.1003387

Lovegrove FE, Gharib SA, Peña-Castillo L, Patel SN, Ruzinski JT, Hughes TR, Liles WC, Kain KC (2008). Parasite burden and CD36-mediated sequestration are determinants of acute lung injury in an experimental malaria model. PLoS Pathog, 4, e1000068. doi: https://doi.org/10.1371/journal.ppat.1000068

Lundqvist J, Larsson C, Nelson M, Andersson M, Bergström S, Persson C (2010). Concomitant infection decreases the malaria burden but escalates relapsing fever borreliosis. Infect Immun, 78, 1924–1930. doi: 10.1128/IAI.01082-09

Luty AJ, Perkins DJ, Lell B, Schmidt-Ott R, Lehman LG, Luckner D, Greve B, Matousek P, Herbich K, Schmid D, Weinberg JB, Kremsner PG (2000). Low interleukin-12 activity in severe *Plasmodium falciparum* malaria. Infect Immun, 68, 3909–3915. doi: 10.1128/IAI.68.7.3909-3915.2000

Maier A G, Matuschewski K, Zhang M, & Rug M (2019). *Plasmodium falciparum*. Trends Parasitol, 35(6), 481–482. https://doi.org/10.1016/j.pt.2018.11.010

Malaguarnera L, Imbesi RM, Pignatelli S, Simpore J, Malaguarnera M, Musumeci S (2002). Increased levels of interleukin-12 in *Plasmodium falciparum* malaria: Correlation with the severity of disease. Parasite Immunol, 24, 387–389. doi: 10.1046/j.1365-3024.2002.00478.x

Mabbott NA (2018). The influence of parasite infections on host immunity to co-infection with other pathogens. Front Immunol, 9, 2579. doi: 10.3389/fimmu.2018.02579

McGuire W, Knight JC, Hill AVS, Allsopp CEM, Greenwood BM, & Kwiatkowski D (1999). Severe Malarial Anemia and Cerebral Malaria Are Associated with Different Tumor Necrosis Factor Promoter Alleles. J Infect Dis, 179(1), 287–290. https://doi.org/10.1086/314533

Mawson AR (2013). The pathogenesis of malaria: A new perspective. Pathog Glob Health, 107(3), 122–129. doi: https://doi.org/10.1179/2047773213Y.0000000084

Man S, Fu Y, Guan Y, Feng M, Qiao K, Li X, Gao H, Cheng X (2017). Evaluation of a major surface antigen of *Babesia microti* merozoites as a vaccine candidate against *Babesia* infection. Front Microbiol, 8, 2545. doi: 10.3389/fmicb.2017.02545

Marsh K, Kinyanjui S (2006). Immune effector mechanisms in malaria. Parasite Immunol, 28, 51–60. doi: 10.1111/j.1365-3024.2006.00808.x

Mayne P (2014). Clinical determinants of Lyme borreliosis, babesiosis, bartonellosis, anaplasmosis, and ehrlichiosis in an Australian cohort. Int J Gen Med, 15. doi: 10.2147/IJGM.S75825

McArdle AJ, Turkova A, Cunnington AJ (2018). When do co-infections matter? Curr Opin Infect Dis, 31, 209–215. doi: 10.1097/QCO.0000000000000447

Medina TS, Costa SP, Oliveira MD, Ventura AM, Souza JM, Gomes TF, Vallinoto AC, Póvoa MM, Silva JS, Cunha MG (2011). Interleukin-10 and interferon-γ levels in *Plasmodium vivax* malaria suggest a reciprocal regulation which is not altered by IL-10 gene promoter polymorphism. Malar J, 10, 264. doi: 10.1186/1475-2875-10-264

Millington OR, Gibson VB, Rush CM, Zinselmeyer BH, Phillips RS, Garside P, Brewer JM (2007). Malaria impairs T cell clustering and immune priming despite normal signal 1 from dendritic cells. PLoS Pathog, 3, e143. doi: 10.1371/journal.ppat.0030143

Mineo S, Niikura M, Inoue S, Kuroda M, Kobayashi F (2013). Development of severe pathology in immunized pregnant mice challenged with lethal malaria parasites. Infect Immun, 81, 3865–3871. doi: 10.1128/IAI.00749-13

Mishra SK, Newton CR JC (2009). Diagnosis and management of the neurological complications of *falciparum* malaria. Nat Rev Neurol, 5, 189–198. doi: 10.1038/nrneurol.2009.23

Miyagami T, Igarshi I, Suzuki M (1987). *Plasmodium berghei*: Long-lasting immunity induced by a permanent attenuated mutant. Zentralblatt Für Bakteriologie, Mikrobiologie Und Hygiene. Series A. Med Microbiol Infect Dis Virol Parasitol, 264, 502–512. doi: https://doi.org/10.1016/S0176-6724(87)80074-3

Molyneux ME, Taylor TE, Wirima JJ, Borgsteinj A. Clinical features and prognostic indicators in paediatric cerebral malaria: a study of 131 comatose Malawian children. QJM: Int J Med, 1989 May 1;71(2):441-59

Mordue DG, Wormser G P (2019). Could the drug tafenoquine revolutionize treatment of *Babesia microti* infection? J Infect Dis, 220, 442–447. doi: https://doi.org/10.1093/infdis/jiz119

Moutailler S, Valiente Moro C, Vaumourin E, Michelet L, Tran FH, Devillers E, Cosson JF, Gasqui P, Van VT, Mavingui P, Vourc'h G, Vayssier-Taussat M (2016). Co-infection of ticks: The rule rather than the exception. PLoS Negl Trop Dis, 10, e0004539. doi: 10.1371/journal.pntd.0004539

Nagayasu E, Nagakura K, Akaki M, Tamiya G, Makino S, Nakano Y, Kimura M, & Aikawa M (2002). Association of a Determinant on Mouse Chromosome 18 with Experimental Severe *Plasmodium berghei* Malaria. Infect Immun, 70(2), 512–516. https://doi.org/10.1128/IAI.70.2.512-516.2002

Nadal C, Bonnet SI, & Marsot M (2022). Eco‑epidemiology of equine piroplasmosis and its associated tick vectors in Europe: A systematic literature review and a meta‑analysis of prevalence. Transbound Emerg Dis, 69(5), 2474–2498. https://doi.org/10.1111/tbed.14261

Narurkar R, Mamorska-Dyga A, Nelson JC, Liu D (2017). Autoimmune hemolytic anemia associated with babesiosis. Biomark Res, 5, 14. doi: 10.1186/s40364-017-0095-6

Na YJ, Chai JY, Jung BK, Lee HJ, Song JY, Je JH, Seo JH, Park SH, Choi JS, Kim MJ (2014). An imported case of severe *falciparum* malaria with prolonged hemolytic anemia clinically mimicking a coinfection with babesiosis. Korean J Parasitol, 52, 667

Okada H, Suzue K, Imai T, Taniguchi T, Shimokawa C, Onishi R, Hirata J, Hisaeda H (2015). A transient resistance to blood-stage malaria in interferon-γ-deficient mice through impaired production of the host cells preferred by malaria parasites. Front Microbiol, 6, 600. doi: 10.3389/fmicb.2015.00600

Ozarslan N, Robinson J F, and Gaw S L (2019). Circulating monocytes, tissue macrophages, and malaria. J Trop Med, 2019, 1–9. doi: 10.1155/2019/3720838

Pais TF, Ali H, Moreira da Silva J, Duarte N, Neres R, Chhatbar C, Acúrcio RC, Guedes RC, Strano Moraes MC, Costa-Silva B, Kalinke U, Penha-Gonçalves C (2022). Brain endothelial STING1 activation by *Plasmodium*-sequestered heme promotes cerebral malaria via type I IFN response. Proc Natl Acad Sci, 119, e2206327119. doi: 10.1073/pnas.2206327119

Perkins SL (2014). Malaria's Many Mates: Past, Present, and Future of the Systematics of the Order *Haemosporida*. J Parasitol, 100(1), 11–25. https://doi.org/10.1645/13-362.1

Percário S, Moreira DR, Gomes BA, Ferreira ME, Gonçalves AC, Laurindo PS, Vilhena TC, Dolabela MF, Green MD (2012). Oxidative stress in malaria. Int J Mol Sci, 13, 16346–16372. doi: 10.3390/ijms131216346

Petra B, Josipa K, Renata BR, & Vladimir M (2018). Canine Babesiosis: Where Do We Stand? Acta Vet, 68(2), 127–160. https://doi.org/10.2478/acve-2018-0011

Rathinasamy V, Poole WA, Bastos RG, Suarez CE, Cooke BM (2019). Babesiosis vaccines: lessons learned, challenges ahead, and future glimpses. Trends Parasitol, 35, 622–635. doi: 10.1016/j.pt.2019.06.002

Redpath SA, Fonseca NM, and Perona-Wright G (2014). Protection and pathology during parasite infection: IL-10 strikes the balance. Parasite Immunol, 36, 233–252. doi: 10.1111/pim.12113

Rico LG, Salvia R, Ward MD, Bradford JA, and Petriz J (2021). Flow-cytometry-based protocols for human blood/marrow immunophenotyping with minimal sample perturbation. STAR Protoc, 2, 100883. doi: 10.1016/j.xpro.2021.100883

Rénia L, Goh YS (2016). Malaria parasites: the great escape. Front Immunol, 7, 463. doi: 10.3389/fimmu.2016.00463

Roberts JA, Kerr JD, Tracey-Patte P (1972). Function of the spleen in controlling infections of *Babesia rodhaini* in mice. Int J Parasitol, 2, 217–226. doi: 10.1016/0020-7519(72)90009-4

Sanches-Vaz M, Temporão A, Luis R, Nunes-Cabaço H, Mendes AM, Goellner S, et al (2019). *Trypanosoma brucei* infection protects mice against malaria. PLOS Pathog, 15, e1008145. doi: 10.1371/journal.ppat.1008145

Sanni LA, Jarra W, Li C, and Langhorne J (2004). Cerebral edema and cerebral hemorrhages in interleukin-10-deficient mice infected with *Plasmodium chabaudi*. Infect Immun, 72, 3054–3058. doi: 10.1128/IAI.72.5.3054-3058.2004

Stevenson MM, and Riley EM (2004). Innate immunity to malaria. Nat Rev Immunol, 4, 169–180. doi: 10.1038/nri1311

Strangward P, Haley MJ, Shaw TN, Schwartz JM, Greig R, Mironov A, de Souza JB, Cruickshank SM, Craig AG, Milner DA Jr, Allan SM, Couper KN (2017). A quantitative brain map of experimental cerebral malaria pathology. PLOS Pathog, 13, e1006267. doi: 10.1371/journal.ppat.1006267

Swanson M, Pickrel A, Williamson J, and Montgomery S (2023). Trends in reported babesiosis cases — United States, 2011–2019. MMWR Morb Mortal Wkly Rep, 72, 273–277. doi: 10.15585/mmwr.mm7211a1

Sevilla E, González LM, Luque D, Gray J, Montero E (2018). Kinetics of the invasion and egress processes of *Babesia divergens*, observed by time-lapse video microscopy. Sci Rep, 8, 14116. doi: 10.1038/s41598-018-32349-7

Skariah S, Arnaboldi P, Dattwyler RJ, Sultan AA, Gaylets C, Walwyn O, Mulhall H, Wu X, Dargham SR, Mordue DG (2017). Elimination of *Babesia microti* is dependent on intraerythrocytic killing and CD4 + T cells. J Immunol, 199, 633–642. doi: 10.4049/jimmunol.1601193

Sobolewski P, Gramaglia I, Frangos JA, Intaglietta M, van der Heyde H (2005). *Plasmodium berghei* resists killing by reactive oxygen species. Infect Immun, 73, 6704–6710. doi: 10.1128/IAI.73.10.6704-6710.2005

Sow F, Nyonda M, Bienvenu AL, Picot S (2015). Wanted *Plasmodium falciparum*, dead or alive. Microb Cell, 2, 219–224. doi: 10.15698/mic2015.07.211

Steiner FE, Pinger RR, Vann CN, Grindle N, Civitello D, Clay K, Fuqua C (2008). Infection and co-infection rates of *Anaplasma phagocytophilum* variants, *Babesia* spp., *Borrelia burgdorferi*, and the rickettsial endosymbiont in Ixodes scapularis (Acari: Ixodidae) from sites in Indiana, Maine, Pennsylvania, and Wisconsin. J Med Entomol, 45, 289–297. doi: 10.1603/0022-2585(2008)45[289:iacroa]2.0.co;2

Stevenson MM, Riley EM (2004). Innate immunity to malaria. Nat Rev Immunol, 4, 169–180. doi: 10.1038/nri1311

Taylor WR J, Canon V, & White N J (2006). Pulmonary manifestations of malaria: recognition and management. Treat Respir Med, 5, 419–428. doi: 10.2165/00151829-200605060-00007

Thakre N, Fernandes P, Mueller AK, & Graw F (2018). Examining the reticulocyte preference of two *Plasmodium berghei* strains during blood-stage malaria infection. Front Microbiol, 9, 166. doi: 10.3389/fmicb.2018.00166

Trinchieri G (2007). Interleukin-10 production by effector T cells: Th1 cells show self control. J Exp Med, 204, 239–243. doi: 10.1084/jem.20070104

Terkawi MA, Cao S, Herbas MS, Nishimura M, Li Y, Moumouni PF, Pyarokhil AH, Kondoh D, Kitamura N, Nishikawa Y, Kato K, Yokoyama N, Zhou J, Suzuki H, Igarashi I, Xuan X

(2015). Macrophages are the determinant of resistance to and outcome of nonlethal *Babesia microti* infection in mice. Infect Immun, 83, 8–16. doi: 10.1128/IAI.02128-14

Trinchieri G (1993). Interleukin-12 and its role in the generation of Th1 cells. Immunol Today, 14, 335–338. doi: 10.1016/0167-5699(93)90230-I

Ty MC, Zuniga M, Götz A, Kayal S, Sahu PK, Mohanty A, Mohanty S, Wassmer SC, Rodriguez A (2019). Malaria inflammation by xanthine oxidase‐produced reactive oxygen species. EMBO Mol Med, 11, e9903. doi: 10.15252/emmm.201809903

Vannier E, Krause P J (2012). Human babesiosis. N Engl J Med, 366, 2397–2407. doi: 10.1056/NEJMra1202018

Van Duivenvoorde LM, Voorberg-van Der Wel A, Van Der Werff NM, Braskamp G, Remarque EJ, Kondova I, Kocken CHM, & Thomas AW (2010). Suppression of *Plasmodium cynomolgi* in rhesus macaques by coinfection with *Babesia microti*. Infect Immun, 78, 1032–1039. doi: 10.1128/IAI.00921-09

Venkatesan P (2022). The future of malaria control in light of RTS,S. Lancet Microbe, 3, e251. doi: https://doi.org/10.1016/S2666-5247(22)00070-2

Vermeil C, Menut J, Miegeville M, Cruziat J, Julienne F, Morin O, Roger AP, Marjolet M, Bouillard C (1983). Babesiasis, pediatric malaria: Does confusion exist in Africa? Bull Soc Pathol Exot, 76, 797–804

Villeval J-L, Gearing A, Metcalf D (1990). Changes in hemopoietic and regulator levels in mice during fatal or nonfatal malarial infections. Exp Parasitol, 71, 375–385. doi: 10.1016/0014-4894(90)90063-I

Vos AJ, Bock RE (2006). Vaccination against bovine babesiosis. Ann N Y Acad Sci, 916, 540–545. doi: 10.1111/j.1749-6632.2000.tb05333.x

Wang G, Efstratiou A, Adjou Moumouni PF, Liu M, Jirapattharasate C, Guo H, Gao Y, Cao S, Zhou M, Suzuki H, Igarashi I, Xuan X (2016). Primary *Babesia rodhaini* infection followed by recovery confers protective immunity against *B. rodhaini* reinfection and *Babesia microti* challenge infection in mice. Exp Parasitol, 169, 6–12. doi: 10.1016/j.exppara.2016.07.003

Weiss L (1989). Mechanisms of splenic control of murine malaria: Cellular reactions of the spleen in lethal (Strain 17XL) *Plasmodium yoelii* malaria in BALB/c mice, and the consequences of pre-infective splenectomy. Am J Trop Med Hyg, 41, 144–160. doi: 10.4269/ajtmh.1989.41.144

Weiss L, Johnson J, Weidanz W (1989). Mechanisms of splenic control of murine malaria: Tissue culture studies of the erythropoietic interplay of spleen, bone marrow, and blood in lethal (strain 17XL) *Plasmodium yoelii* malaria in BALB/c mice. Am J Trop Med Hyg, 41, 135–143. PMID: 2774062

Welsh RM, Che JW, Brehm MA, and Selin LK (2010). Heterologous immunity between viruses: Heterologous immunity between viruses. Immunol Rev, 235, 244–266. doi: https://doi.org/10.1111/j.0105-2896.2010.00897.x

White DJ, Talarico J, Chang H-G, Birkhead GS, Heimberger T, Morse DL (1998). Human babesiosis in New York State: Review of 139 hospitalized cases and analysis of prognostic factors. Arch Intern Med, 158, 2149. doi: 10.1001/archinte.158.19.2149

World Malaria Report (2022). Geneva: World Health Organization; 2022. Licence: CC BY-NC-SA 3.0 IGO

Wu Y, Wang QH, Zheng L, Feng H, Liu J, Ma SH, Cao YM (2007). *Plasmodium yoelii*: Distinct CD4+ CD25+ regulatory T cell responses during the early stages of infection in susceptible and resistant mice. Exp Parasitol, 115, 301–304. doi: 10.1016/j.exppara.2006.09.015

Xu X, Sumita K, Feng C, Xiong X, Shen H, Maruyama S, Kanoh M, Asano Y (2001). Down-regulation of IL-12 p40 gene in *Plasmodium berghei*-infected mice. J Immunol, 167, 235–241. doi: 10.4049/jimmunol.167.1.235

Xue X, Ren S, Yang X, Masoudi A, Hu Y, Wang X, Li H, Zhang X, Wang M, Wang H & Liu J (2021). Protein regulation strategies of the mouse spleen in response to *Babesia microti* infection. Parasit Vectors, 14, 61. doi: 10.1186/s13071-020-04574-5

Yeruham I, Hadani A, Galker, F (1998). Some epizootiological and clinical aspects of ovine babesiosis caused by Babesia ovis—a review." Vet Parasitol, 74, 153-163. doi: https://doi.org/10.1016/S0304-4017(97)00143-X

Yi W, Bao W, Rodriguez M, Liu Y, Singh M, Ramlall V, Cursino-Santos JR, Zhong H, Elton CM, Wright GJ, Mendelson A, An X, Lobo CA, Yazdanbakhsh K (2018). Robust adaptive immune response against *Babesia microti* infection marked by low parasitemia in a murine model of sickle cell disease. Blood Adv, 2, 3462–3478. doi: 10.1182/bloodadvances.2018026468

Young KM, Corrin T, Wilhelm B, Uhland C, Greig J, Mascarenhas M, Waddell LA (2019). Zoonotic *Babesia*: A scoping review of the global evidence. PLoS One, 14, e0226781. doi: 10.1371/journal.pone.0226781

Yoneto T, Yoshimoto T, Wang CR, Takahama Y, Tsuji M, Waki S, Nariuchi H (1999). Gamma interferon production is critical for protective immunity to infection with blood-stage *Plasmodium berghei* XAT but neither NO production nor NK cell activation is critical. Infect Immun, 67, 2349–2356. doi: https://doi.org/10.1128/IAI.67.5.2349-2356.1999

Zhou X, Li SG, Chen SB, Wang JZ, Xu B, Zhou HJ, Ge HX, Chen JH, Hu W (2013). Co-infections with *Babesia microti* and *Plasmodium* parasites along the China-Myanmar border. Infect Dis Poverty, 2, 24. doi: 10.1186/2049-9957-2-24

Zintl A, Mulcahy G, Skerrett HE, Taylor SM, Gray JS (2003). *Babesia divergens*, a bovine blood parasite of veterinary and zoonotic importance. Clin Microbiol Rev, 16, 622–636. doi: 10.1128/CMR.16.4.622-636.2003

Zivkovic D, Speksnijder JE, Kuil H, Seinen W (1984). Immunity to *Babesia* in mice II. Cross protection between various *Babesia* and *Plasmodium* species and its relevance to the nature of *Babesia* immunity. Vet Immunol Immunopathol, 5, 359–368. doi: 10.1016/0165-2427(84)90004-7